U.S. DEPARTMENT OF ENERGY

PNNL-22235

Techno-economic Performance Evaluation of Compressed Air Energy Storage in the Pacific Northwest

BP McGrail
CL Davidson
DH Bacon
MA Chamness
SP Reidel
FA Spane
JE Cabe
FS Knudsen
MD Bearden
JA Horner
HT Schaef
PD Thorne

February 2013

Pacific Northwest NATIONAL LABORATORY

Proudly Operated by Battelle Since 1965

DISCLAIMER

PACIFIC NORTHWEST NATIONAL LABORATORY
operated by
BATTELLE
for the
UNITED STATES DEPARTMENT OF ENERGY
under Contract DE-AC05-76RL01830

Printed in the United States of America

Available to DOE and DOE contractors from the
Office of Scientific and Technical Information,
P.O. Box 62, Oak Ridge, TN 37831-0062;
ph: (865) 576-8401
fax: (865) 576-5728
email: reports@adonis.osti.gov

Available to the public from the National Technical Information Service
5301 Shawnee Rd., Alexandria, VA 22312
ph: (800) 553-NTIS (6847)
email: orders@ntis.gov <http://www.ntis.gov/about/form.aspx>
Online ordering: http://www.ntis.gov

This document was printed on recycled paper.
(8/2010)

PNNL-22235

Techno-economic Performance Evaluation of Compressed Air Energy Storage in the Pacific Northwest

BP McGrail
CL Davidson
DH Bacon
MA Chamness
SP Reidel
FA Spane
JE Cabe
FS Knudsen
MD Bearden
JA Horner
HT Schaef
PD Thorne

February 2013

Prepared for Bonneville Power Administration
under Intergovernmental Contract #54177

Pacific Northwest National Laboratory
Richland, Washington 99352

Project Highlights

In the first project of its kind, the Bonneville Power Administration teamed with the Pacific Northwest National Laboratory and a full complement of industrial and utility partners to evaluate the technical and economic feasibility of developing compressed air energy storage (CAES) in the unique geologic setting of inland Washington and Oregon. The basic idea of CAES is to capture and store compressed air in suitable geologic structures underground when off-peak power is available or additional load is needed on the grid for balancing. The stored high-pressure air is returned to the surface and used to produce power when additional generation is needed, such as during peak demand periods. To date, there are two operating CAES plants in the world; a 110 MW plant in McIntosh, Alabama, commissioned in 1991 and a 290 MW plant in Huntorf, Germany built in 1978. Both plants store air underground in excavated salt caverns produced by solution mining. Since underground salt formations are in relatively few locations geographically and are specifically not present in the Pacific Northwest, the project team extended analysis of traditional CAES storage in salt caverns to much more prevalent underground porous and permeable rock structures. Doing so resulted in a set of significant advancements to CAES concepts and to its fundamental value proposition beyond traditional peak to off-peak load shifting. Details regarding the project's assumptions, analysis methods, and findings are provided in the Executive Summary and in the main body of this report. However, the key overarching conclusions from this study are:

- Eastern Washington and Oregon are rich with potentially suitable sites for CAES. Screening criteria were applied to identify more favorable site locations and included constraints on distance to both natural gas pipelines and transmission lines (230 kV or greater), presence of deep, thick, and laterally extensive geologic traps, and proximity to previously drilled deep exploration wells to constrain storage reservoir properties. Application of the screening criteria yielded five candidate locations, which were narrowed to two areas for detailed assessment of subsurface storage capacity, power plant design, transmission interconnection, and economic feasibility.
- A conventional CAES plant was designed and analyzed for a first site located at Columbia Hills. The plant design offers 231 MW of load during storage and 207 MW of generation. Storage capacity at this site was estimated at approximately 1.5 million metric tons of air, representing potential for approximately 40 days of continuous injection at plant capacity and simulations indicate a capability of over 400 hours of subsequent generation without further injections. Simplified economic analysis indicates the installed capital cost would be similar to conventional combined-cycle gas turbines at a levelized cost of electricity (LCOE) as low as 6.4 cents per kilowatt-hour (kWh), competitive with most generating options within the region.
- A new type of no-fuel hybrid geothermal CAES plant was designed for a site located near Yakima Canyon north of Selah (Yakima Minerals). Constraints on natural gas supply were identified after this site was selected, which necessitated development of this new CAES plant configuration. The plant design at this location offers 150 MW of load during storage and 83 MW of generation capacity. The storage reservoir at this site is very deep, being more than 10,000 ft below ground surface. Pressures at those depths result in higher density of air being stored, which combined with a very large reservoir structure provide for a very large air storage capacity. Simulations of continuous injection for 1 year representing 4 MMT of air filled less than 20% of the reservoir volume. The hybrid Yakima Minerals plant LCOE was estimated to be 11.8 cents per kWh and could be competitive with the region's peaking and renewables generation.

- Both plant configurations evaluated would be capable of providing balancing (increasing or decreasing reserve), energy production, and peaking capacity within ten minute response time standards.

Utilization of the very large air storage capacity available in porous rock structures enables a CAES plant to offer a unique combination of attributes including grid-scale energy storage capacity, seasonal load shifting, load balancing, peaking reserve, and traditional diurnal peak to off-peak load shifting. CAES appears to offer a storage and generation option that could integrate well into the region's resource portfolio, with the ability to tailor plant design, storage reservoir siting and development, and project management to the operator's specific needs and business case.

Executive Summary

The mismatch between the timing of wind-based power generation and the demand for electricity has resulted in the frequent over-generation and under-generation of power within the Bonneville Power Administration (BPA) service area. In a number of instances, the issue is compounded in the spring when high water flows have led to the curtailment of power production from wind resources, and environmental dispatch requirements mandate the use of hydroelectric turbines (rather than spilling all the excess flow over the dams) to maintain dissolved gases in the Columbia River at appropriate levels. For these reasons, and because of the significant growth in wind generation capacity to date (Figure ES.1) and additional growth expected over the coming years, there is strong interest in novel opportunities for integrating these intermittent renewable resources while ensuring the stability and reliability of transmission in BPA's service territory.

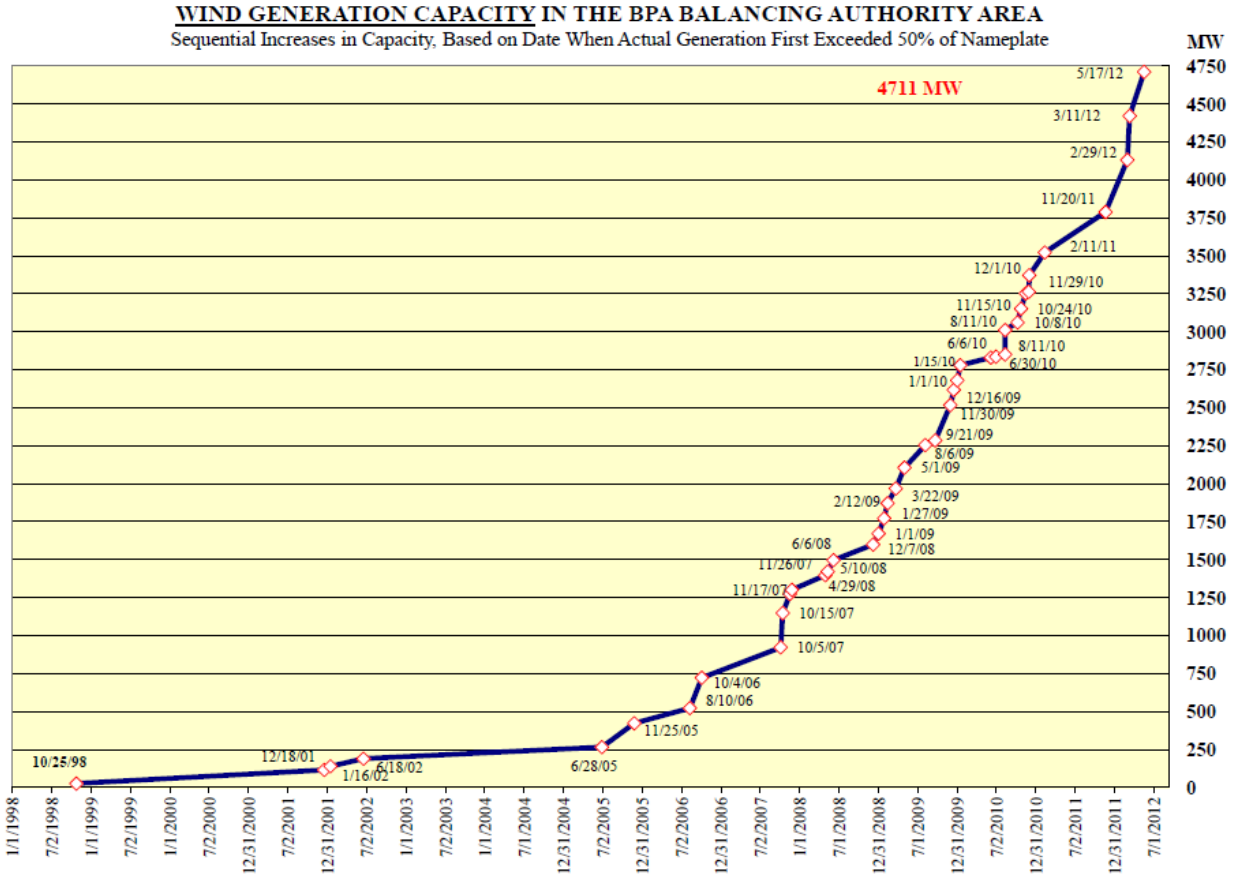

Figure ES.1. Wind installed capacity in BPA balancing authority area[1]

BPA has identified energy storage as one of 19 critical technologies with the potential to enhance grid stability, increase operational transfer capability, and prevent and mitigate the impacts of extreme events to the grid. BPA's Transmission Technology Roadmap (BPA, 2011a) indicates that technology breakthroughs are needed that dramatically reduce the costs of large-scale (gigawatt-hour level) energy

[1] Wind Installed Capacity Plot. Accessed at: http://transmission.bpa.gov/business/operations/Wind/WIND_InstalledCapacity_Plot.pdf

storage systems to drive revolutionary changes in the design and operation of the electric power system. This project has been undertaken to provide a preliminary, region-specific analysis of costs, seasonality, capacity, and duration of strategic options for subsurface energy storage.

This study began with a regional reconnaissance-level site suitability evaluation that identified five candidate areas that could generically support a compressed air subsurface reservoir, and corresponding compressed air energy storage (CAES) power plant. Of these, two sites were selected for core geologic simulation work, which in turn was used to inform design and modeling of preliminary plant configurations. The characteristics of each site and especially the constraints on natural gas supply at one site resulted in very different design and operational approaches. However, in both cases, a technologically viable first-order[1] configuration was designed and modeled to take the greatest advantage of local surface and subsurface conditions, and to best mitigate the challenges at each site. Site-specific system designs and costs, including levelized costs of electricity (LCOEs) were developed based on the chosen designs.[2]

While the sites discussed below reflect the most appealing locations based on the siting process described above, the flexibility of off-the-shelf component technologies used in CAES plants indicates that final configurations could be tailored to the specific strengths and challenges of a site or operational purpose. One primary finding of this study—that there are areas within the Columbia River Basalt where storage capacities, injectivities, and geometries comprise a suitable storage reservoir for compressed air—suggests that CAES projects may be viable at a number of sites beyond those examined here.

CAES Project Siting

The Pacific Northwest region east of the Cascade Mountain Range is dominated by the Columbia Plateau Province (CPP). The CPP predominantly consists of a set of continental flood basalt deposits that cover over 81,000 mi^2 of portions of eastern Washington, northeastern Oregon, and western Idaho, with a total composite volume of more than 53,700 mi^3 (REIDEL et al., 2002). As shown in Figure ES.2, the Columbia River Basalt Group (CRBG) portion extends and is coincident with a very large fraction of the wind and thermal power generation resources in the region, as represented by their CO_2 emissions. Flood basalts fill large basins through multiple (up to several hundred) outpourings of deep mantle lavas from feeder dikes. Total composite thickness of basalt in the deepest part of these basins can exceed 4 km, with subsurface temperatures exceeding 175°C at depth in some areas.

[1] It is important to note that actual built plant configurations for these sites are heavily dependent upon geologic site characterization to quantitatively determine reservoir conditions, which will affect compression, injection, and production system design.

[2] As a technical siting and feasibility study, the consumption of grid-supplied energy during compression was maintained as a zero cost attribute.

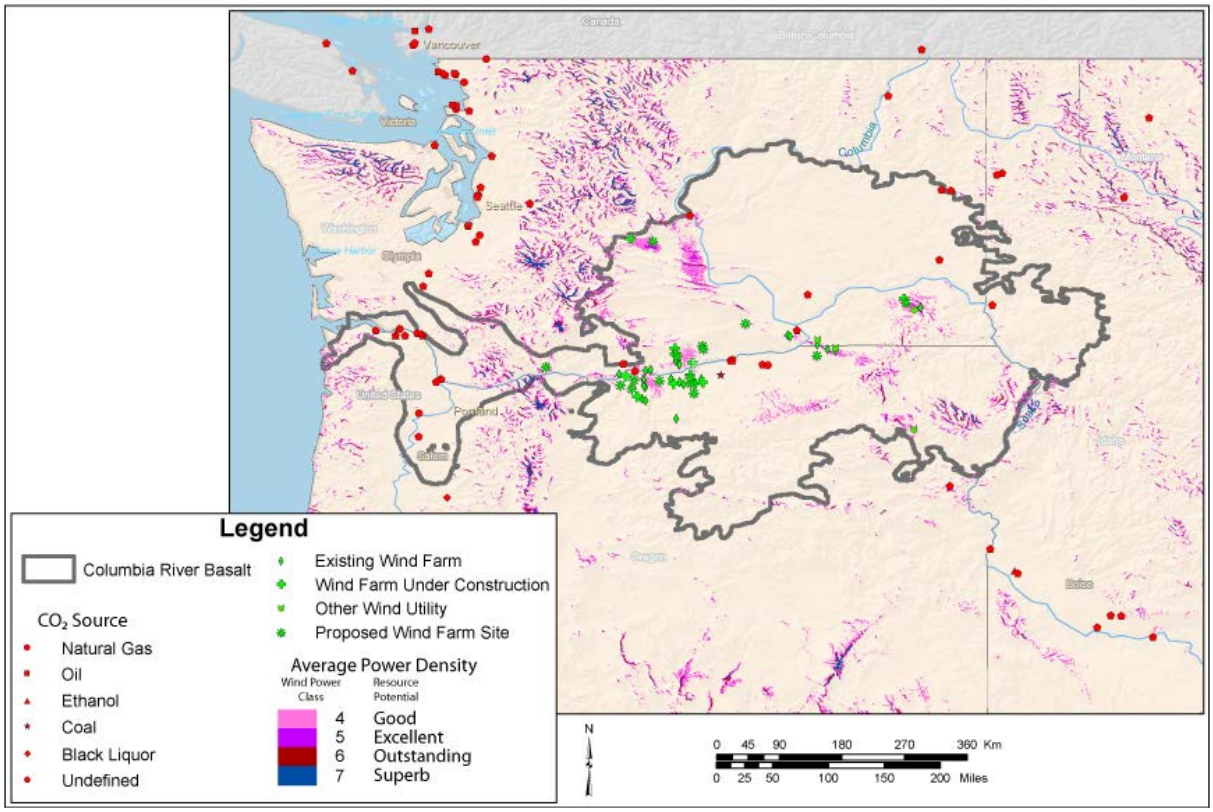

Figure ES.2. Map showing coincidence of wind and major thermal power station resources with Columbia River Basalt (outlined in gray) target for energy storage

CRBG represents a considerable barrier for oil and natural gas exploration in the underlying sub-basalt sediments, and potential reservoirs within these basins filled with flood basalts have not been extensively investigated as compared to typical, conventional sedimentary basins in other regions of the U.S. Only very limited data are available on deep reservoir temperatures, and especially deep aquifer hydrogeologic properties critical to any quantitative assessment of potential for CAES in the basalts and the sub-basalt sedimentary units. Recent advances in drilling technology and geophysical data acquisition methods have helped to overcome subsurface access barriers, and deep oil and gas exploration wells are beginning to fill some of the data gaps with respect to the geology and hydrogeology in flood basalt provinces. Data collected from natural gas exploration wells recently drilled in the Pacific Northwest as well as the extensive characterization work being done on the Columbia River Basalt for CO_2 sequestration pilot testing (McGrail et al., 2009) provides an opportunity for the first time to advance quantitative assessment of CAES potential in this unique regional geologic setting.

Regional identification of potentially suitable CAES sites began with the storage reservoir parameters required to implement a commercial scale storage project. Areas were evaluated for four key criteria:

- Reservoir thickness ($\geq$ 30 ft)
- Reservoir permeability (k $\geq$ 500 millidarcies)
- Effective porosity ($\varepsilon \geq 0.1$), and
- Overlying low-permeability, caprock thickness ($\geq$ 100 ft; $\leq$ 10-1 microdarcies).

Preliminary reservoir simulation work undertaken using the STOMP (Subsurface Transport Over Multiple Phases) model showed that, while air injected into a low or no dip reservoir tends to migrate quite slowly, such a storage configuration presented difficulties in recovering a significant fraction of the injected compressed air before water intrusion into the well occurred. For this reason, the above criteria were modified to include the presence of an anticlinal structure to increase air recovery efficiency and to prevent migration of the compressed air away from the storage project boundaries.

The requirements above imply a need for data upon which to base a quantitative evaluation. Because, as discussed earlier, relatively few wells exist in this region at candidate storage depths, minimizing uncertainty in the site assessment process necessitated a focus in areas near existing deep boreholes in the CRBG. The limitations presented by this exclusive use of available data significantly constrained the areas available for evaluation in this study. However, because a high percentage of deep wells drilled outside the Hanford site were sited based upon proprietary oil and gas exploration information, it is likely that these sites represent the most likely candidates for high injectivities, good capacities, and structural suitability. Site areas also were selected to include those within 20 miles of transmission lines (230+ kV), and locations with proximity to natural gas pipelines. Figure ES.3 shows the five zones (A through E) initially investigated in this study.

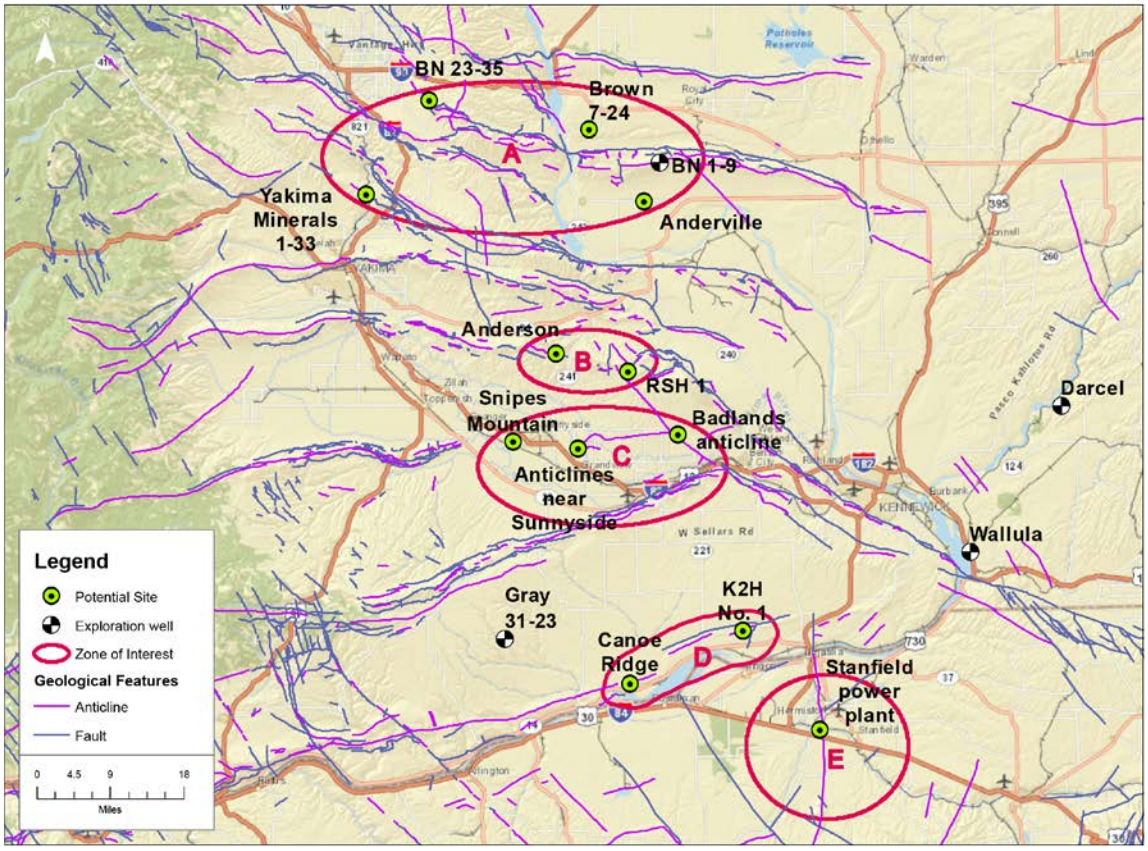

Figure ES.3. Location of deep exploration wells and five potential zones of interest

Based on a multidisciplinary evaluation that included consultation between subject area experts at BPA and Pacific Northwest National Laboratory, these five sites were narrowed to two. A conventional CAES approach—where compressed air is used to increase the efficiency of a natural gas plant by decreasing the amount of process power needed to run the gas turbine—is presented for the Columbia Hills site (Zone D), which sits only a few miles from several pipelines with large, available gas supplies.

A similar initial assessment of site suitability identified Zone A as a second preferred site option. However, detailed analysis of natural gas supply availability on pipelines in the area made it clear that, without construction of a dedicated gas line to the project site, Zone A and any site north of the major supply lines running along the Washington-Oregon border would not be able to secure sufficient gas to support a natural gas-fired thermal plant. Rather than omit all sites not adjacent to suitable gas lines, a no-fuel option was evaluated in which compressed air would be injected and then extracted as the sole source of power generation at the surface. This option was examined at the Yakima Minerals site (Zone A) just north of Selah, Washington.

Key findings and considerations for both the Columbia Hills and Yakima Minerals sites are discussed in more detail in the following sections.

Columbia Hills CAES Plant

The Columbia Hills CAES plant design presented in this study represents a conventional system design that has achieved commercial success when paired with cavern-based air storage. The novel use of deep flood basalts as the air storage reservoir is a distinguishing difference from a “standard” CAES plant deployed elsewhere. The power plant is a decoupled system; the compressor is only used for the injection air into the subsurface. Extraction and combustion of the stored air during power production mode does not require, nor is it modeled with an air compressor to supply combustion air. Because there is no parasitic compressor load during power production, the heat rate of the gas-fired CAES plant is excellent when compared to other gas-fired generating technologies. Qualitatively, this extends to the compression cycle as well, where the consumption of grid-supplied energy is assumed to consist of excess capacity, which is shown to consist predominantly of wind and hydroelectric generation, rather than thermally produced electricity. The CAES plant has a generation capacity of 207 MW, a total capital cost of $1,112/kW and a levelized cost of electricity of 6.41 cents per kilowatt-hour at 25% capacity factor. This is competitive with most regionally based new build generating alternatives, and is significantly better than a directly comparable simple-cycle combustion turbine. In addition to energy production, the plant as configured would be expected to capitalize on additional revenue streams, such as the provision of ancillary services. Figure ES.4 is a block flow representation of the conventional natural gas-fired CAES plant evaluated at the Columbia Hills site.

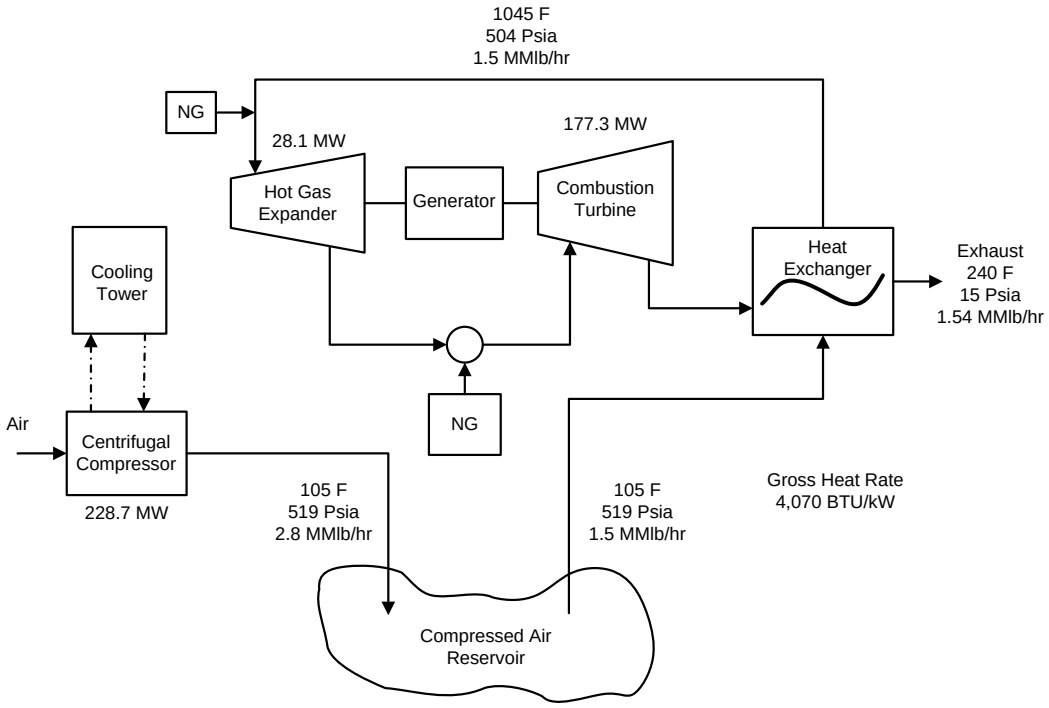

Figure ES.4. Columbia Hills CAES plant

The selected site offers numerous advantages in terms of land ownership, proximity to critical infrastructure (natural gas pipeline and transmission), and nearby exploration wells that reduce risk of encountering unexpected hydrogeologic conditions at the site. The geologic structure examined for storage in this case, while smaller relative to the storage capacity present at the Yakima Minerals site, is capable of meeting compression requirements for 40 days before injected air begins to transition beyond the boundaries of the storage area. Simulation results show that approximately 40% of the stored air volume could be extracted before formation water breakthrough occurs, which suggests the importance of maintaining an adequately sized volume of cushion air when managing the reservoir.

Its relatively small storage capacity and the limited injectivity of the subsurface reservoir are the primary constraints at the Columbia Hills site. Based on assumed reservoir properties, four injection wells use up all available injection capacity at the site, which would effectively limit future expansion of the CAES facility beyond the 231 MW compression load under cases analyzed in this report. While the subsurface parameters are the limiting factor for maximum capacity of the surface facility, it is worth noting that the plant is both readily scalable (up or down) and capable of being sited anywhere the compressed air reservoir can be established and maintained.[1] If higher capacity or storage requirements are needed at the Columbia Hills site, fracture stimulation of the reservoir should be factored into any future analysis. Reservoir stimulation would offer two key benefits by 1) significantly reducing uncertainty around encountering less favorable hydrologic properties than expected at the site, and 2) reducing the pressure required to achieve the targeted injection rate and increasing the air storage volume efficiency in the structure. Both factors will improve the plant operating efficiency and reduce financial risk associated with developing a project at this site.

[1] Subject to the availability of additional infrastructure required by the plant configuration (e.g., natural gas, cooling water, transmission).

As a consequence of the CO_2 sequestration pilot study underway near Wallula, Washington (MCGRAIL et al., 2011), the Washington State Department of Ecology (WADOE) now has experience in permitting unique activities associated with large-scale injections of gases into the Columbia River Basalts. The injection wells envisioned for the Columbia Hills site would most likely be permitted as Class V wells under the state's Underground Injection Control Program. One aspect of the envisioned completions, however, will require concurrence from WADOE. Well completions that connect distinct aquifer units are prohibited in Washington State under WAC 173-160-420. The well design for the Columbia Hills site envisions a completion across three members in the Grande Ronde Basalt. Compressed air storage results in a dewatered zone around an injection well. Hence, as long as the CAES plant was operational, water transfer between these interflow zones would not be possible and the injection wells would comply with the intent of the regulation in WAC 173-160-240. Nevertheless, WADOE would need to approve the well completion plan for a project utilizing a similar well design as outlined in this report.

Yakima Minerals Hybrid Plant

The Yakima Minerals site, located in the Yakima Canyon north of Selah, Washington, is home to the Yakima Minerals 1-33 exploration well, sited at the crest of an anticline. The geology at this site includes a basalt sequence underlain by thick sub-basalt sandstones with excellent permeability, suggesting high injectivities and a relatively compact air storage zone, making it an attractive target for fluid injection and storage. Based on subsurface modeling, the site would readily accommodate a large degree of capacity expansion should it be needed in the future; whereas the Columbia Hills structure could accommodate 40 days of compressed air injection before reaching the structure's spill point, corresponding simulations at the Yakima Minerals site showed that no loss of compressed air was seen even after a year of injection. The site however lacks access to natural gas supplies via existing pipelines as well as cooling water. Based on these infrastructure restrictions, and given the storage reservoir is far deeper than any CAES plant considered to date, the Yakima Minerals plant necessitated an unconventional design approach.

The hybrid CAES plant at Yakima Minerals would utilize geothermal and geopressure resources to produce power. During the compression phase (air injection), compression would supply air to the deep compressed air reservoir. Heat of compression would be captured and stored in molten salt, while trim cooling for the centrifugal compressor intercoolers would be provided by ammonia absorption refrigeration. Upon extraction, geothermal resources would be used to preheat the pressurized air for high-pressure turbo-expansion, and then the molten salt would be used to supplement the compressed air flow with additional heat for the low-pressure/high temperature expansion.

The very deep storage reservoir (>10,000 ft) and modeled fracture pressure of the subsurface compressed air reservoir enables the compressor and turbo-expander equipment to operate at substantially higher pressures than conventional CAES plants. As designed and modeled, this results in maximum compression capacity relative to airflow, as well as significant power output from a non-phase change geothermal plant. Figure ES.5 provides a block flow representation of the hybrid CAES plant modeled for the Yakima Minerals site.

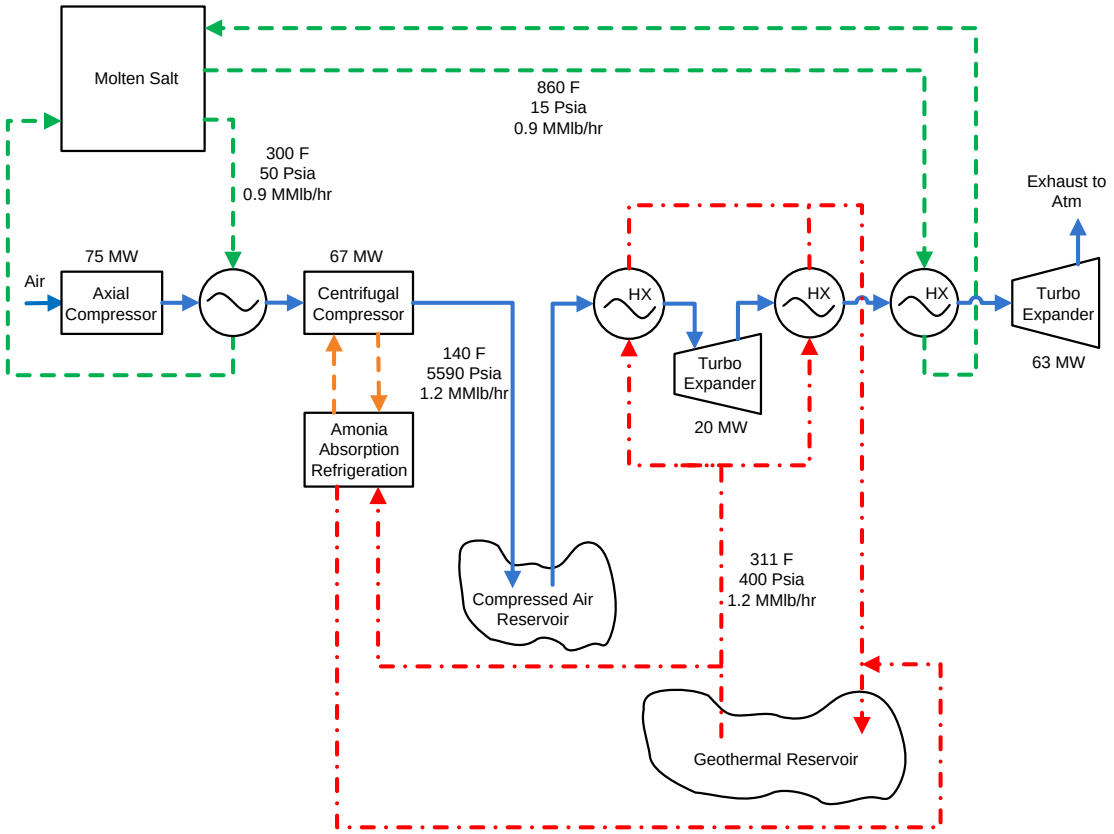

Figure ES.5. Yakima Minerals hybrid CAES plant

Perhaps the single most valuable aspect of the hybrid CAES plant based on the assumptions made is that it is a technically feasible, non-fossil fired energy source that can be dispatched to produce or consume energy with essentially no environmental releases. The hybrid CAES plant has a generation capacity of 83 MW, a total capital cost of $2,738/kW and a levelized cost of electricity of 11.84 cents per kilowatt-hour at 25% capacity factor. In addition to energy production, the plant as configured would be expected to capitalize on additional revenue streams, such as the provision of ancillary services.

Compressor cooling is a significant design issue at the Yakima Minerals site. For maximum compressor efficiency, implementation of a shallow groundwater source cooling water return system and/or cooling tower would be preferred over air-cooling if readily accessible. However, groundwater source cooling would require a substantial flow rate based on heat exchanger duty, access to shallow and very permeable sediment or basalts near the power plant site, and large diameter wellbore completions. Implementing a cooling tower option at this site drastically reduces the groundwater flow requirements, and would directly reduce capital and operating expenses from what is currently modeled.[1]

The nearest available surface water to implement a cooling water option would be the Yakima River. Due to excess demand on the Yakima River, obtaining a water right permit for out-of-stream use of Yakima River water may be difficult and would take an extended period. One mitigating factor is that the primary withdrawals from the Yakima River would coincide with periods of excess spring run-off and the

[1] The air cooling and ammonia absorption equipment cost is $7.8 million. Total installed cost would be higher, and would include construction, instrumentation, piping, and ancillary line items such as insulation and paint.

largest continuous compressor load; hence, a negligible impact on overall management of the resource would be possible. To address these concerns, staff incorporated the geothermal driven ammonia absorption cooling system into final process flow diagrams, and eliminated the need for cooling water. The geothermal flows required for the cooling process were balanced against the duty required for trim cooling, and are envisioned to be used for both compression and generation cycles. In Washington State, closed-loop heating and cooling water return flow wells are rule-authorized wells under WAC 173-218-100 provided no chemicals or other products are added to the water. Hence, both the geothermal heat extraction and the injection wells would be rule-authorized as envisioned for this plant. The air injection well(s) would be completed in a single defined sub-basalt sedimentary formation and hence should comply with all well construction requirements under WAC 173-160-420.

Economic Co-optimization of Surface and Subsurface Design

The diversity of the plant designs and reservoir parameters for the two sites modeled here speaks to the breadth of settings across which CAES projects could potentially be developed in the Pacific Northwest, and represents a viable solution to bridging the need for regional energy storage. This first-order effort to identify the best known sites based on a number of surface and subsurface siting criteria, and to pair those sites with the suite of compression and generation technologies best suited to commercial-scale projects at each site, clearly demonstrated feasibility of CAES for economical grid-scale energy storage in the Pacific Northwest. The LCOE analysis (Figure ES.6) presented in this report is the first such analysis for CAES in the region, and provides a meaningful basis for considering this technological option alongside other balancing and generation alternatives. The conventional CAES configuration at Columbia Hills could provide power at just over 6 cents per kilowatt-hour, which is competitive with natural gas combined cycle, and unsubsidized wind when adjusted for comparable capacity factors; and is significantly lower than natural gas fired simple cycle combustion turbines operating at comparable capacity factors. The hybrid CAES configuration at Yakima Minerals with an LCOE of 11.8 cents per kilowatt-hour could be economically competitive with peaking gas, as well as other renewable energy sources such as solar photovoltaics, concentrating solar, and distributed generation technologies (non-utility level wind, solar, and biomass).

The cost of energy estimate provided in this siting and technical feasibility study does not include provisions or estimates for the cost of compression, particularly during diurnal operations. While the working volume of compressed air in the storage reservoir would initially come from zero cost excess grid capacity, diurnal operations would in most cases need to consider and account an associated energy cost for compression. Additional value, not monetized for this report, would be expected for the facility due to its ability to dispatch for both power generation and power consumption thereby offsetting the potential cost of compression, and generating additional revenue streams as applicable.

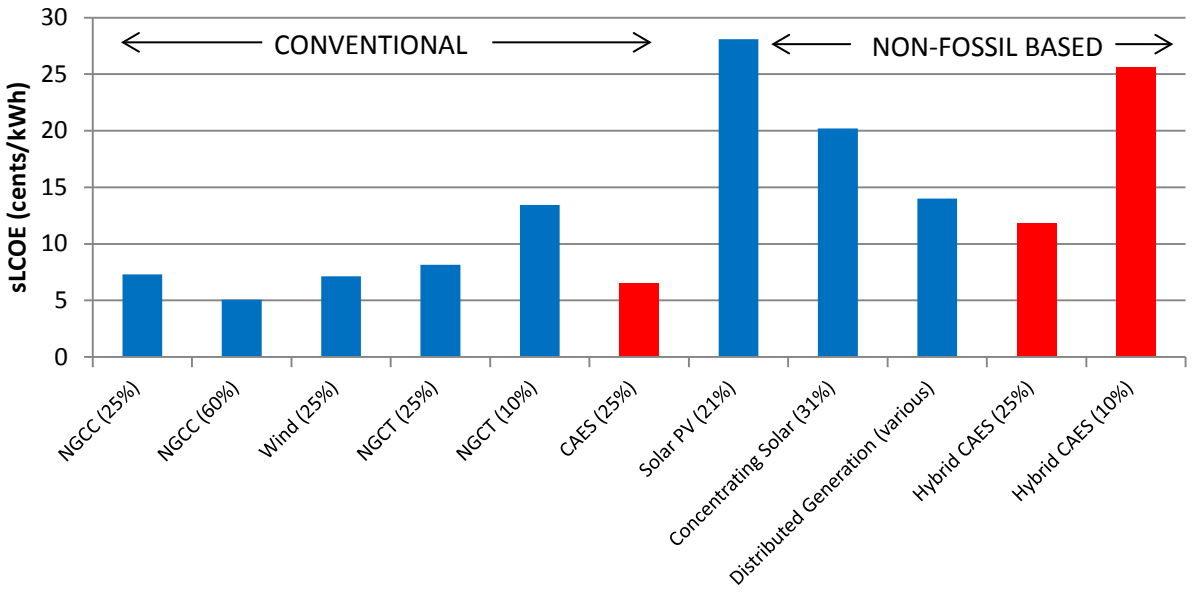

Figure ES.6. Levelized cost of electricity and relevant generating alternatives[1]

Design flexibility allows paired surface-subsurface systems to be tailored to the needs of the project. Their flexibility would allow either of the CAES configurations described in this report to serve a number of purposes—mitigation of over-generation events, routine energy production via diurnal arbitrage, and provision of ancillary services, making it a unique resource within the BPA service territory. For the purpose of this evaluation, the technical feasibility of a utility level CAES configuration at a specific location was assessed recognizing that the economic optimization of the design, operation, and management of these plants was outside of the current scope of the project. To that regard, the capital cost estimate provided for facility build-out includes the compression and power generation plant, the storage reservoir development, and transmission interconnection, but does not include items such as fee, insurance, and bonds. Additionally, because aspects of financing are neither estimated nor disclosed, items such as allowance for funds used during construction (AFUDC) are not included in the total cost estimate. A full breakdown of capital costs are provided in each respective section.

In addition to providing a proof of concept that CAES is feasible in storage reservoirs within the CRBG, configurations and associated LCOEs presented here provide a starting point for discussing the value CAES may have in enabling the integration of intermittent renewables energy while maintaining stable, reliable production and delivery of electricity in the BPA service area. Additional economic modeling—including baseload generation, balancing and power arbitrage, and ways to allow a portion of the rents associated with increased hydroelectric dispatch to accrue the CAES project operator—will enable more specific modeling of the revenue streams and allow greater iteration on plant design and storage reservoir management.

[1] Additional generating alternatives evaluated using data from the National Renewable Energy Laboratory's Transparent Cost Database and modified for comparative capacity factors and fuel cost as necessary. Accessed at http://en.openei.org/apps/TCDB/ January 9, 2013.

Acronyms and Abbreviations

μD	microdarcy
amu	atomic mass units
Aspen IPE	Aspen Process Economic Analyzer
BAA	balancing authority area
BPA	Bonneville Power Administration
Btu	British thermal units
BWIP	Basalt Waste Isolation Project
CAES	compressed air energy storage
CAISO	California Independent System Operator
CPP	Columbia Plateau Province
CRBG	Columbia River Basalt Group
DOGAMI	Oregon Department of Geology and Mineral Industries
DOE	U.S. Department of Energy
EGS	enhanced geothermal system
fsp	feldspar
GIS	Geographic Information System
HP	high-pressure
J/kg-K	joule per kilogram kelvin
kWh	kilowatt-hour
LCOE	levelized cost of electricity
LP	low-pressure
mag	magnetite
Mlb	million pounds
MMBtu	million British thermal units
mD	millidarcy
MMT	million metric tons
MWh	megawatt-hour
NREL	National Renewable Energy Laboratory
O&M	operation and maintenance
PNNL	Pacific Northwest National Laboratory
psia	pounds per square inch absolute
px	pyroxene
RPS	renewable portfolio standards
scm	standard cubic meters
SEM	scanning electron microscopy
sLCOE	simplified levelized cost of electricity

STOMP	Subsurface Transport Over Multiple Phases
USGS	U.S. Geological Survey
W/m-K	watt per meter kelvin
WADOE	Washington State Department of Ecology
WDNR	Washington State Department of Natural Resources
WECC	Western Electricity Coordinating Council

Contents

Executive Summary iii
CAES Project Siting vi
Columbia Hills CAES Plant ix
Yakima Minerals Hybrid Plant xi
Economic Co-optimization of Surface and Subsurface Design xiii
Acronyms and Abbreviations xv
1.0 Introduction 1
1.1 Description and Major Objectives 1
1.2 Technology Gap 2
1.2.1 Background 2
1.2.2 Research Needs 4
2.0 Site Identification 6
2.1 Regional Suitability Analysis 6
2.1.1 Area Covered by CRBG 8
2.1.2 Depth to Basalt Reservoirs 8
2.1.3 Access to Key Infrastructure 9
2.1.4 Potential geologic traps 11
2.1.5 Reservoir and Caprock Thickness 13
2.1.6 Reservoir Permeability and Effective Porosity 14
2.1.7 Non-potable Water in Reservoir 14
2.1.8 Geothermal Energy Recovery Potential 15
2.1.9 Site Selection 15
3.0 Subsurface Modeling and Experimental Research 24
3.1 STOMP Simulator 24
3.2 Scoping Simulations 24
3.3 Geologic Model Development 26
3.4 CAES Simulation: Columbia Hills Site 28
3.4.1 Spill Point 36
3.4.2 Water Breakthrough 38
3.4.3 Diurnal Injection/Extraction 40
3.5 CAES Simulation: Yakima Minerals Site 42
3.5.1 Spill Point 44
3.5.2 Water Breakthrough 44
3.5.3 Diurnal Injection/Extraction 46
3.6 Yakima Minerals Site Geothermal Heat Recovery 48
3.7 Summary of Simulation Results 51

4.0 Basalt-Air Reactivity Experimental Results 52
5.0 Energy Storage and Demand Analysis 54
6.0 Columbia Hills Site Design and Analysis 60
6.1 Plant Design Assumptions 61
6.1.1 Injection 61
6.1.2 Extraction 62
6.1.3 Well Bore Diameter 63
6.2 CAES Plant Model and Aspen Plus Simulation 64
6.2.1 Injection and Extraction Simulation 64
6.2.2 CAES Plant Simulation 66
6.2.3 CAES Plant Water Balance 69
6.3 Plant Operations 71
6.3.1 Capacity and Heat Rate 71
6.3.2 Energy Production 72
6.4 CAES Capital and Levelized Costs 73
6.4.1 Well Field Drilling and Development 74
6.4.2 CAES Plant 74
6.4.3 Transmission and Interconnection 76
6.4.4 Levelized Cost of Electricity 76
7.0 Yakima Minerals Hybrid CAES Plant 80
7.1 Compression and Cooling Requirements 80
7.2 Injection and Extraction Simulation 82
7.3 Geothermal Cycle Hybrid CAES Plant Model and Simulation 85
7.4 Geothermal/Molten Salt Hybrid CAES Plant Model and Simulation 88
7.5 Plant Operations 94
7.6 Hybrid CAES Plant Capital and Levelized Cost 95
7.6.1 Well Field Drilling and Development 96
7.6.2 Hybrid CAES Plant Capital Equipment 97
7.6.3 Transmission and Interconnection 98
7.6.4 Levelized Cost of Electricity 99
8.0 Ancillary Services and Revenue Sources 101
8.1 Balancing Services 101
8.2 Arbitrage 101
8.3 Other Energy Services 103
9.0 Key Findings: Project Implementation 104
9.1 Core Considerations for CAES siting 104
9.2 Columbia Hills CAES Plant 105
9.3 Yakima Minerals Hybrid Plant 106
9.4 Conclusions and Next Steps 108

10.0 Literature Cited 109

Figures

Figure 1. Map showing coincidence of wind and major thermal power station resources with Columbia River Basalt (outlined in gray) target for energy storage 4
Figure 2. Stratigraphy of the Grande Ronde Basalt 6
Figure 3. Location of deep boreholes and inferred thickness of Columbia River Basalt Group 9
Figure 4. Key infrastructure, existing generation, and extent of the Columbia River Basalt Group in the current region of interest 10
Figure 5. Map showing zones based on distance between natural gas pipelines and transmission lines carrying 230 kV or more 11
Figure 6. Example of a geologic trap in an anticline (adapted from REIDEL et al. (2002)) 12
Figure 7. Location of deep exploration and characterization wells providing data on the deep basalt and sub-basalt across the primary area of investigation 13
Figure 8. Generalized area of high chloride and fluoride in groundwater in the Grande Ronde Basalt (REIDEL et al., 2002) 15
Figure 9. Location of deep exploration wells and five potential sites 16
Figure 10. Stratigraphic and temperature data for the Yakima Minerals 1-33 well indicate potential reservoirs for both CAES and geothermal source development 17
Figure 11. The existing wells within Zone A are largely located within a short distance of high voltage electricity transmission, but only the Yakima Minerals well is near a natural gas pipeline, which was found to be capacity constrained 18
Figure 12. Regional cross section (taken from an unpublished PNNL report) with Zone B noted ("Area B") 19
Figure 13. Existing infrastructure and land ownership by type for Zone B 19
Figure 14. Existing infrastructure and land ownership for Zone C 20
Figure 15. Stratigraphy for K2H-1 and 100 Circles (Canoe Ridge) wells 21
Figure 16. Existing infrastructure and land ownership for Zone D. Note the large contiguous parcel ownership and the excellent proximity to high voltage transmission and the natural gas pipeline running west along the river. 22
Figure 17. Plume radii for air injection with a closed outer boundary at 4.3 days (top left), 14.3 days (top right) and 71.6 days (bottom) 25
Figure 18. Simulation of one injection-withdrawal cycle at 50 kg/s for various sizes of air storage. *Over-estimate due to mass loss across outer boundary 26
Figure 19. Air plume after 3 months of drift with 5-degree formation dip 26
Figure 20. Drift of center of mass of air plume over 3-month period 26
Figure 21. Surface topography and reconstructed top of the permeable Sentinel Bluffs basalt flow top at the Columbia Hills site 28
Figure 22. Model grid and layering at the Columbia Hills site. Target layers have finer grid spacing and are labeled 29
Figure 23. Compressed air in target formations after 30-day single-well injection at the Columbia Hills site 31

Figure 24. Compressed air in target formations after 30-day injection using two wells at the Columbia Hills site 32
Figure 25. Compressed air in target formations after 30-day injection using three wells at the Columbia Hills site 32
Figure 26. Compressed air in target formations after 30-day injection using four wells at the Columbia Hills site 33
Figure 27. Compressed air in target formations after 30-day injection using five wells at the Columbia Hills site 33
Figure 28. Compressed air in target formations after 30-day injection using seven wells at the Columbia Hills site 34
Figure 29. Air mass injected vs. time for multiple well scenarios at the Columbia Hills site 34
Figure 30. Air injected at 30 days vs. number of wells 35
Figure 31. Total air injection rate vs. time 35
Figure 32. Air flow rate from four wells at the Columbia Hills site after 30 days of injection 36
Figure 33. Extent of injected air plume after 40 days of injection, isosurface gas saturation = 0.5 37
Figure 34. Extent of injected air plume after 60 days of injection, isosurface gas saturation = 0.5 37
Figure 35. Extent of injected air plume after 90 days, isosurface gas saturation = 0.5 38
Figure 36. Total amount of remaining air at Columbia Hills site during extraction period 39
Figure 37. Air plume in Columbia Hills formation after 30 days of injection followed by 80 days of extraction 39
Figure 38. Total mass of compressed air at the Columbia Hills site during 30 days of diurnal injection/extraction cycles 40
Figure 39. Extent of compressed air plume at the Columbia Hills site after 30 days of injection and an additional 30 days of diurnal injection/extraction cycles 41
Figure 40. Grid and layering in the sub-basalt region at the Yakima Minerals site. Depths are below the mean surface elevation of 2,085 ft. 42
Figure 41. Cumulative mass of air injected over 30 days at the Yakima Minerals site 43
Figure 42. Gas saturation after 30 days of injection at the Yakima Minerals site 43
Figure 43. Injected air plume at the Yakima Minerals site after 1 year of continuous injection 44
Figure 44. Total amount of remaining air at Yakima Minerals site during extraction period 45
Figure 45. Air plume at the Yakima Minerals site after 30 days of injection followed by 56 days of extraction 46
Figure 46. Total mass of compressed air at the Yakima Minerals site during 30 days of diurnal injection/extraction cycles 47
Figure 47. Extent of compressed air plume at the Yakima Minerals site after 30 days of injection and an additional 30 days of diurnal injection/extraction cycles 47
Figure 48. Cross-section of model grid and layering for Yakima Minerals deep geothermal wells simulation 49
Figure 49. Pressure distribution in formation at the end of a 6-hr injection period 49
Figure 50. Formation temperature after 14 days of water injection at 220°F 50
Figure 51. Water temperature at geothermal extraction and injection wells 50

Figure 52. Residual gas analyses of gases obtained from the reactor containing basalt, water, and air (red) and the reactor with only water and air (black) 52
Figure 53. Microphotograph of an unreacted basalt chip (Wanapum formation) with distinguishable grains of titanium rich magnetite (mag), feldspar (fsp), and pyroxene (px) as observed by SEM 53
Figure 54. Microphotograph of an reacted basalt chip (Wanapum formation) with distinguishable grains of titanium rich magnetite (mag), feldspar (fsp), and pyroxene (px) as observed by SEM 53
Figure 55. Wind installed capacity in BPA balancing authority area 54
Figure 56. BPA Balancing and Reserves Deployed 56
Figure 57. Columbia Hills CAES plant block flow diagram 57
Figure 58. Yakima Minerals hybrid CAES plant block flow diagram 59
Figure 59. Schematic of the Huntorf CAES facility 60
Figure 60. Schematic of the McIntosh CAES facility 60
Figure 61. Well field conceptual layout 62
Figure 62. Gross power vs. well bore diameter 63
Figure 63. Injection and extraction process flow diagram 65
Figure 64. CAES plant process flow diagram 67
Figure 65. Compressor cooling water process flow diagram 70
Figure 66. Impact of capacity factors on sLCOE for CAES plant 78
Figure 67. Impact of natural gas price on future sLCOE 78
Figure 68. Comparative LCOE for new build generating options 79
Figure 69. Injection and extraction for hybrid CAES plant 83
Figure 70. Injection and extraction for geothermal/molten salt hybrid CAES 84
Figure 71. Adiabatic geothermal hybrid CAES plant (compression) 86
Figure 72. Adiabatic geothermal hybrid CAES plant (power generation) 87
Figure 73. Geothermal/molten salt compression cycle 90
Figure 74. Molten salt process flow 91
Figure 75. Geothermal driven ammonia absorption cooling for hybrid CAES plant 92
Figure 76. Adiabatic geothermal/molten salt hybrid CAES plant (generation) 93
Figure 77. LCOE of hybrid CAES and additional generating resources 100

Tables

Table 1. Layering at the Columbia Hills site 29
Table 2. Initial pressures and temperatures at the location of Well 1 (ENSTOR #1) 30
Table 3. Initial formation pressure and injection pressure at the top of the upper screened interval in each injection well. For the 5-well scenario, the locations of Wells 1 and 2 were shifted slightly to locations 1b and 2b for optimum spacing. 31
Table 4. Relative advantages and disadvantages to hybrid configurations 58
Table 5. Material balance for injection and extraction 64
Table 6. Material balance for CAES plant 68
Table 7. Material balance for water and cooling system 69
Table 8. Flow sheet load and duty 71
Table 9. Calculated CAES heat rate 72
Table 10. Estimated capital costs for CAES plant at Columbia Hills 73
Table 11. Well drilling estimate for Columbia Hills locations 74
Table 12. Overnight capital cost of CAES facility 75
Table 13. Interconnection costs by kV rating 76
Table 14. Simplified LCOE calculation for conventional CAES plant 77
Table 15. Heat and material balance for geothermal hybrid plant (compression) 88
Table 16. Heat and material balance for geothermal hybrid CAES plant (power generation) 88
Table 17. Utility and consumption for geothermal hybrid CAES plant 88
Table 18. Heat and material balance for geothermal/molten salt hybrid CAES plant 94
Table 19. Utility and consumption for geothermal/molten salt hybrid CAES plant 94
Table 20. Estimated capital costs for hybrid CAES plant at Yakima Minerals 96
Table 21. Well drilling estimate for Yakima Minerals location 97
Table 22. Overnight capital costs of hybrid CAES facility 98
Table 23. Interconnection costs by kV rating 99
Table 24. Simplified LCOE calculation for hybrid CAES plant 100
Table 25. Arbitrage values ($/kW-year) for CAES 102

1.0 Introduction

1.1 Description and Major Objectives

The electric grid in the Pacific Northwest is facing an increasingly complex operating environment with rapid growth in wind generation capacity combining with seasonal periods of high stream flows to produce an increasing frequency of over-generation events (BPA, 2011b). The Bonneville Power Administration (BPA) is managing these events, in part, by offering zero priced power and reducing the output of hydroelectric dams through additional spill; but the use of stream flow spillage as a supply management option is limited due to associated adverse dissolved gas level increases in the Columbia River and its tributaries, which may pose a danger to federally protected fish. As a result, BPA has been increasingly required to curtail wind generation due to lack of load under certain surplus-power conditions. This could cause wind power developers to see a net reduction in value of current generation capacity and to lose federal production tax credits and renewable energy credits, potentially hampering new wind development in the region.

In addition to seasonal over-generation problems, BPA has experienced large increases in the requirement to hold capacity reserves on the system to respond quickly to unscheduled ramps by the fleet of wind generation. These balancing reserve requirements have surpassed 1,000 MW in the BPA balancing authority area (BAA) and have nearly exhausted the capability of the hydroelectric system to meet the balancing needs within the BAA.

Grid-scale energy storage could help manage over-generation events and provide continuous balancing reserves with lower overall costs and fewer mid- to long-term barriers to additional renewables development in the Pacific Northwest. A variety of options have been considered for energy storage, including pumped hydro, underground pumped hydro, various types of batteries, compressed air energy storage (CAES), flywheels, ultra capacitors, and superconducting magnetic energy storage. Pumped hydro and subsurface energy storage methods, in general, appear to be the only options in this set that are technically feasible at the scale (DOTY et al., 2010) needed to address a significant fraction of 100 MW-month and potentially up to 1,100 MW-month over-generation events anticipated by BPA (2011b). Technical and economic analysis of pumped hydro energy storage has been previously reported (KINTNER-MEYER et al., 2010). This report is the first attempt to examine the potential for subsurface energy storage in suitable geologic formations present in the Pacific Northwest.

Although considerable work on various CAES concepts has been done, surprisingly, there has been no published study of CAES implemented in flood basalts, which represent the predominant regional geologic formation within the Pacific Northwest east of the Cascade Mountain Range. Pacific Northwest National Laboratory (PNNL) has pioneered both laboratory (MCGRAIL et al., 2006) and field pilot studies (MCGRAIL et al., 2009) examining the potential for large-scale injection and storage of CO_2 and natural gas storage in flood basalts (REIDEL et al., 2002). The results of these studies clearly suggest the potential of utilizing flood basalts for CAES.

In addition to technical feasibility, a cost analysis has been performed that includes a careful evaluation of 1) the marginal return from electricity sales, 2) likely number and duration of storage cycles per year, 3) permitting and site monitoring requirements, and 4) operation and maintenance (O&M) costs.

These cost factors are critical for reliable estimation of life-cycle costs and to ensure that a realistic assessment can be made for energy storage versus other options for managing over-generation events.

1.2 Technology Gap

Energy storage was identified by BPA as one of 19 critical technologies that have the potential to enhance grid stability, increase operational transfer capability, and prevent and mitigate extreme events to the grid. BPA's Transmission Technology Roadmap (BPA, 2011a) indicates that technology breakthroughs are needed that dramatically reduce the costs of large-scale megawatt-level energy storage systems to drive revolutionary changes in the design and operation of the electric power system. This project has been undertaken to provide a preliminary region-specific analysis of costs, seasonality, capacity, and duration of strategic options for subsurface energy storage.

1.2.1 Background

In a CAES system, compressors use electrical energy to compress air, increasing its pressure sufficiently to be injected and stored in an underground geologic formation. Compression is performed when excess (off-peak) electricity is available on the grid. When electricity is needed on the grid, the compressed air is withdrawn from the geologic reservoir and expanded back to atmospheric pressure. Energy is produced as the pressurized air moves through successive stages of an expansion turbine. During expansion, heat must be supplied to compensate for Joule-Thompson cooling that occurs as the air expands. Typical CAES plants supply that heat through combustion of natural gas. A CAES plant, therefore, can produce the same power output as a conventional simple cycle natural-gas fired power plant but using approximately 60% less natural gas on a heat rate basis.[1]

In the 1970's and 1980's, considerable work was undertaken by the U.S. Department of Energy (DOE) and private industry evaluating various CAES options (ALLEN et al., 1985). In the U.S., this work resulted in the commissioning of a 110 MW CAES plant in Alabama in 1991. This plant stores air in an excavated salt cavern produced by solution mining. However, CAES has been considered in more widely distributed porous sedimentary rocks where water displaced during injection can provide a nearly constant hydrostatic backpressure during withdrawal. For example, advanced evaluations were conducted for a CAES facility near Des Moines, Iowa utilizing "aquifer storage" in a Mt. Simon sandstone domal structure. Unfortunately, the project was cancelled due to discovery of unsuitable hydrogeologic conditions after exploratory drilling (SCHULTE et al., 2012).

In the Pacific Northwest region east of the Cascade Mountain Range, the area is dominated by the Columbia Plateau Province (CPP). The CPP predominantly consists of a set of continental flood basalt deposits that cover over 81,000 mi^2 of portions of eastern Washington, northeastern Oregon, and western Idaho, with a total composite volume of more than 53,700 mi^3 (REIDEL et al., 2002). As shown in Figure 1, the Columbia River Basalt Group (CRBG) portion extends and is coincident with a very large fraction of the wind and fossil fuel based power generation resources in the region, as represented by their CO_2 emissions. Flood basalts fill large basins through multiple (up to several hundred) outpourings of deep mantle lavas from feeder dikes. Total composite thickness of basalt in the deepest part of these basins can exceed 4 km, with subsurface temperatures exceeding 175 °C at depth in some areas. CRBG represents a

[1] 10,830 Btu/kWh (HHV) heat rate of Frame 6FA simple cycle: 4,070 Btu/kWh heat rate of CAES plant simulated.

considerable barrier for oil and natural gas exploration in the underlying sub-basalt sediments, and potential reservoirs within these basins filled with flood basalts have not been extensively investigated as compared to typical, conventional sedimentary basins in other regions of the U.S. Only very limited data are available on deep reservoir temperatures, and especially deep aquifer hydrogeologic properties critical to any quantitative assessment of potential for CAES in the basalts and the sub-basalt sedimentary units. Perhaps that is why there have been no published studies of CAES in this region.

Recent advances in drilling technology and other geophysical methods have helped to overcome subsurface access barriers, and deep oil and gas exploration wells are beginning to fill some of the data gaps with respect to the geology and hydrogeology in flood basalt provinces. Data collected from natural gas exploration wells recently drilled in the Pacific Northwest as well as the extensive characterization work being done on the Columbia River Basalt for CO_2 sequestration pilot testing (McGrail et al., 2009) provides an opportunity for the first time to quantitatively advance CAES assessments in this unique regional geologic setting.

In addition to the CRBG, a Jurassic, Cretaceous, and Paleocene igneous and metamorphic crystalline rock basement complex underlies the CRBG. Data from deep exploratory wells show that the area extending west into the Pasco Basin has up to 15,000 ft of non-marine sedimentary and volcanogenic rocks that occur between the CRBG and the underlying crystalline basement complex. The sedimentary/volcanogenic rock sequence below the CRBG includes Eocene sedimentary rocks, fluvial sandstone and coals of the Roslyn Formation, and volcanic flows, tuff beds, and arkosic sandstones of the Eocene and Oligocene Naches Formation, and the Oligocene Ohanapecosh, Wenatchee, and Wildcat Creek Formations. These sub-basalt formations are presently the target of gas exploration activities in certain portions of the Columbia Basin. The presence of potential commercial-grade reservoirs of natural gas also suggests the potential for CAES within these sub-basalt sedimentary formations.

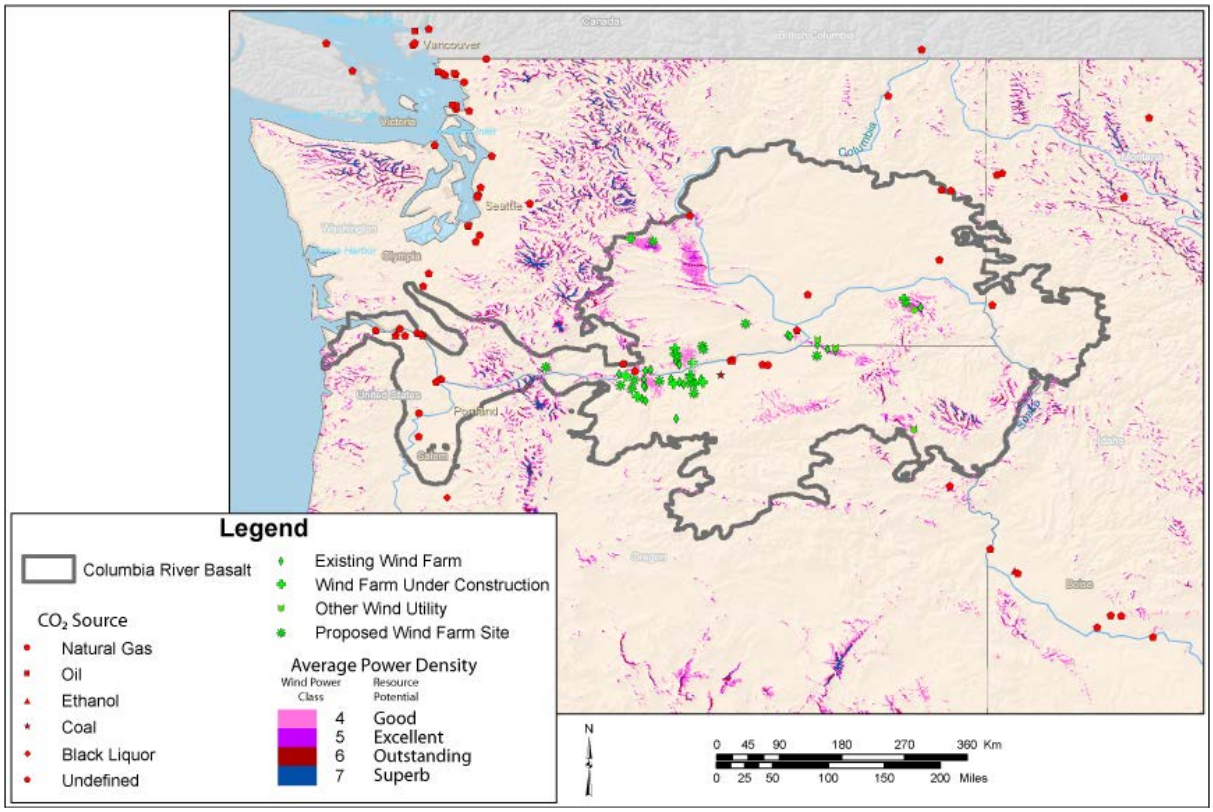

Figure 1. Map showing coincidence of wind and major thermal power station resources with Columbia River Basalt (outlined in gray) target for energy storage

1.2.2 Research Needs

Implementing CAES in flood basalts will require a considerably different approach than has been considered in previous CAES studies. CAES requires injection of significant volumes of air, 10^7 standard cubic meters (scm) or more. Accommodating that kind of volumetric storage capacity with relatively short cycle times of hours to days for load and generation balancing requires utilization of high permeability structures in the basalt (or sub-basalt sediments). This is very similar to requirements for CO_2 storage where 80 ktons or more of CO_2 would need to be injected per month from a relatively small coal or biomass fueled power plant. To accommodate those kinds of volumetric rates, PNNL has developed the following criteria for suitable injection horizons in the CRBG:

- reservoir thickness ($\geq$ 30 ft)
- reservoir permeability (k $\geq$ 500 millidarcies (mD))
- effective porosity ($\varepsilon \geq 0.1$)
- overlying low-permeability, caprock thickness ($\geq$ 100 ft; $\leq$ 10-1 microdarcies (μD)).

A hypothetical CO_2 injection scenario PNNL has developed as part of this commercial feasibility study includes use of "multiple-stacked" basalt injection reservoirs. Assuming six injection zones with average properties that are equivalent to the minimum values listed above, computer simulations indicate that over 3 ktons per day of CO_2 can be readily accommodated in a single injection well. That is

equivalent to approximately 1 x 10^6 scm of air per day, enough to operate a 250 MW CAES plant for about 30 hours. Actual air injection simulations are needed to determine whether higher volumetric rates could be accommodated in areas with known higher permeability than in this example.

Basalts are also chemically reactive reservoir rocks, and compressed air injection could potentially induce precipitation of iron oxyhydroxides and carbonate minerals that would degrade reservoir permeability over time. Recent work at PNNL has shown that treatment with sulfur compounds can coat the basalt and halt carbonate formation even when the basalt is exposed to supercritical CO_2 (SCHAEF et al., 2010). Experiments are needed exposing Columbia River Basalt to air at high pressure to determine the extent of secondary mineral formation and determine whether mitigation measures would be necessary for long-term operation.

2.0 Site Identification

2.1 Regional Suitability Analysis

Basalt flows and sub-basalt sediments in the Columbia Basin are proposed as possible reservoirs for CAES. Some of the hydrogeologic characteristics of the basalt flows in the CRBG favorable to CAES include the large areal extent and thickness of the CRBG and individual flows, lateral continuity, higher permeability zones between flows (interflow zones) for storage sandwiched between low-permeability zones to serve as caprock, structural features that may serve as geologic traps, and compressive strength properties. Some of the unfavorable characteristics may include decreasing injectivity and storage capacity with increasing depth and the potential for major faults to act as leakage pathways or boundaries to lateral movement. Figure 2 illustrates the CRBG members discussed in this study. Youngest flows are at the top of the column, oldest at the bottom. Each basalt member may consist of one or many individual flows.

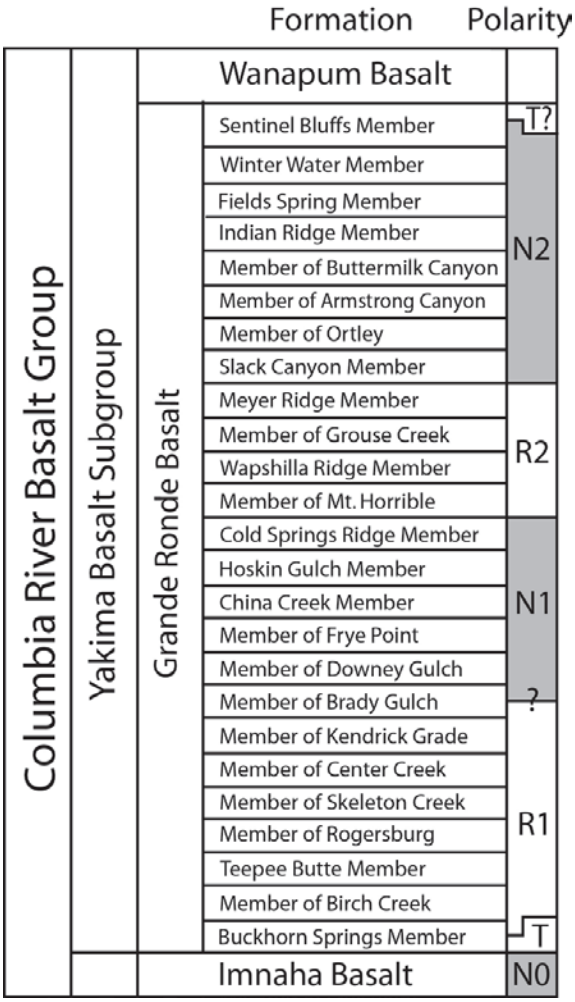

Figure 2. Stratigraphy of the Grande Ronde Basalt

Criteria were established to guide a search for possible sites within the Columbia Basin in Washington and Oregon. These criteria evolved during the site evaluation process as information was

evaluated and preliminary models were run to evaluate the effect of buoyancy in various subsurface storage scenarios. The following is a discussion of these criteria and the ultimate identification of two sites for further consideration.

Several sources of information were used to identify potential sites for CAES, including available hydrogeologic data used in the U.S. Geological Survey (USGS) Hydrology Model (BURNS et al., 2011), data found on the Oregon Department of Geology and Mineral Industries (DOGAMI) geologic data compilation webpage, and geologic and geophysical well log data available from a variety of sources, including:

- oil and gas well logs found on the Washington State Department of Natural Resources (WDNR) webpage (WDNR, 2012a)
- logs from wells drilled on the Hanford Site for the Basalt Waste Isolation Project (BWIP)
- logs from wells drilled to support natural gas storage or CO_2 sequestration
- logs for water wells available from the Washington State Department of Ecology (WADOE, 2012).

It should be noted that deep oil and natural gas exploration boreholes, basalt characterization wells on the Hanford Site, and natural gas storage and CO_2 sequestration characterization wells are referred to as deep wells here unless specifically called out. Also, recent unpublished studies provided new interpretations of basalt stratigraphy and structure. In addition to the above sources of information, geothermal data from the WDNR (2012b) and DOGAMI (2012b) webpages were used to evaluate potential sites for underground thermal energy recovery to support a no-fuel CAES option at one of the selected sites.

When possible, Geographic Information System (GIS) data from the above sources were incorporated into a single GIS map, allowing integration of data from a variety of sources into a single working environment.

The following criteria were used to narrow the search area during the site selection process. Each criterion is discussed in more detail in subsequent sections:

1. Within area covered by CRBG
2. For CAES in basalt, depth of injection reservoir must be $\geq$ 1,500 ft
3. Less than 20 miles from both natural gas pipelines and transmission lines (230 kV or greater)
4. Potential geologic traps
5. No known paths for vertical movement nearby
6. Total reservoir thickness is $\geq$ 30 ft and caprock thickness is $\geq$ 100 ft
7. Reservoir permeability (k) is $\geq$ 500 mD and effective porosity (n_e) is $\geq$ 0.1
8. May want zones with non-potable water even though compressed air would be clean
9. For geothermal energy recovery, permeable reservoir rocks with temperatures $\geq$ 150°C are needed

The following sections briefly describe the impact of each of these constraints on the site selection process used in this study.

2.1.1 Area Covered by CRBG

The CRBG covers approximately 81,000 mi^2 of the Pacific Northwest (Figure 3). Hundreds of basalt flows were erupted from fissures in eastern Washington and Oregon and western Idaho. The flows are laterally continuous across large distances, and each basalt flow commonly consists of a relatively permeable flow top overlying a dense, relatively impermeable basalt flow interior; some flows may also have a permeable flow bottom. The combination of a permeable flow bottom and an underlying basalt flow top are commonly referred to collectively as a basalt interflow zone. Sediments may be found intercalated between basalt flows where the ancestral Columbia River system and its tributaries flowed across the basalt surfaces or where lacustrine environments may have developed. The concept of using the relatively permeable zones sandwiched between impermeable zones as a sequence of potential reservoirs and caprocks has been extensively investigated for CO_2 sequestration (MCGRAIL et al., 2006; MCGRAIL et al., 2009) and natural gas storage (REIDEL et al., 2002; REIDEL et al., 2005). Existing maps of basalt extent (REIDEL et al., 1989; TOLAN et al., 1989) were used to constrain the area of investigation.

2.1.2 Depth to Basalt Reservoirs

A depth of at least 1,500 ft is desired for CAES reservoirs to maximize efficiencies in storing and retrieving compressed air. Greater depths correlate to higher storage densities; higher storage densities result in smaller plume areas for a given mass of air storage. Areas with sufficient basalt thickness were initially identified using existing geologic maps that show the areal extent and thickness of basalt flows. As shown in Figure 3, the CRBG is thickest near the center of its areal extent. Those areas along the margins of the Columbia Basin where basalt thins to less than 1,500 ft thick were removed from further consideration. Data on thickness of basalt and underlying rocks come from a limited number of deep wells (i.e., deep oil and gas exploration boreholes, basalt characterization wells on the Hanford Site, and natural gas storage and CO_2 sequestration characterization wells) scattered across the Columbia Basin (Figure 3). Detailed technical information obtained from these wells provides the most reliable means for identifying potential reservoirs. Therefore, areas with existing deep well data were selected for further review.

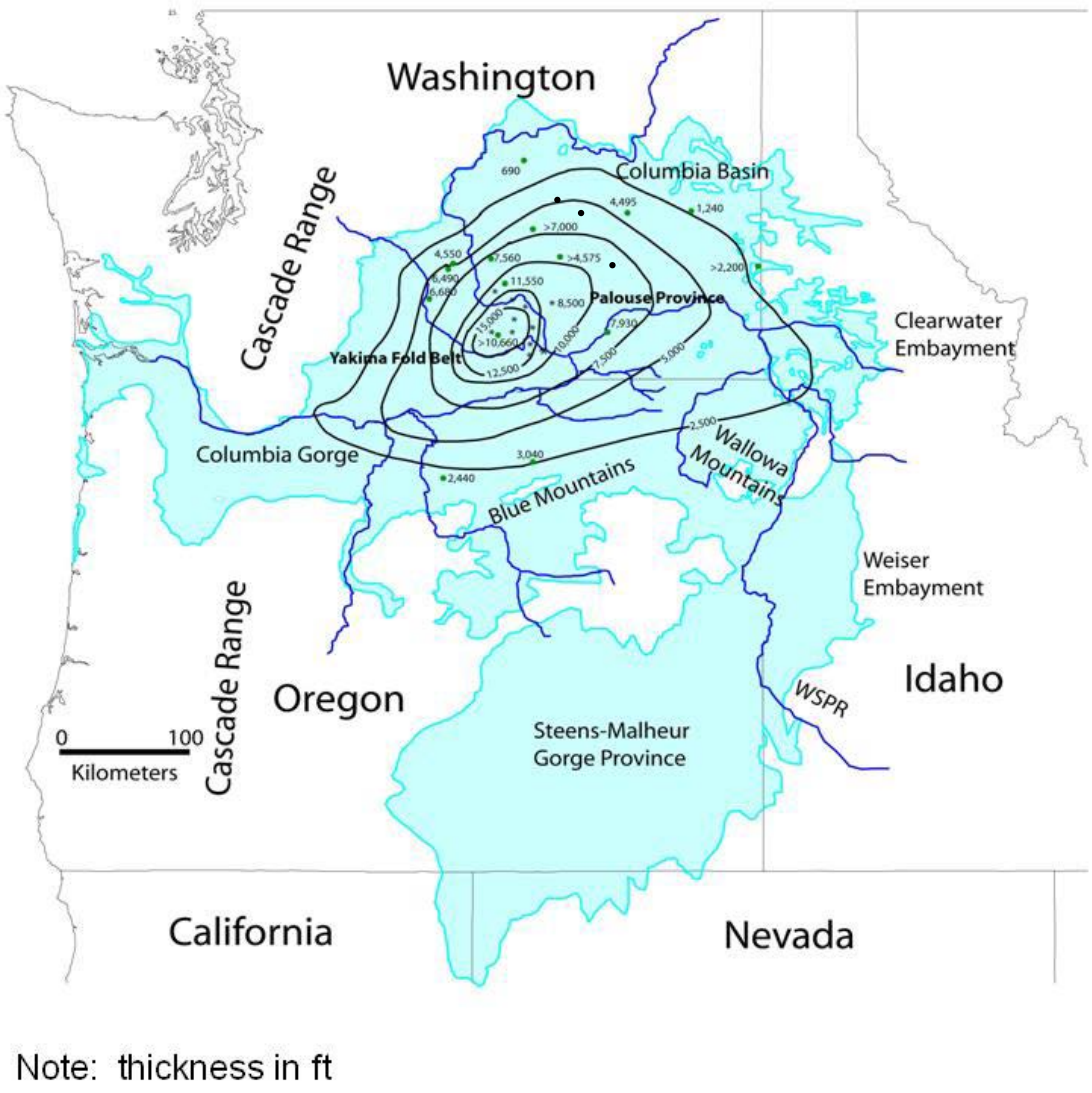

Figure 3. Location of deep boreholes and inferred thickness of Columbia River Basalt Group

2.1.3 Access to Key Infrastructure

To minimize costs associated with new grid connections and access to natural gas supply, efforts were focused on areas within 20 miles of both existing high voltage transmission (230 kV or higher) and natural gas pipelines. Figure 4 shows the location of transmission, natural gas pipelines, and power generation by type over the extent of the CRBG. A map showing distance to natural gas pipelines and transmission lines was developed to facilitate tiered prioritization of areas according to their distance to both types of infrastructure (Figure 5). Areas where natural gas pipelines and transmission lines are within 5, 10, or 20 miles of each other are shown as different colors. Most areas outside the 20-mile zone (shown as yellow in Figure 5) were not considered further while areas within the 5-mile zone (orange areas in Figure 5) were given higher preference over those farther away.

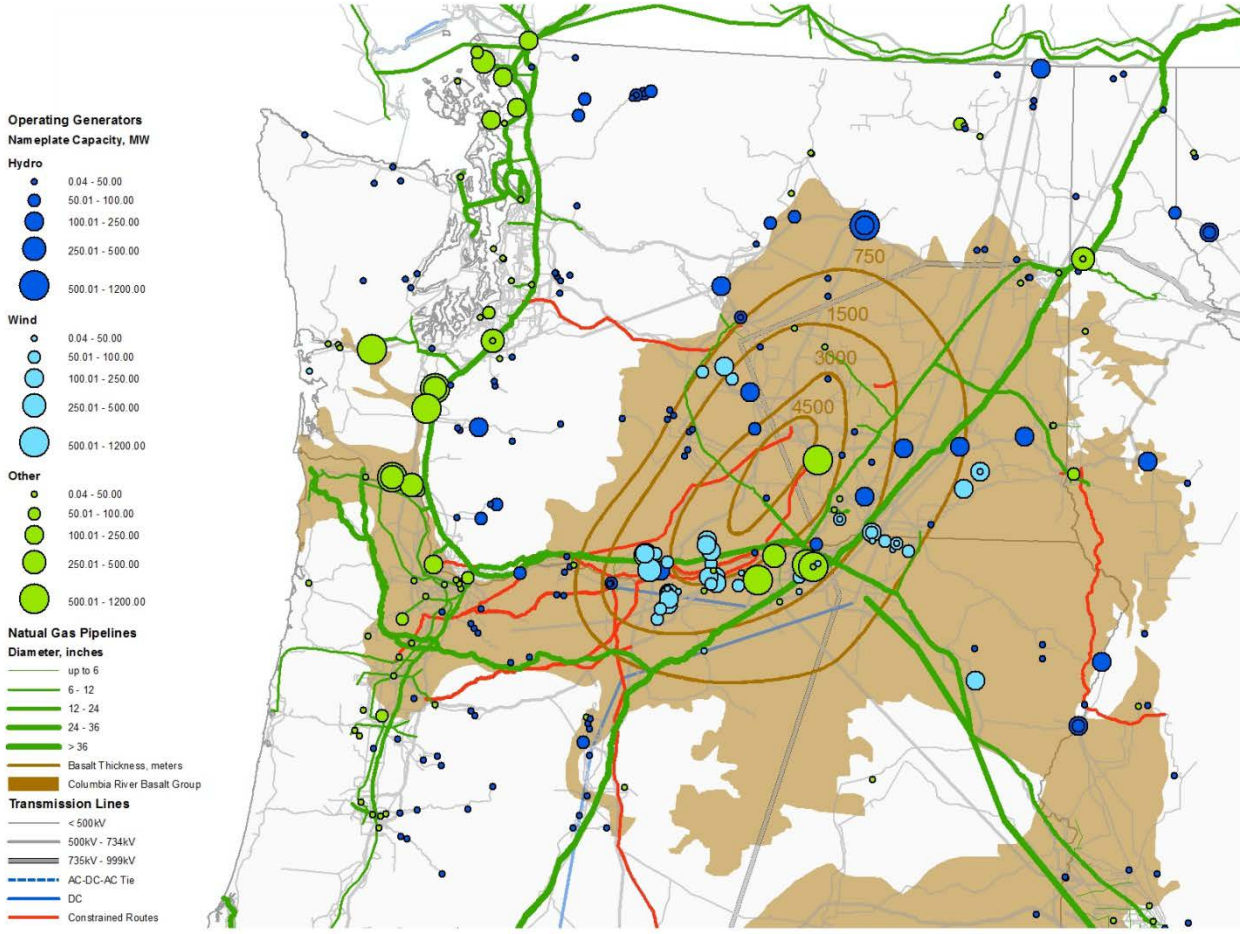

Figure 4. Key infrastructure, existing generation, and extent of the Columbia River Basalt Group in the current region of interest

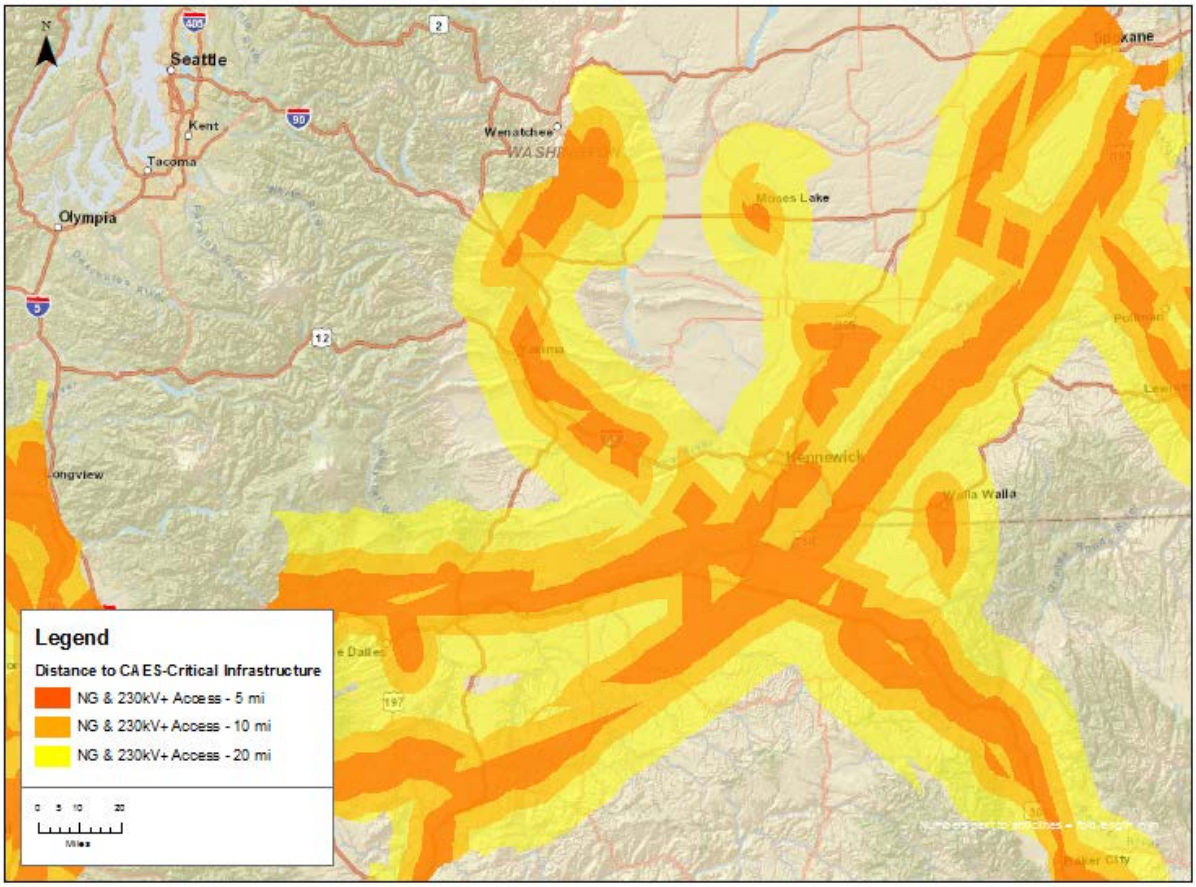

Figure 5. Map showing zones based on distance between natural gas pipelines and transmission lines carrying 230 kV or more

2.1.4 Potential geologic traps

Geologic traps are features that may help contain compressed air or heated fluids near the point of injection. Traps could be formed by rock layers folded into anticlines (rocks bent into a downward facing U) or synclines (an upward facing U), lateral changes in permeability within a rock layer, or in some cases faults that cut across layers (Figure 6).

Multi-phase simulations were run to examine the effect on stored air if layers are tilted from 0 to 5 degrees. Results of the additional modeling indicated that gas moved greater distances from the point of injection with increased tilt. For a tilt of 5 degrees, the center of injected mass moves up to 1/2 mile from the point of injection over potential storage timeframes examined.

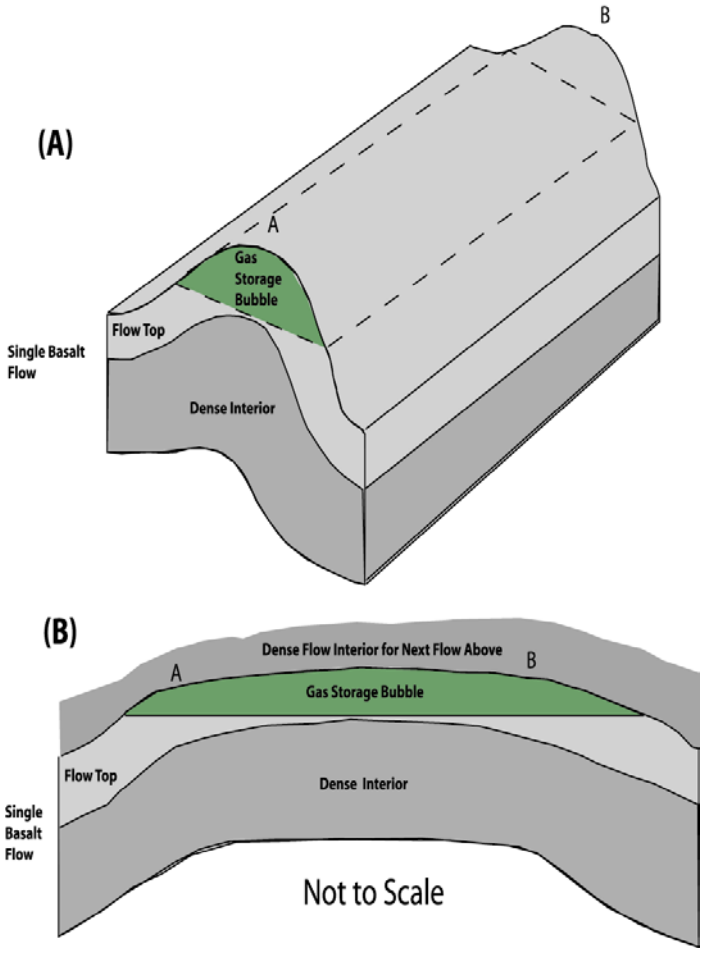

Figure 6. Example of a geologic trap in an anticline (adapted from REIDEL et al. (2002))

Using the buoyancy of the compressed air to keep it in the highest part of the reservoir beneath the caprock in anticlinal structures appears to provide the best containment scenario. In particular, geologic domes or doubly plunging anticlines, where layers dip down in all directions from a high point, could be particularly effective as a structural trap. Consequently, areas were selected that contain anticlines with a closure encompassing an area with minimum radius of approximately 5,000 ft, sufficient to store 50,000 megawatt-hours (MWh) of energy.

Major anticlines seen at the surface generally extend to the base of the basalt and may extend into the sub-basalt sedimentary rocks. Anticlines in the Columbia Basin are associated with deep through-going thrust faults that dip down beneath the anticlines. In some places, faults may provide vertical pathways for groundwater and/or natural gas movement while in other places faults inhibit lateral fluid movement. The character of any particular fault can change laterally or with depth and is often unknown.

Subsurface geologic structures such as folds and faults are known only from the integration of deep well data and detailed surface geophysical surveys. Much of the surface geophysics data are proprietary but can be purchased. For this investigation, it was not cost-effective to purchase surface geophysical data for the entire area under consideration for this project, although it may be reasonable to explore purchase of specific data sets after a specific site or sites are selected. Some geologic and hydraulic data

from deep exploration and characterization wells are publicly available from WDNR. These data indicate the presence and character (i.e., water-bearing or impermeable) of any faulting that may have been encountered within the wells.

Review of potential geologic traps focused on known anticlines and potential dome structures along those anticlines lying within the 20-mile zone shown in Figure 5. The location of deep wells with available hydrogeologic information is also shown in Figure 7. Where possible, areas near major faults were avoided because of lack of data on the characteristics of the fault system.

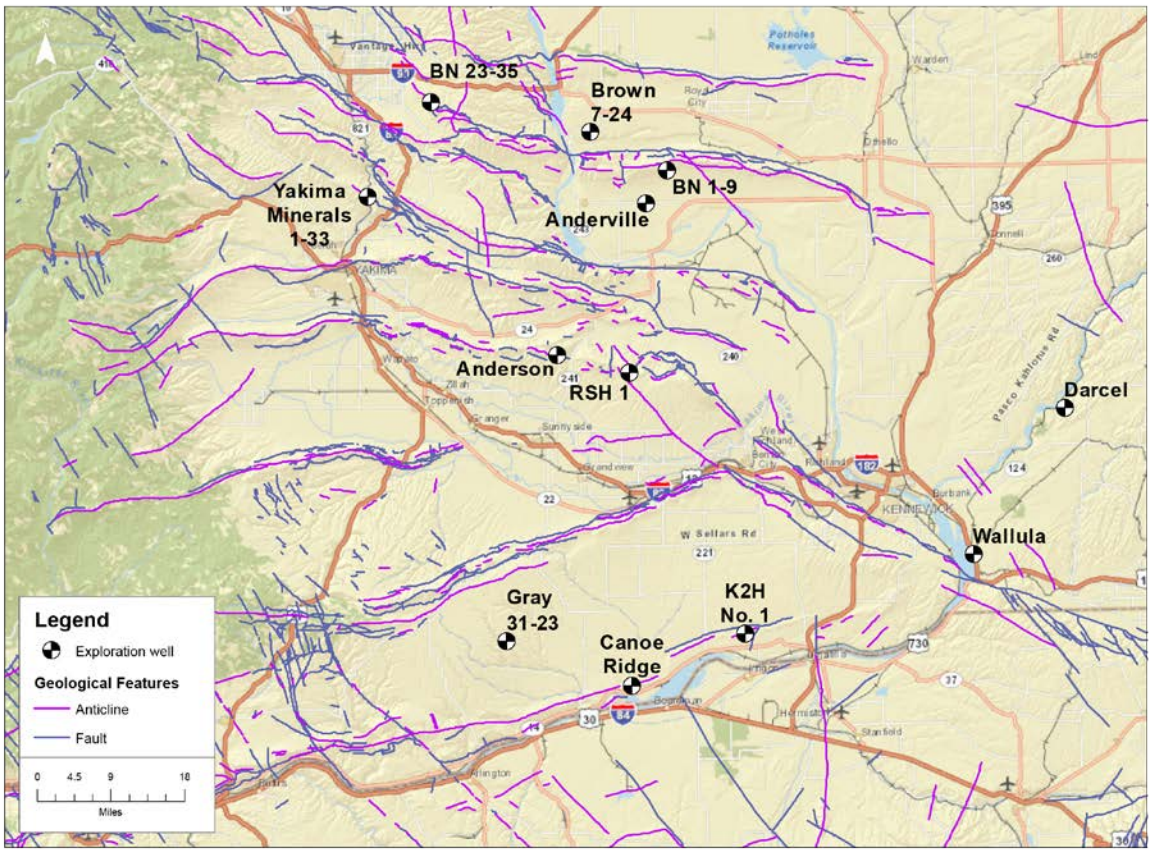

Figure 7. Location of deep exploration and characterization wells providing data on the deep basalt and sub-basalt across the primary area of investigation

2.1.5 Reservoir and Caprock Thickness

Data on thickness of individual basalt flow tops and flow interiors at depths greater than 1,500 ft are sparse because relatively few water wells penetrate to that depth. Informal geologic descriptions of rocks encountered during drilling of deep water wells are usually reported by drillers, and typically drillers' reports do not provide adequate technical information to identify specific basalt flows or flow components.

Geologic log descriptions available for wells drilled for BWIP on and around the Hanford Site, the characterization wells for natural gas storage and exploration near Umatilla, Oregon, and the CO_2 sequestration test well near Wallula, Washington, provide excellent control on basalt flow geochemistry

and flow contacts. Downhole geophysical logs and mud logs from the deep exploration wells provide additional information on the thickness of flows and flow components. Geochemistry for many of the basalt flows was used to identify specific flows.

2.1.6 Reservoir Permeability and Effective Porosity

Wells drilled for BWIP and the natural gas storage and CO_2 sequestration projects provide hydrologic test data from discrete basalt flow tops and flow interiors rather than testing multiple water-bearing zones, which is typical of water wells for agricultural or drinking water use. Oil and gas exploration wells rarely tested zones within the basalt unless there was a show of gas or oil. An analysis of available quality data obtained from hydrologic tests performed in flow tops within the Grand Ronde Basalt suggests that transmissivity ranges across 8 orders-of-magnitude with a geometric mean of 2.03 ft^2 per day. The range in transmissivity appears to be randomly distributed and there does not seem to be a categorical decrease in transmissivity with depth. The statistical analysis suggests there is a 20% probability that any individual Grande Ronde Basalt flow encountered in a well will have a transmissivity of 36 ft^2 per day, which is equivalent to the characteristics desired for a CAES facility (i.e., permeability of 500 mD for an interval thickness of 30 ft with a hydraulic conductivity of 1.2 ft per day).

2.1.7 Non-potable Water in Reservoir

The current concept for a CAES facility will store compressed atmospheric air. To be conservative in site selection, only those areas where Grande Ronde Basalt flows are thought likely to have high chloride and fluoride content exceeding drinking water standards were considered further. REIDEL et al. (2002) examined areas within the Columbia Basin suitable for natural gas storage within CRBG flows. Criteria for natural gas storage are similar to those for compressed air storage and include requirements for non-potable water in potential reservoir horizons. Figure 8 shows their interpretation of favorable and less favorable areas for natural gas storage in CRBG flows.

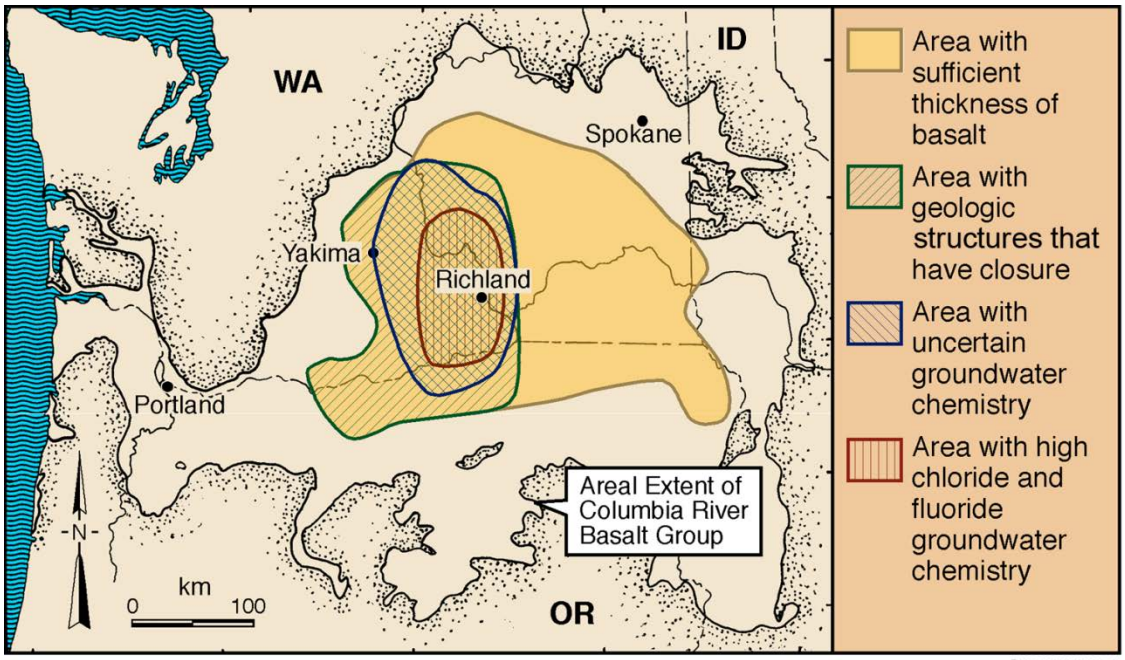

Figure 8. Generalized area of high chloride and fluoride in groundwater in the Grande Ronde Basalt (REIDEL et al., 2002)

2.1.8 Geothermal Energy Recovery Potential

To support a no-fuel CAES option, locations where moderate temperature water ≥150°C could be recovered were considered. Quality downhole temperature logs are available from a few deep wells while only bottom-hole temperatures are available for other wells. Temperature gradients were calculated for each well and used to estimate the depth below ground surface required to reach 150°C. Depths ranged from 8,200 ft to more than19,000 ft below ground surface. Rocks at these depths are predicted to be in sub-basalt formations.

The only wells that have intersected the entire basalt section are the deep oil and gas exploration wells. In the western portion of the Columbia Basin, sub-basalt formations are dominated by volcanic and volcaniclastic rocks, while the basalt in the eastern portion of the Basin is underlain by granitic and metamorphic basement rocks. Rivers draining toward the middle of the Basin deposited sediments ranging in size from mud to conglomerates. These sub-basalt sedimentary units may include the Wenatchee, Ohanapecosh, Roslyn, Teanaway, and Swauk Formations (REIDEL et al., 2002; WILSON et al., 2008).

2.1.9 Site Selection

As data were collected in a geologic information system, it quickly became evident that the only data available for areas where basalt depths are 1,500 ft or more that also meet the criteria for distance to infrastructure, geologic traps, and non-potable water come from the deep exploration wells and the natural gas storage and CO_2 sequestration characterization wells. Numerous wells on the Hanford Site meet most of the criteria for CAES but are too far from natural gas pipelines, and nothing is known of the sub-basalt rocks in that area. Those wells shown in Figure 9 are thought to have potential reservoirs in both the

basalt and sub-basalt rocks based on gas shows, groundwater inflow, and limited hydraulic testing. It may be possible to re-enter and use the deep oil and gas wells for a CAES facility since some of the wells, such as RSH-1, are still open over much of their depth. More detailed data from these wells and supporting surface geophysics also may be available for purchase and could be analyzed to better determine the suitability of a particular site.

Four zones of interest were identified based on their geology, and a fifth zone was selected based on proximity to infrastructure and the presence of a natural gas power plant (Figure 9). Potential sites are labeled from north to south without any preference inferred by the labeling.

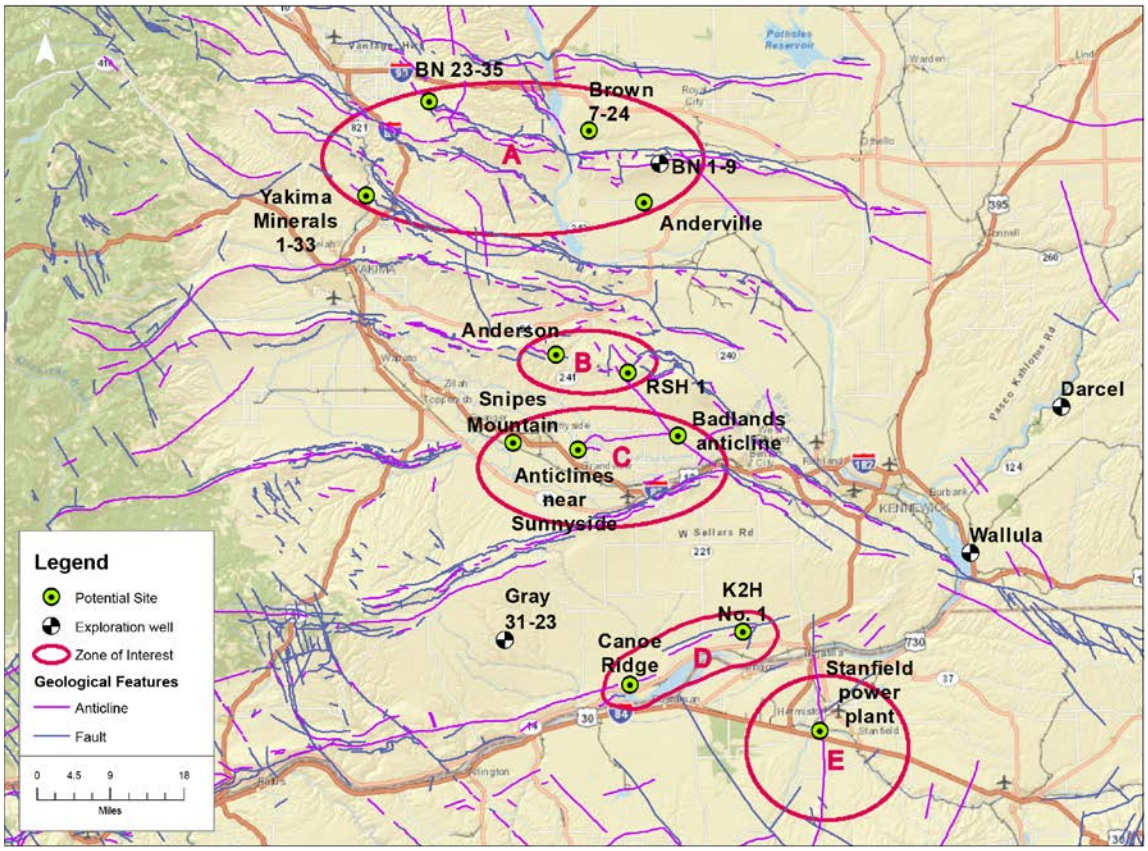

Figure 9. Location of deep exploration wells and five potential sites

Zone A

This zone covers a large area between Ellensburg and Yakima, Washington, that contains multiple large anticlines and several abandoned deep exploration wells that encountered shows of gas in sub-basalt formations and in some cases in the deeper basalt interflow zones. There are intervals presumed to be suitable for CAES reservoirs in basalt interflow zones and potential reservoir rocks in the sub-basalt formations with temperatures in excess of 150°C that could be used for a geothermal source based on shows of gas (Figure 10). The gas exploration wells, in addition to providing important data on the reservoirs present at these locations, may also provide an opportunity for re-entering the wells to save on construction costs.

As shown in Figure 11, although the eastern portion of Zone A is more than 20 miles away from gas pipelines, the western portion is generally within 10 miles of both gas and power. There several large land parcels (including large federal- and state-owned parcels) that might simplify surface and subsurface rights negotiations. The anticlines are large in this area, providing options for plant capacity expansion if needed. Disadvantages to this zone are the rugged terrain, depth to temperatures ≥150°C predicted at greater than 12,000 ft. Also, upon detailed investigation of natural gas supply, the existing radial gas line to the west of the Yakima Minerals well was found to be capacity constrained, which would require significant expansion of the pipeline from the main line along the Columbia River to supply gas for a conventional CAES plant.

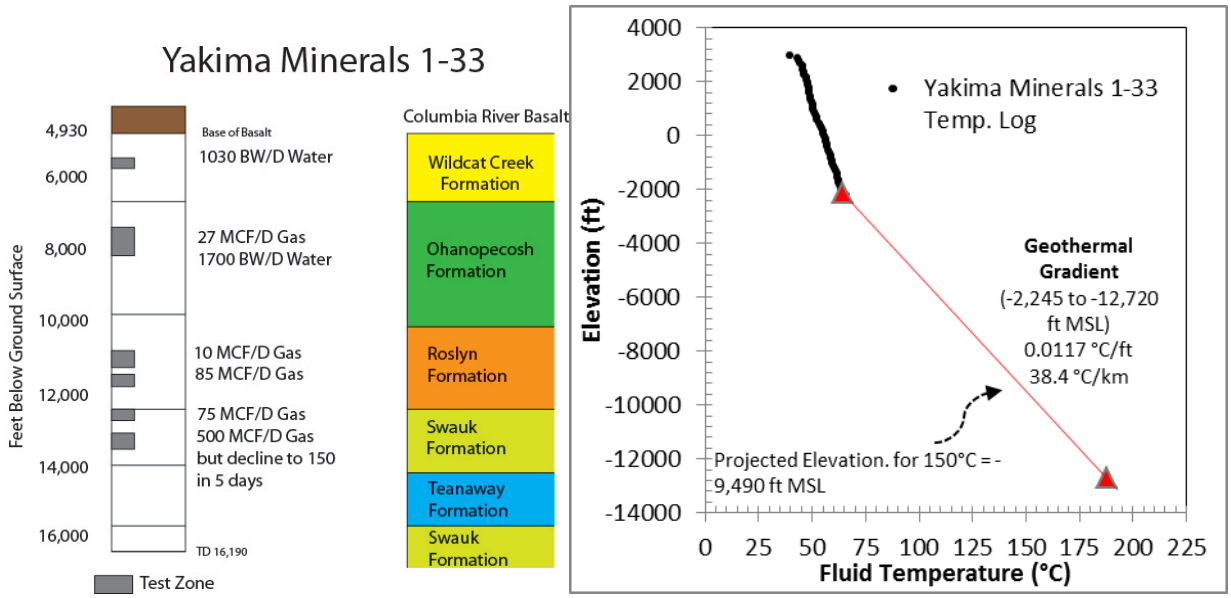

Figure 10. Stratigraphic and temperature data for the Yakima Minerals 1-33 well indicate potential reservoirs for both CAES and geothermal source development

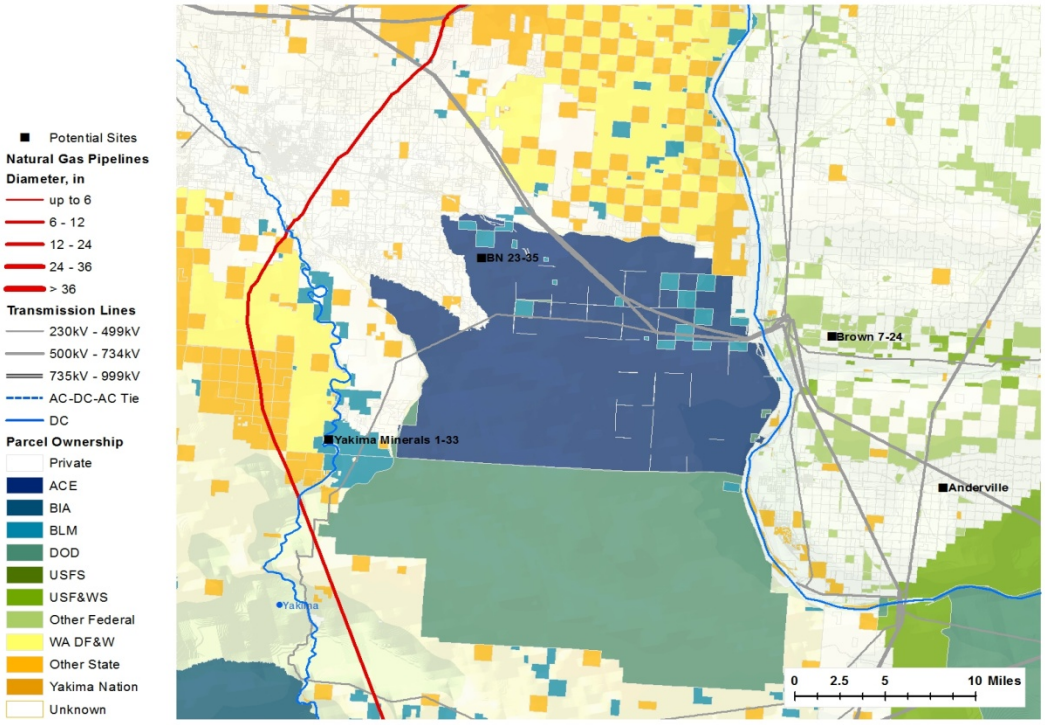

Figure 11. The existing wells within Zone A are largely located within a short distance of high voltage electricity transmission, but only the Yakima Minerals well is near a natural gas pipeline, which was found to be capacity constrained

Zone B

This is an area east of Toppenish, Washington, that is centered near two gas exploration wells. The zone contains several major and minor anticlines that could provide geologic structural traps (Figure 12). Hydraulic test data from RSH-1 are available for select interflow and dense interior zones (GEPHART et al., 1979). Both deep exploration wells are located near the center of the Columbia Basin, where the basalt is over 13,000 ft thick, and are on large blocks owned by a single landowner, which may simplify land use discussions (Figure 13). The thicker basalt section offers more potential interflow zones for possible CAES reservoirs. Temperatures $\geq$ 150°C are predicted at depths of between 10,000 and 13,000 ft. Sub-basalt volcaniclastics of the Roslyn Formation may provide suitable geothermal reservoirs. The RSH-1 well is still open to a depth of more than 9,000 ft, which could potentially be re-entered at a minimal cost and used as part of the facility.

While both wells are within 4 miles of transmission lines, they are more distant from the natural gas pipeline. Although considerably closer to the main pipeline along the Columbia River, this is the same radial supply line as discussed in Zone A, and would require significant expansion if the final plant configuration were larger than 300 MW.

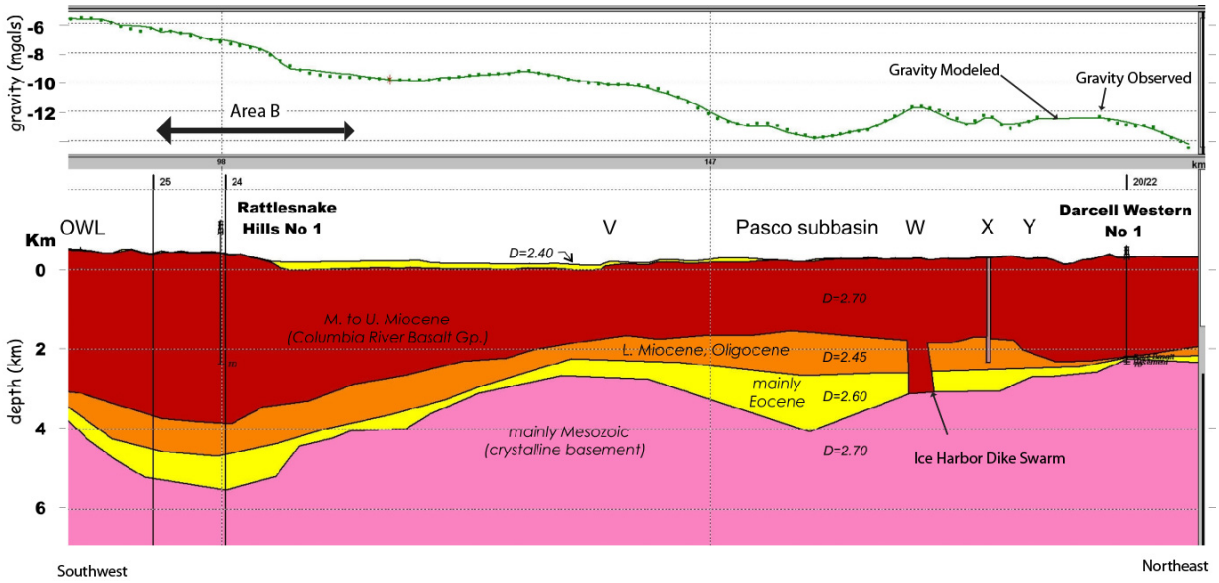

Figure 12. Regional cross section (taken from an unpublished PNNL report) with Zone B noted ("Area B")

Figure 13. Existing infrastructure and land ownership by type for Zone B

Zone C

This is an area near Sunnyside, Washington, that contains several doubly plunging anticlines that could provide good closure as geologic structural traps. There are no deep exploration wells near or within this zone, but the anticlines are within 15 miles of the Anderson and RSH-1 deep gas wells in Zone B and the stratigraphy and thickness of the formation are expected to be similar. These doubly plunging anticlines are extensions of larger, major anticlines and are therefore thought to extend some distance into the subsurface, although their character may change with depth. The two westernmost potential sites are located within 5 to 10 miles of gas and power lines, while the Badlands anticline is between 10 and 20 miles from infrastructure. Disadvantages to sites within this zone of interest are the lack of site-specific knowledge of characteristics of the basalt section, character of the sub-basalt formations, and structural character of the anticlines with depth. Additionally, land parcels are generally smaller, which may add complexity to land use negotiations.

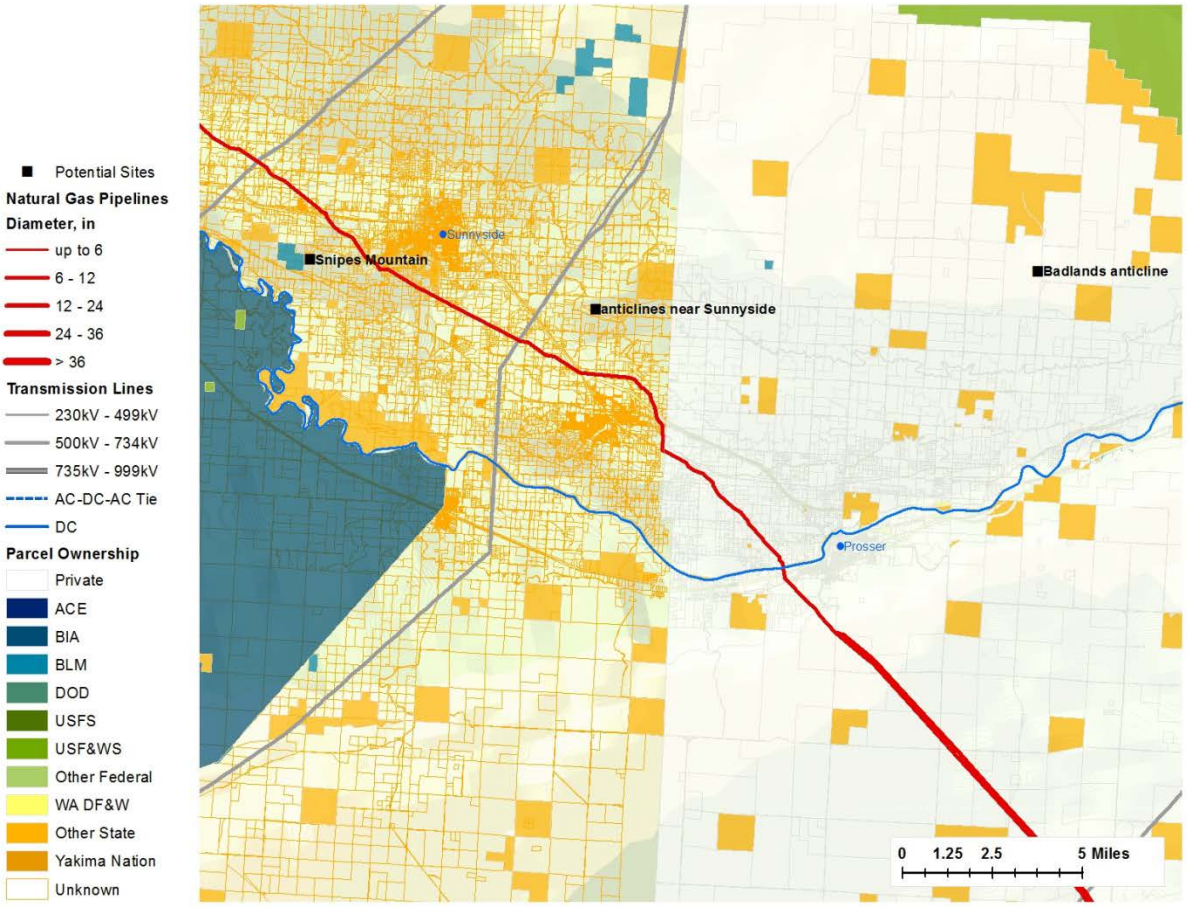

Figure 14. Existing infrastructure and land ownership for Zone C

Zone D

This zone lies north of the Columbia River and Boardman, Oregon, along the extension of the major Columbia Hills anticline. In this area, several smaller amplitude doubly plunging anticlines could provide good closure as structural traps. The zone is within 2 miles of both gas and power lines and is on large parcels of land, which may simplify land use negotiations. There are several relatively shallow natural

gas storage characterization wells close by that were drilled to depths of 3,500 to 3,800 ft, and it may be possible to re-enter these wells for future use. Some permeable interflow zones in the basalt were tested and some of those data are publicly available. In this area, the base of basalt is predicted to be at a depth of 12,000 ft or more. Ancestral Columbia River sediments may also occur in sub-basalt formations, but no deep wells have been drilled in the area to provide stratigraphic detail. Disadvantages of this area of interest are the lack of knowledge at depths greater than 3,800 ft and inadequate data on some of the key permeable zones important for a CAES plant.

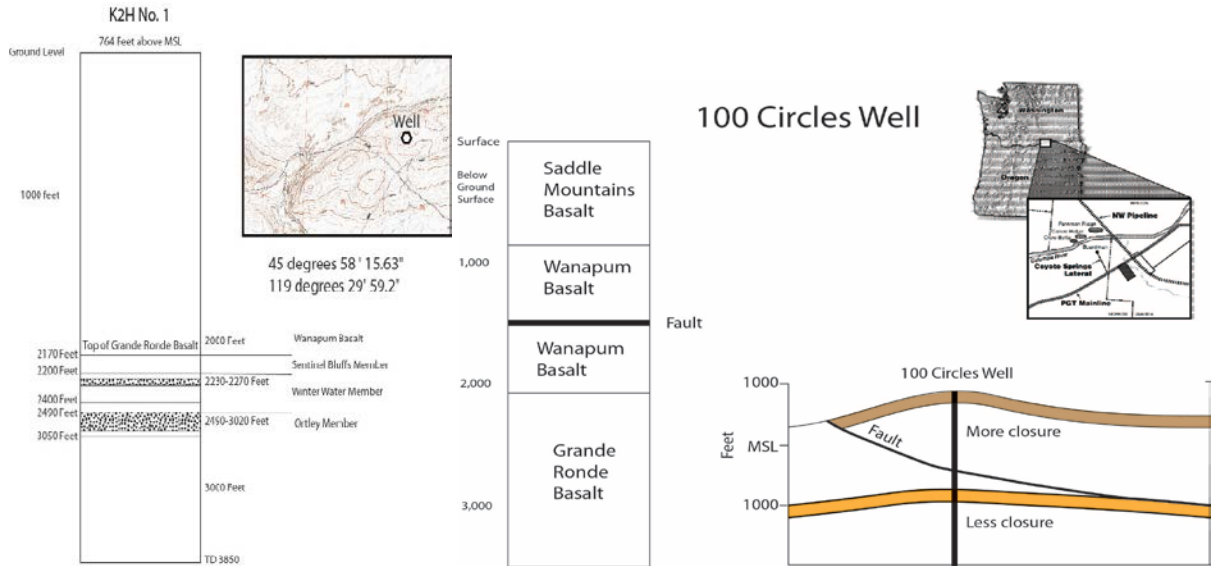

Figure 15. Stratigraphy for K2H-1 and 100 Circles (Canoe Ridge) wells

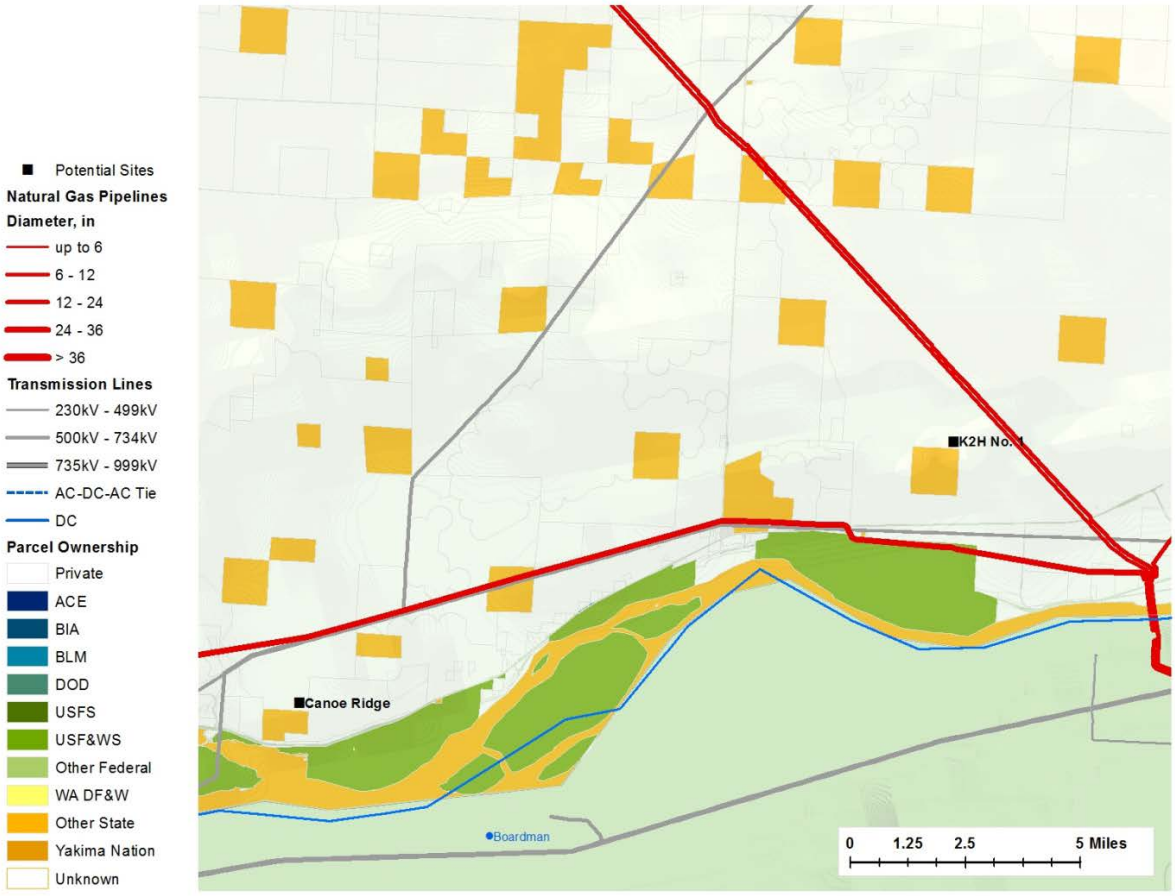

Figure 16. Existing infrastructure and land ownership for Zone D. Note the large contiguous parcel ownership and the excellent proximity to high voltage transmission and the natural gas pipeline running west along the river.

Zone E

Zone E was primarily selected based on its proximity to existing power and gas lines near Hermiston, Oregon. The zone lies within a large syncline along a small amplitude feature that is mapped as an anticline in Oregon but that corresponds to a mapped fault in Washington. Sub-basalt geology within the zone of interest is unknown but may consist of ancestral Columbia River sediments. The basalt section is predicted to be about 7,500 ft thick in this area.

Area of Interest Downselection

In the process of evaluating all five zones of interest, two were identified as having the highest priority for more detailed CAES plant siting study: Zone A and Zone D. Within Zone A, the area near the Yakima Minerals well was chosen for more detailed modeling, as was the area near the Enstor well (also known as the K2H-1 well) within Zone D.

While Zone A has favorable geologic and other conditions for a CAES plant, there is no natural gas availability without costly expansion of the existing pipeline infrastructure. Although pipeline construction costs would be expensive for this option, due to the strong potential for compressed air and

thermal energy recovery, this area was selected for evaluation of a no-fuel hybrid CAES/geothermal plant option, which is described in more detail in Section 3.5.

The Yakima Minerals well in Zone A was used to model both CAES and geothermal heat recovery in sub-basalt sediments. This well is located at the bottom of the scenic and narrow Yakima River canyon, which could prove problematic for facility siting. Air injection simulation work used depths based on an injection well location at the top of the adjacent ridge along the same anticline, 1,500 ft above the canyon bottom. Sub-basalt rocks encountered at a depth of nearly 6,400 feet below the canyon bottom include tuffs, shales, and fluvial sands and sandstones. Caprocks are provided by the less permeable portions of each basalt flow and by the shales and some tuffs in the sub-basalt formations. The well is situated along the axis of an anticline approximately 34,000 ft long by 14,000 ft wide that extends to the northwest and southeast of the well site and is cut on the southern limb by a thrust fault, repeating part of the basalt section. Information on how this anticline and related fault(s) changes with depth is not publicly available, but shows of gas at multiple depths in sub-basalt formations indicate the presence of geologic traps. Because much of the information at depth is proprietary, assumptions were made about conditions at depth that are used in the detailed modeling. Assumptions include a hydrostatic gradient of 0.433 psi/ft for fresh water and a thermal gradient of 0.02°F/ft, reservoir porosity of 10% and a hydraulic conductivity of 0.48 ft per day, overlain by a caprock with a porosity of 0.05% and hydraulic conductivity of 2.7×10^{-4} ft per day.

The Enstor (K2H-1) well is the basis for detailed modeling for CAES at the Columbia Hills site in Zone D, which included evaluation of a conventional CAES plant using a natural gas fired combustion turbine and turbo-expander train for power generation. The well reached a depth of 3,851 ft below ground surface; this is above the sub-basalt sediments that are estimated to be found approximately 10,000 ft below ground surface. The relatively small secondary anticlines on the larger Columbia Hills anticline form potential traps; the anticline into which the Enstor well is drilled is approximately 18,000 ft long by 3,900 ft wide. Drill logs indicate several water-bearing zones within the basalt. The model uses two of these zones and two others at greater depths based on data from other wells in the Pasco Basin. Actual data on conditions at depth are very sparse. Consequently, modeling used the same assumptions for hydrostatic and temperature gradients used for the model of Zone A. Caprock porosity and hydraulic conductivity (0.001 ft per day) were assumed to be the same for each of the four zones modeled. A porosity of 10% was used for all four reservoir layers in the model while hydraulic conductivity was set to either 1 or 3 ft per day based on drilling information.

Air injection and recovery simulations at both site locations, and water injection/recovery simulations for the Yakima Minerals site, are discussed in greater detail in the next section. Results from these simulations were then used to configure specific plant designs for each site.

3.0 Subsurface Modeling and Experimental Research

A series of simulations were performed to determine the technical feasibility of CAES at Zone A and Zone D. These simulations were performed using STOMP (Subsurface Transport Over Multiple Phases), a multiphase, nonisothermal subsurface flow simulator. STOMP is able to accurately simulate two-phase flow of water and a variety of gases, including air, under the high pressure and temperature conditions found in deep subsurface formations. First, a series of scoping simulations were performed in hypothetical permeable basalt flow tops. Then, a series of simulations were performed at two potential CAES sites, designated as Columbia Hills (Zone D) and Yakima Minerals (Zone A).

3.1 STOMP Simulator

The simulations conducted for this investigation were executed with the STOMP-WAE (water, air, energy) simulator. Partial differential conservation equations for fluid mass and energy comprise the fundamental equations for STOMP-WAE. Coefficients within the fundamental equations are related to the primary variables through a set of constitutive relations. The conservation equations for fluid mass and energy are solved simultaneously. The fundamental coupled flow equations are solved following an integral volume finite-difference approach with the nonlinearities in the discretized equations resolved through Newton-Raphson iteration. The dominant nonlinear functions within the STOMP simulator are the relative permeability-saturation-capillary pressure (k-s-p) relations. The STOMP simulator allows the user to specify these relations through a large variety of popular and classic functions. Two-phase (gas-aqueous) k-s-p relations can be specified with hysteretic or nonhysteretic functions or nonhysteretic tabular data. Two-phase k-s-p relations span both saturated and unsaturated conditions. The aqueous phase is assumed to never completely disappear through extensions to the s-p function below the residual saturation and a vapor pressure-lowering scheme.

A simple pressure-controlled well model was used to simulate the injection or extraction of air from the reservoir. The well model is a source/sink term that extends over several cells in the model, representing the screened interval of the well in the reservoir. The pressure at the well screen is specified, and the injection or extraction rate is calculated. The injection/extraction rate is proportional to the pressure difference between the well and the formation, the permeability of the formation, the density of the fluid, and the area of the well screen.

3.2 Scoping Simulations

Simulations of CAES in a hypothetical basalt reservoir with no vertical dip were developed to aid in site selection. First, simulations of air injection into a 30-ft-thick basalt layer at a depth of 3,000 ft were conducted. The formation was assumed to have a porosity of 10% and a permeability of 0.5 darcies. A freshwater hydraulic gradient of 0.433 psi/ft and a thermal gradient of 0.02°F/ft were assumed. Simulations for both a closed and open outer boundary were conducted. Given a compressor air injection rate of 50 kg/s, injections were run for periods of 4.3, 14.3, and 71.6 days, resulting in air plumes with radii of 2, 4, and > 7 km (Figure 17).

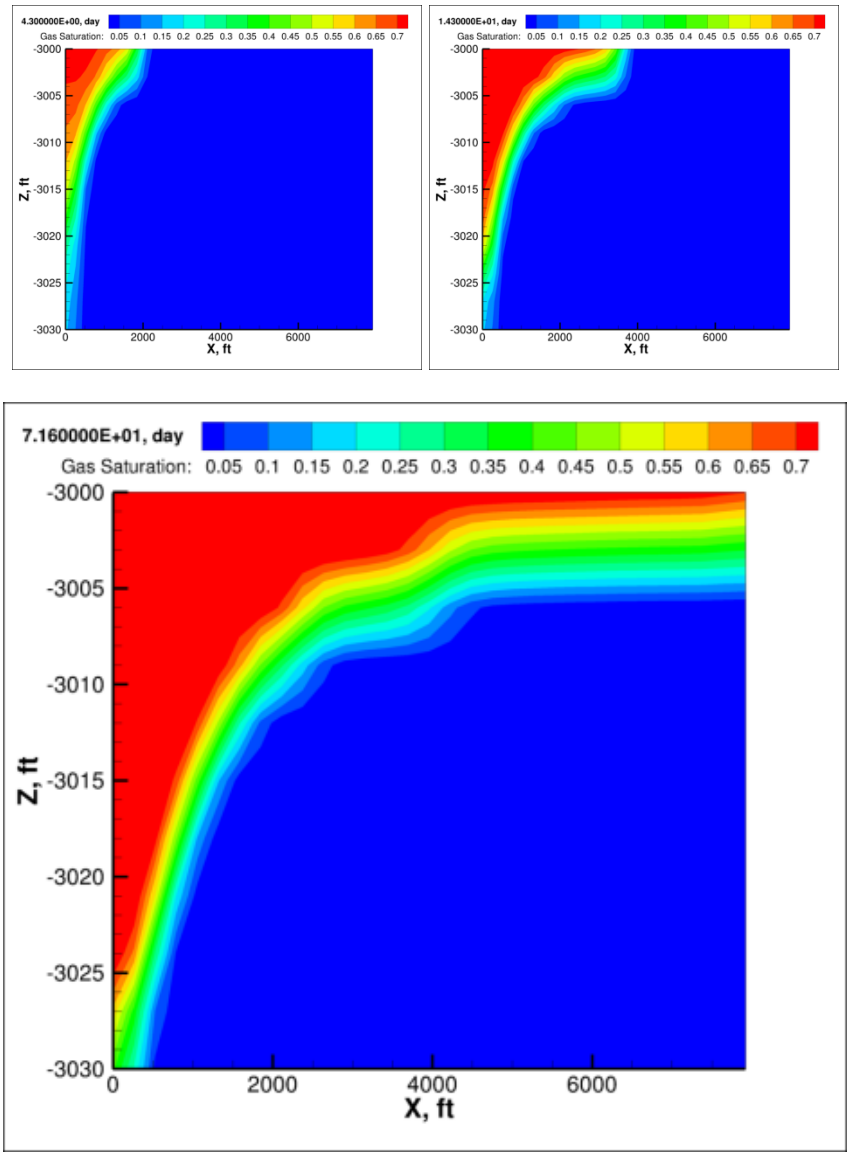

Figure 17. Plume radii for air injection with a closed outer boundary at 4.3 days (top left), 14.3 days (top right) and 71.6 days (bottom)

Next, simulations were conducted to assess how much air could be removed at a withdrawal rate of 50 kg/s before the well would begin to pull water. For the best performance, two wells were required. The injection well was assumed to be screened across the entire formation depth to avoid exceeding the fracture pressure of the formation. The withdrawal well opening was placed at the very top of the formation to take advantage of buoyant rise of the injected air. In general, 40% to 45% of the injected air mass could be removed (Figure 18) before water breakthrough occurred. Due to the low recovery percentages and the need for two wells to implement injection and extraction (thus increasing capital costs), these simulations strongly suggested that anticlinal structures should be the focus of site selection.

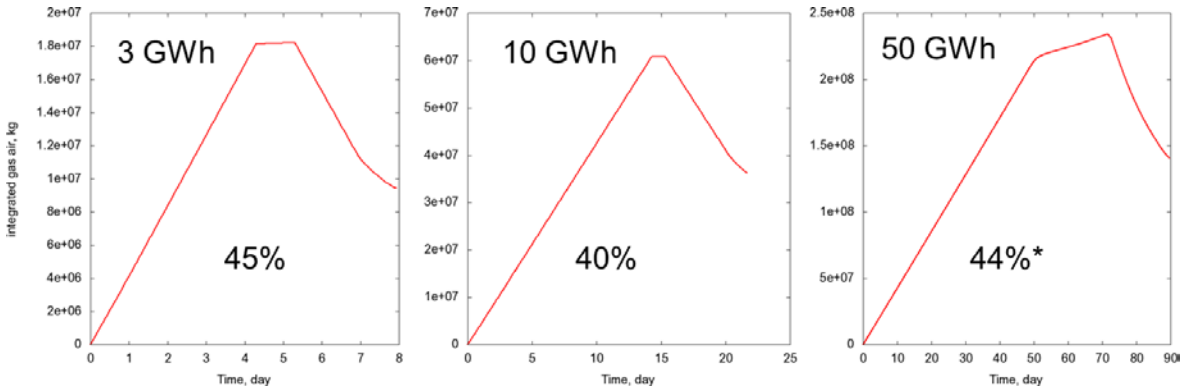

Figure 18. Simulation of one injection-withdrawal cycle at 50 kg/s for various sizes of air storage. *Over-estimate due to mass loss across outer boundary.

The effect of formation dip on injected air plume migration also was considered. Three-dimensional air injection simulations were conducted for formation dips of 0 to 5 degrees. Air was injected for 14.3 days at a rate of 50 kg/s and then the plume allowed to drift for 3 months. The shape of the plume for the case of 5 degrees of tilt is shown in Figure 19. The movement of the center of mass for all cases is summarized in Figure 20. The center of mass of the plume migrates up to 1/2 mile for the 5-degree tilt case. Results suggest that low-dip anticlinal structures would be the most favorable option for air injection in deep basalts.

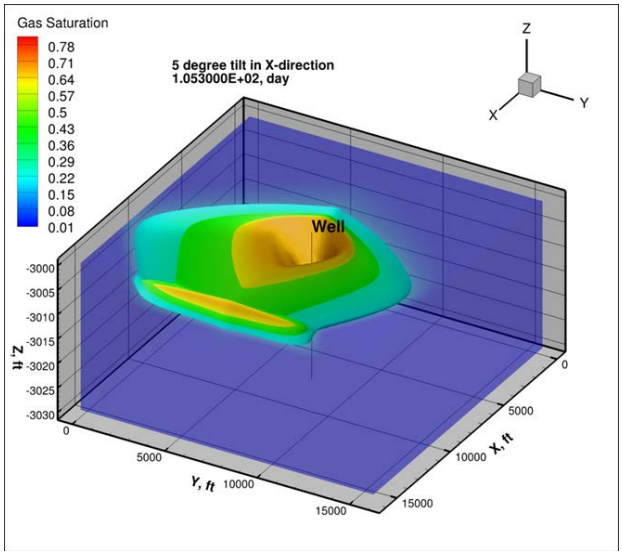

Figure 19. Air plume after 3 months of drift with 5-degree formation dip

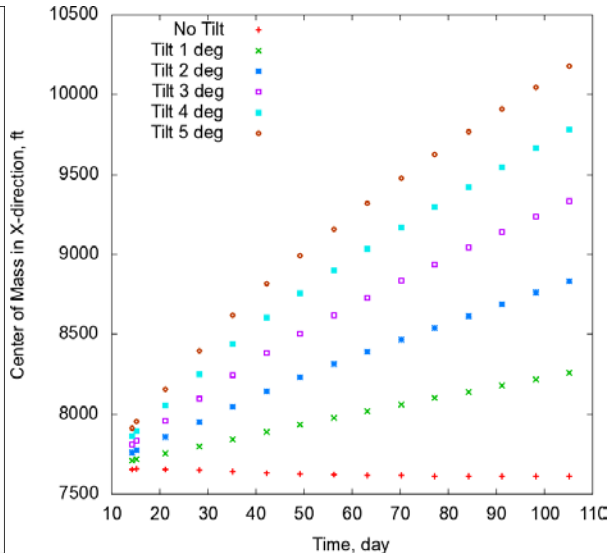

Figure 20. Drift of center of mass of air plume over 3-month period

3.3 Geologic Model Development

Hydrogeologic conceptual models were developed to support numerical flow modeling for two potential CAES sites, referred to as the Columbia Hills and Yakima Minerals sites. The potential storage reservoirs are situated within permeable basalt flow tops at the Columbia Hills site; and in both permeable

basalt flow tops and sub-basalt sandstone at the Yakima Minerals site. Caprock at both sites was assumed to be formed by multiple dense basalt flow interiors that overlie the selected reservoir horizons.

Both potential storage sites were formed by uplift and occur within folded anticlinal structures. Detailed subsurface structural information pertaining to these geologic features is only available for one or two borehole locations in proximity to the sites. The general surface topography, however, reflects the shape and orientation of the underlying structures, but has been altered by erosion of the basalt layers and deposition of surficial sediments in lower topographic areas.

For each site, a 10-m resolution digital elevation model was obtained from the USGS National Elevation Dataset (USGS, 2006). Based on exposure of basalt layers located on the upper portion of the anticline, where they were not covered by sediment, the degree of erosion from the top of the digital elevation model anticline was estimated and a "non-eroded" surface was reconstructed to represent the shape of the deeper basalt flows. The deeply buried basalt flows were emplaced as relatively flat layers and were generally not subjected to significant erosion. This "non-eroded" basalt surface was projected downward to the correct depth of the target caprock and reservoir layers to represent the shape of those layers in the model. Each of the model layers, therefore, mimics the reconstructed basalt surface. The model for each site was also aligned with the anticline axis to allow for more efficient numerical flow modeling.

Figure 21 shows the surface topography and the reconstructed elevation of the surface at the top of the permeable flow top found in the Sentinel Bluffs Member at the Columbia Hills site. Depths for the reservoir and caprock layers at each site were obtained from well logs from the existing boreholes, the 100 Circles well for the Columbia Hills site and the Yakima Minerals well for the Yakima Minerals site. The reservoir and caprock thickness are fixed/equal to the value occurring at the existing well. The Petrel geologic modeling software package was used to construct the three-dimensional sequence of reservoir and caprock layers.

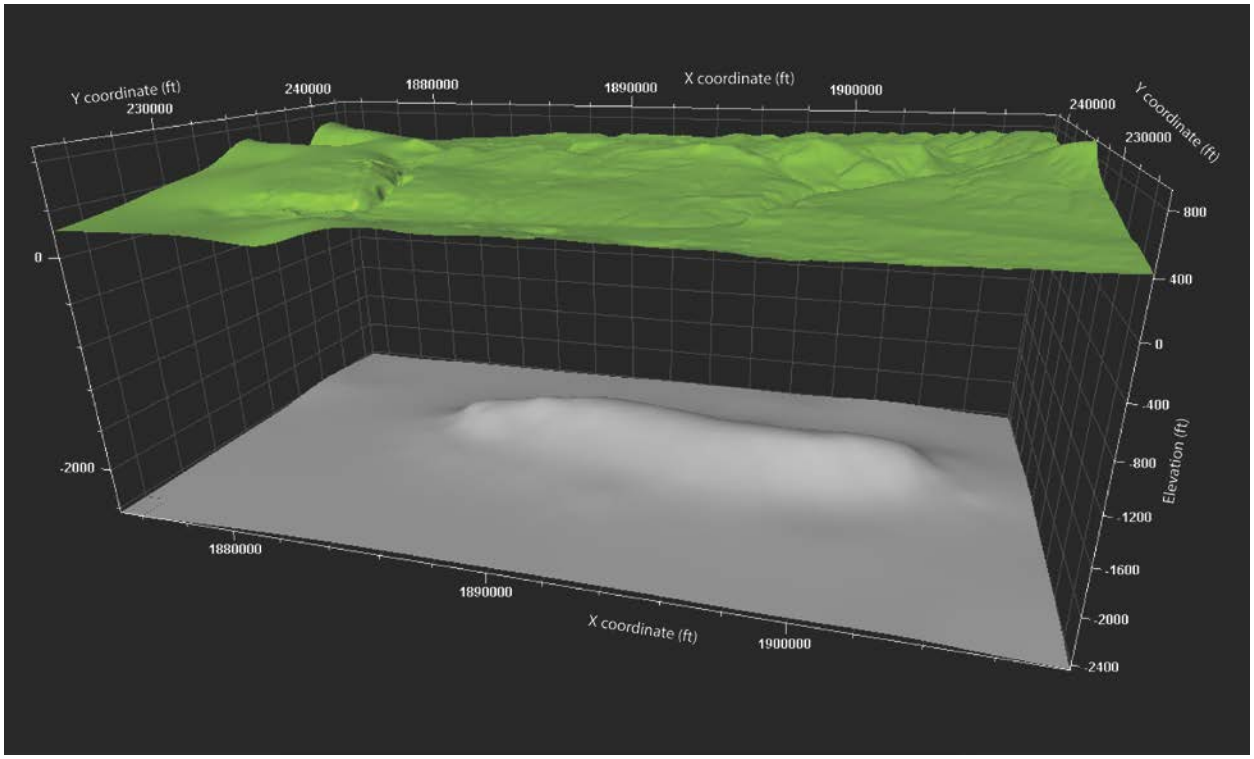

Figure 21. Surface topography and reconstructed top of the permeable Sentinel Bluffs basalt flow top at the Columbia Hills site

Hydraulic flow properties were assigned to the permeable reservoir layers based on test results from wells at the specific sites, where available. This included the Ortley #1 flow top and the Sentinel Bluffs #5 flow top at the Columbia Hills site based on REIDEL et al. (2005). For basalt flow top reservoirs without site-specific data, the statistical analysis of hydraulic properties for Grande Ronde Basalt flow tops was used to estimate hydraulic properties. The probability analysis of 67 regional test results indicated that there is a ~20% probability that any individual Grande Ronde flow top intersected within a borehole will exhibit a transmissivity value of 36 ft^2 per day (i.e., K = 1.2 ft per day, b = 30 ft, k = 0.50 darcies) or higher.

The Petrel geologic modeling software package was used to construct the three-dimensional sequence of reservoir and caprock layers. The layer structure and hydraulic properties were exported from the Petrel geologic model into a file that could be translated to a STOMP model input file.

3.4 CAES Simulation: Columbia Hills Site

A three-dimensional, multiphase flow model of CAES was developed for the Columbia Hills site using the STOMP multiphase flow simulator. The model contains four target formations: the bottom 50 ft of the Sentinel Bluffs Member and 90 ft of rubbly flow top of the Ortley member, separated by 290 ft of impermeable flow interior, and two lower target layers based on the frequency of permeable flow tops in the region (Figure 22). The porosity, hydraulic conductivity, and thickness of each layer are shown in Table 1. The ratio of horizontal to vertical hydraulic conductivity was assumed to be 10:1.

The initial conditions assumed a hydrostatic gradient of 0.433 psi/ft and a thermal gradient of 0.02°F/ft. At the location of the existing K2H-1 injection well, at the top of the upper layer, these assumptions result the initial formation pressures and temperatures at the top of each target formation shown in Table 2. The upper and lower boundaries were assumed impermeable and the lateral boundaries were held at hydrostatic pressure and the initial temperatures.

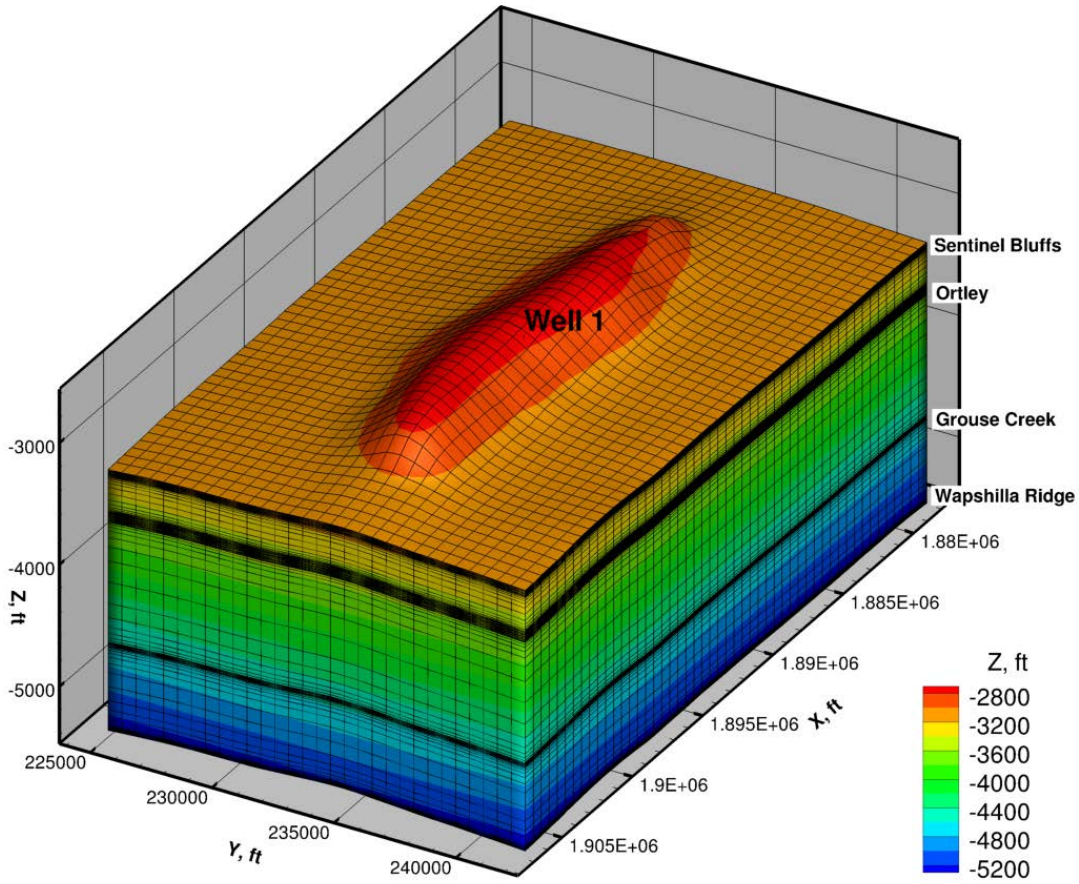

Figure 22. Model grid and layering at the Columbia Hills site. Target layers have finer grid spacing and are labeled.

Table 1. Layering at the Columbia Hills site

Layer	Formation	Hydraulic Conductivity (ft per day)	Porosity (%)	Thickness (ft)
1	Sentinel Bluffs	1	10	50
2	Flow Interior	0.001	1	290
3	Ortley	3	10	90
4	Flow Interior	0.001	1	
5	Grouse Creek	1	10	40
6	Flow Interior	0.001	1	
7	Wapshilla Ridge	1	10	35

Table 2. Initial pressures and temperatures at the location of Well 1 (K2H-1)

Layer	1 (upper)	2	3	4 (lower)
TVD, ft	2,763	3,103	4,179	4,870
Node pressure, psi	1,196	1,343	1,809	2,108
Node temperature, °F	105.3	112.1	133.6	147.4

Injection occurred assuming a fixed pressure in the injection well, set equal to the fracture pressure at the top of the upper layer. Assuming a fracture pressure gradient of 0.7 resulted in an injection pressure of 1,934 psi. This injection pressure exceeds the prevailing hydrostatic formation pressure in the upper three permeable layers, but not in the lower layer, so no air can be injected in that deepest layer. Over a 30-day injection period, 0.319 million metric tons (MMT) of air could be injected into the upper three permeable layers (Figure 23) via a single injection well. Very little air is injected into the third lowest permeable layer because of the low pressure differential between the injection well and the formation.

To determine the maximum amount of air that could be injected into the full anticline structure over a 30-day period, multiple-well analysis with 2 to 7 wells along the ridge of the anticline was conducted. The formation pressures and injection pressures, assuming a hydrostatic gradient of 0.433 psi/ft and a fracture pressure gradient of 0.7 psi/ft are shown in Table 3.

Figure 24 through Figure 28 show the air plume size for 2-, 3-, 4-, 5-, and 7-well injection scenarios, respectively. For the 5-well scenario, the locations of Wells 1 and 2 were shifted slightly to locations 1b and 2b for optimum spacing. Up to four wells can be used with a linear increase in the amount of air injected vs. time (Figure 29). With more than four wells (Figure 30), pressure perturbations from each well interfere (e.g., Figure 28), reducing the pressure gradient between each well and the formation, and reducing the amount of air injected at each well.

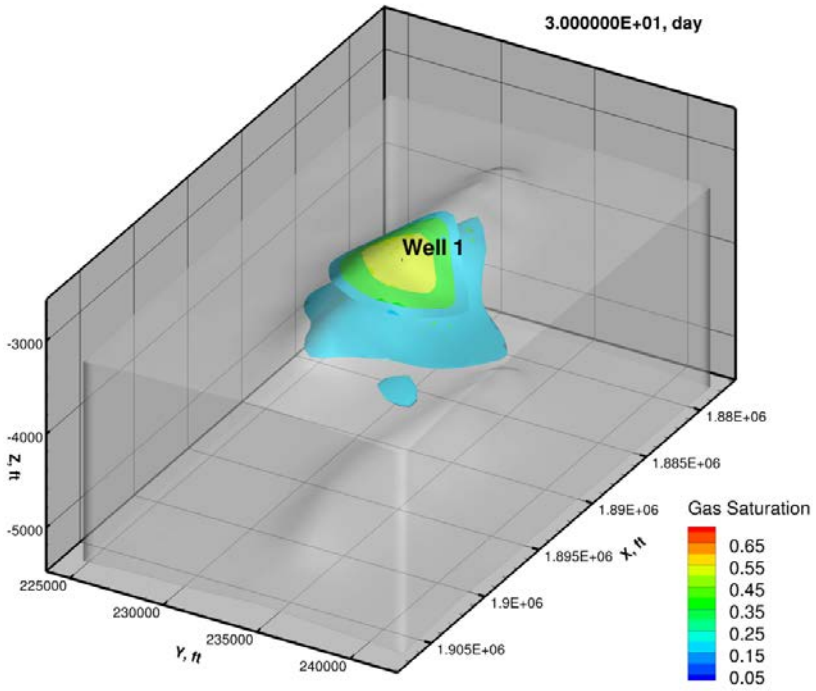

Figure 23. Compressed air in target formations after 30-day single-well injection at the Columbia Hills site

Table 3. Initial formation pressure and injection pressure at the top of the upper screened interval in each injection well. For the 5-well scenario, the locations of Wells 1 and 2 were shifted slightly to locations 1b and 2b for optimum spacing.

Well	Depth (ft)	Formation Pressure (psi)	Injection Pressure (psi)	Temperature (°F)
1	2763	1196	1934	105.3
1b	2723	1179	1906	104.5
2	2696	1167	1887	103.9
2b	2718	1177	1903	104.4
3	2718	1177	1903	104.4
4	2862	1239	2003	107.3
5	2714	1175	1899	104.3
6	2724	1179	1907	104.5
7	2740	1186	1918	104.8

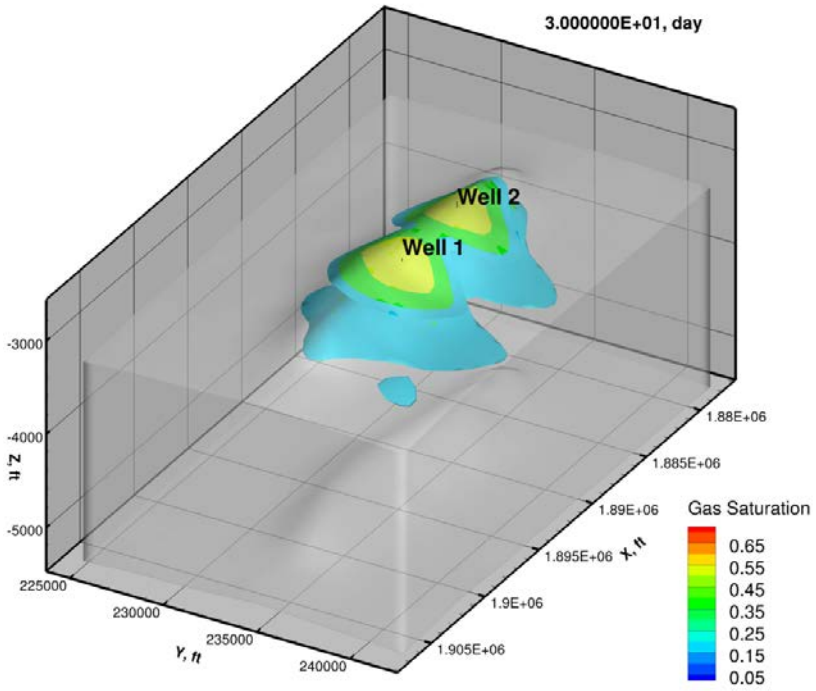

Figure 24. Compressed air in target formations after 30-day injection using two wells at the Columbia Hills site

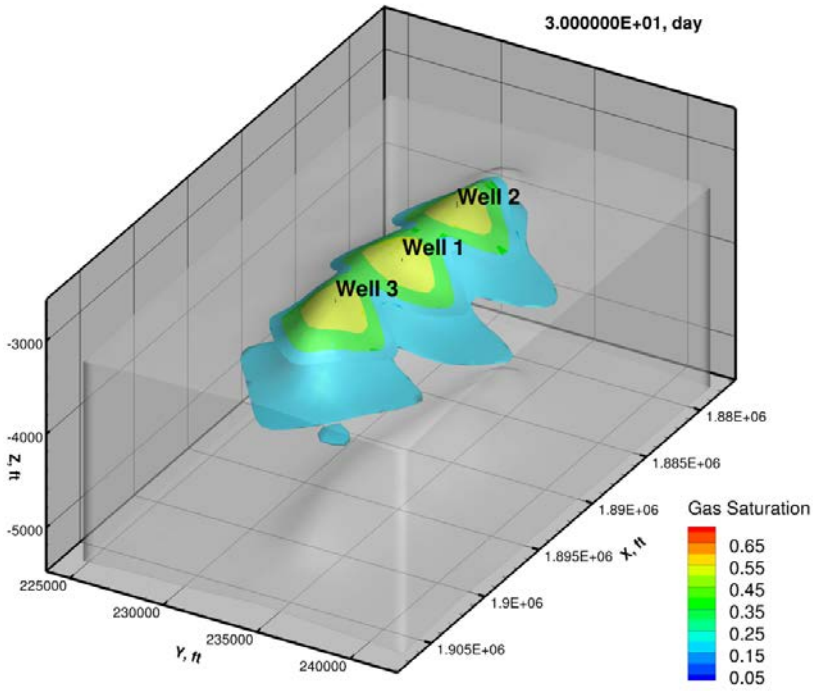

Figure 25. Compressed air in target formations after 30-day injection using three wells at the Columbia Hills site

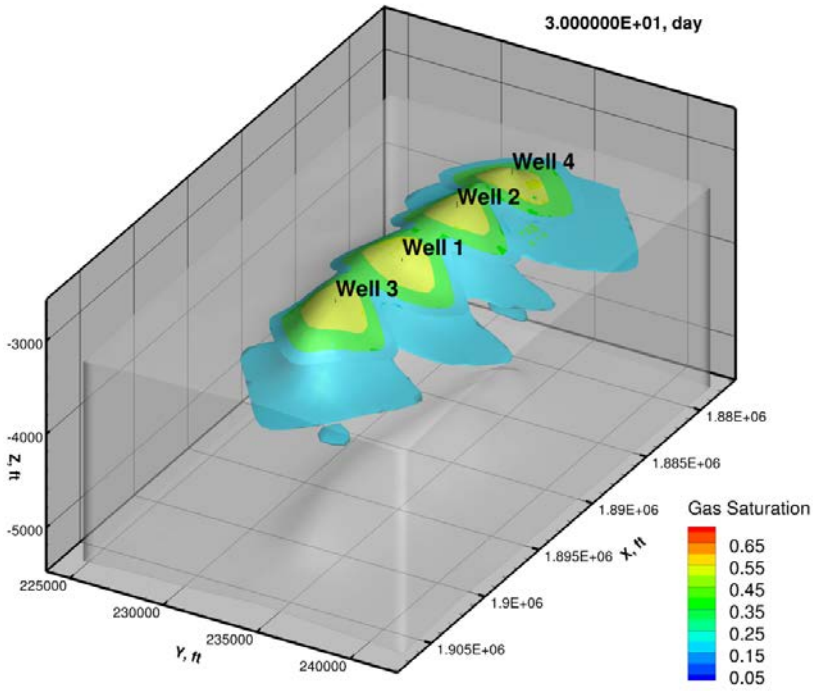

Figure 26. Compressed air in target formations after 30-day injection using four wells at the Columbia Hills site

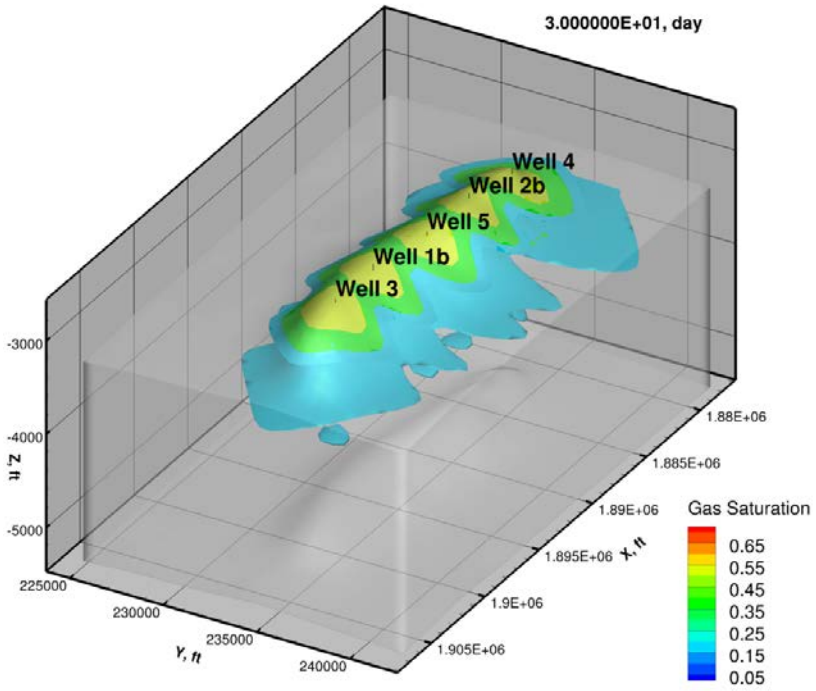

Figure 27. Compressed air in target formations after 30-day injection using five wells at the Columbia Hills site

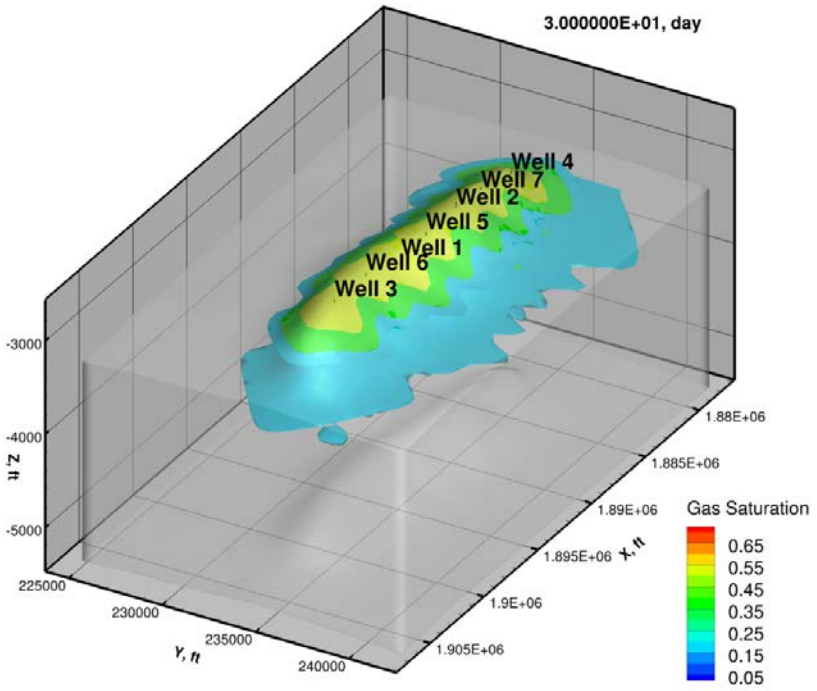

Figure 28. Compressed air in target formations after 30-day injection using seven wells at the Columbia Hills site

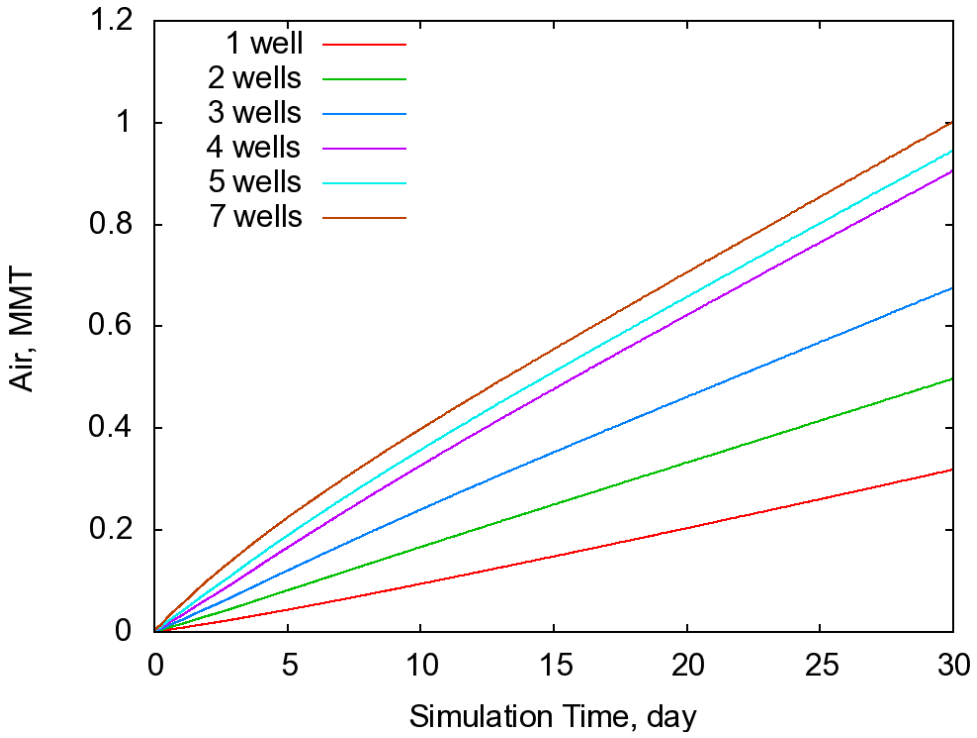

Figure 29. Air mass injected vs. time for multiple well scenarios at the Columbia Hills site

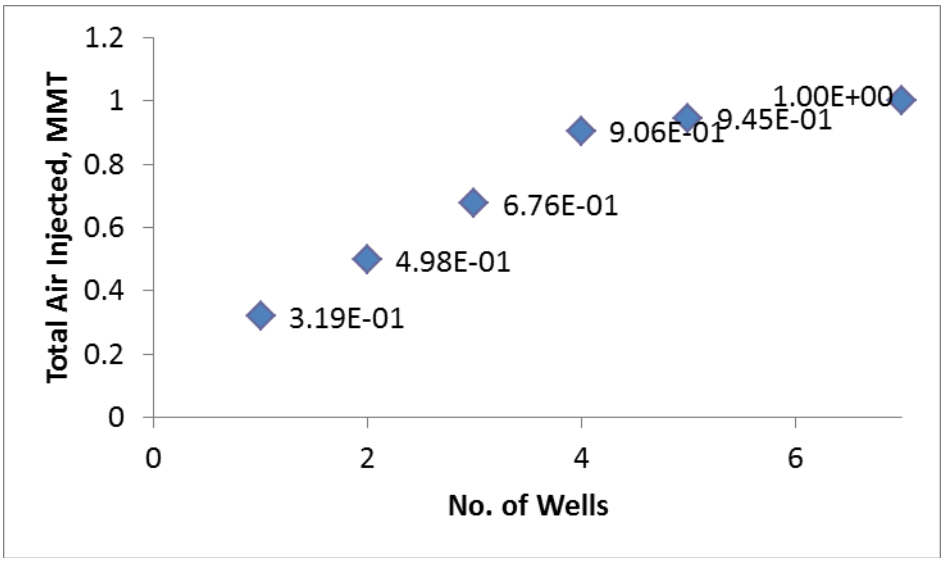

Figure 30. Air injected at 30 days vs. number of wells

With the 4-well configuration providing the reasonable maximum number of wells given the fixed injection pressure (equivalent to formation fracture pressure), an analysis was completed to describe potential air flows over time that the reservoir could support. Modeling indicated that the air injection rate is proportional to the difference between the pressure in the wellbore and the pressure in the formation at the well screen. Therefore, as the well bore pressure is raised or lowered to a constant value, the formation pressure at the well screen gradually increases or decreases, which causes the flow rate to vary over time. The constant pressure boundary condition dampens the pressure changes at the well screen, but does not hold them fixed. Figure 31 indicates that the flow rate over time, while not static, is relatively consistent with the proposed output of the compressor.

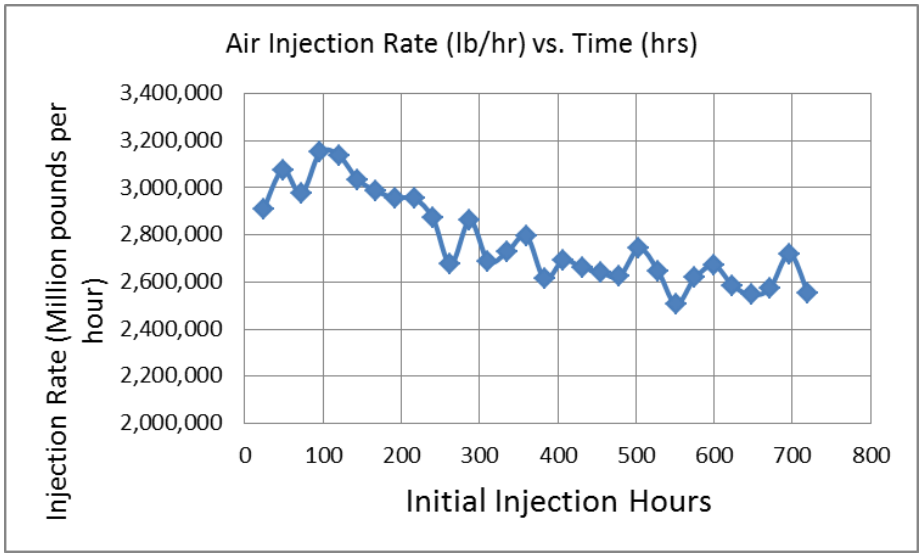

Figure 31. Total air injection rate vs. time

For the 4-well scenario, a 1-week simulation with air extraction was performed to estimate the length of time that significant rates of air extraction could be maintained. The well pressure was reset and held

at the initial formation pressure before injection and the extraction rate calculated versus time. This was meant to simulate the rate at which air would naturally flow from the pressurized formation. Simulation results indicate that a flow rate of greater than 400 kg/s could be maintained for 17.8 hours (Figure 32).

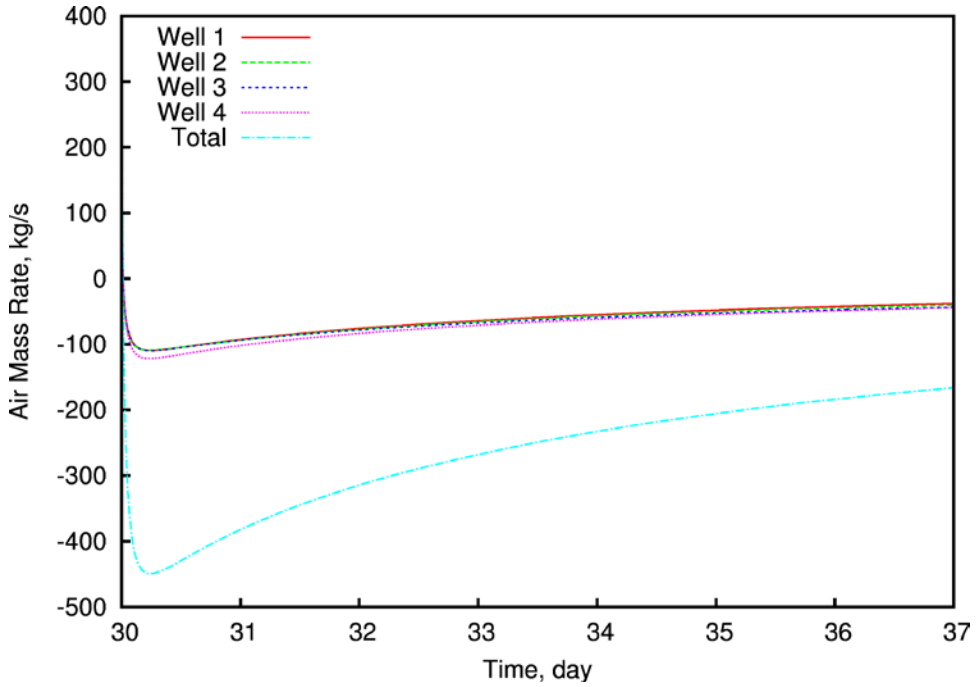

Figure 32. Air flow rate from four wells at the Columbia Hills site after 30 days of injection

Several extended simulations were run beyond the initial 30-day compressed air injection. First, an extended injection simulation was run to determine how long it would take to reach the spill point of the anticline. Second, an extended extraction simulation was run to determine how long it would take until the wells began to draw water. Finally, a 30-day simulation was run with diurnally alternating injection and extraction periods.

3.4.1 Spill Point

Starting with the initial 30-day injection period, compressed air injection continued for a total of 90 days of total injection time. The portion of the pore space occupied by air is variable throughout the plume, with higher air saturations nearer the well and lower air saturations further away. For this analysis, the edge of the plume is taken to be the 0.5 (50%) saturation contour. The spill point is taken to be the horizontal location of the -3000-ft contour at the top of the uppermost formation.

At the end of 40 days injection totaling 1.0 MMT (Figure 33), the air plume has extended past the spill point at several locations in the lower formation. By 60 days of injection totaling 1.5 MMT (Figure 34), the air plume has extended past the spill point at several locations in the upper formation, and the air plume has reached the boundary near $X = 1.88 \times 10^6$ ft. By 90 days of injection totaling 2.2 MMT of injected air (Figure 35), the air plume has reached the model boundary at several points in the upper and lower formations. Due to uncertainties regarding formation extent and dip extending out beyond the modeled boundary, it is not possible to determine whether air transitioning the “spill point” would ultimately be unrecoverable during extraction. However, the results do clearly indicate limited potential

for storage expansion without accessing another set of deeper basalt interflow zones at this site through a separate set of wells.

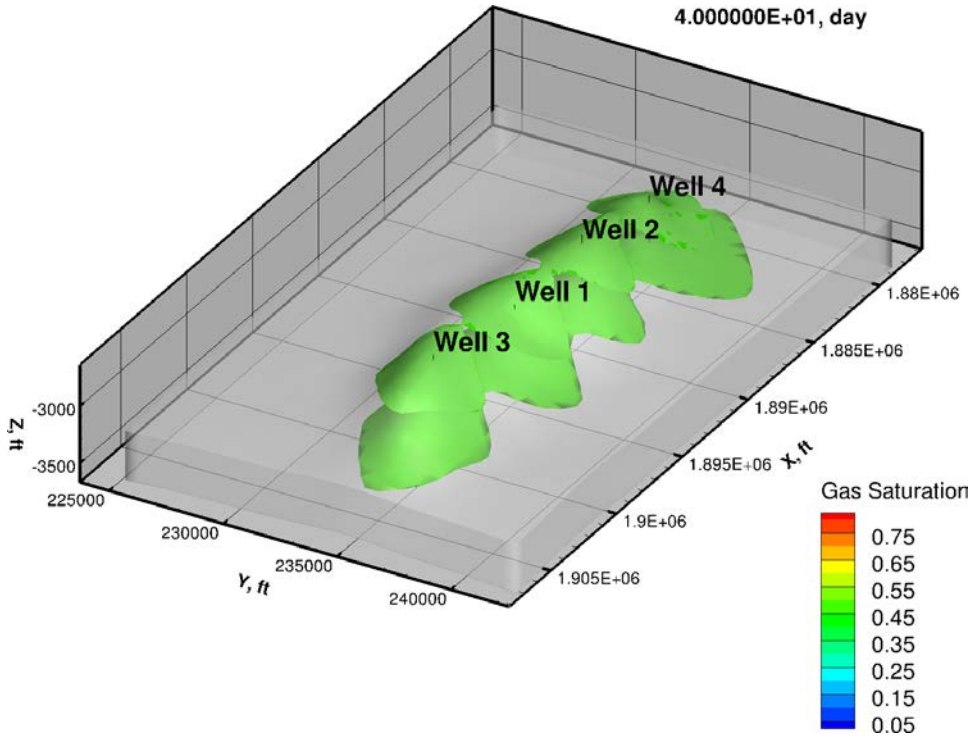

Figure 33. Extent of injected air plume after 40 days of injection, isosurface gas saturation = 0.5

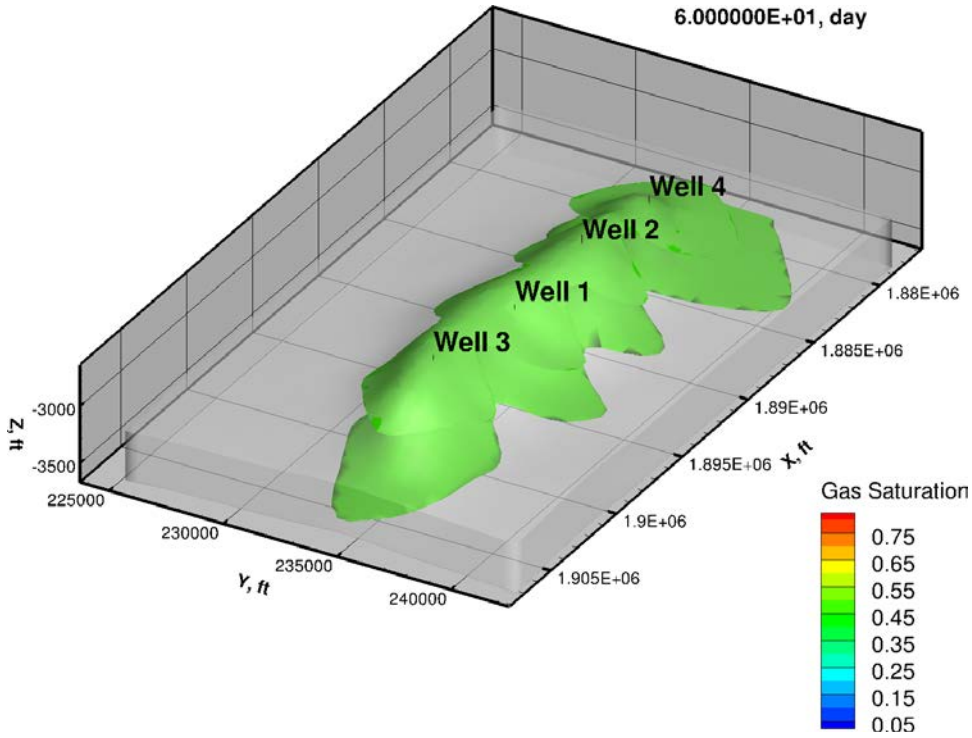

Figure 34. Extent of injected air plume after 60 days of injection, isosurface gas saturation = 0.5

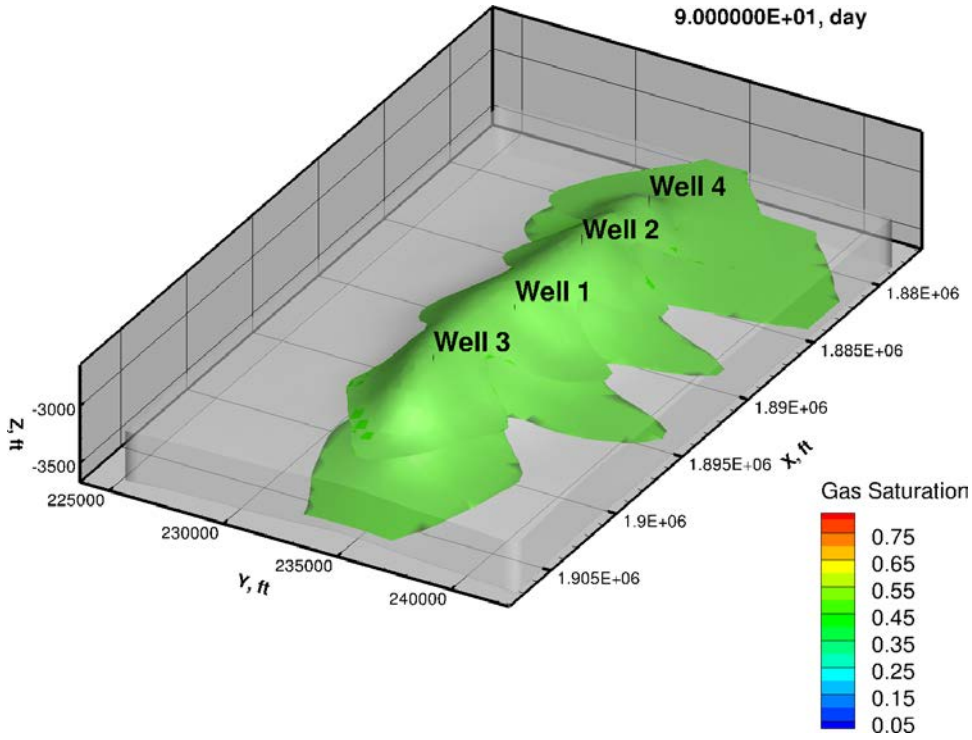

Figure 35. Extent of injected air plume after 90 days, isosurface gas saturation = 0.5

3.4.2 Water Breakthrough

For this scenario, 30 days of injection is followed by air extraction for 6 hours a day at a rate of 189 kg/s, divided equally between each of the four wells. Breakthrough occurs at 110 days, or 80 days after the start of extraction (Figure 36), although noticeable pressure decreases in Well 1 can be seen beginning at a simulation time of 50 days after the start of extraction.

Pressures in each of the four wells decrease steadily with time, and are significantly different. This is an artifact of the model stemming from the assumption of equal withdrawal rates from each well. In the actual facility, the four wells would be tied together at the surface, so that the withdrawal pressure would be the same for each well and the total withdrawal rate would be divided between each of the four wells in proportion to the effective air permeability in each borehole over time. The ability to link multiple wells together is not currently available in STOMP.

The pressure in Well 1 is noticeably lower and breakthrough occurs there first. This is because Well 1 was placed at the actual location of an existing well, and is slightly off the main axis of the anticline, and therefore below the peak. The other three wells were optimally placed at the peak of the anticline, and are able to withdraw from the buoyant air plume for a longer duration. The total mass of air decreases from 0.8 to 0.47 MMT. Fifty-nine percent of the injected air mass remains in the two flow top layers (Figure 37).

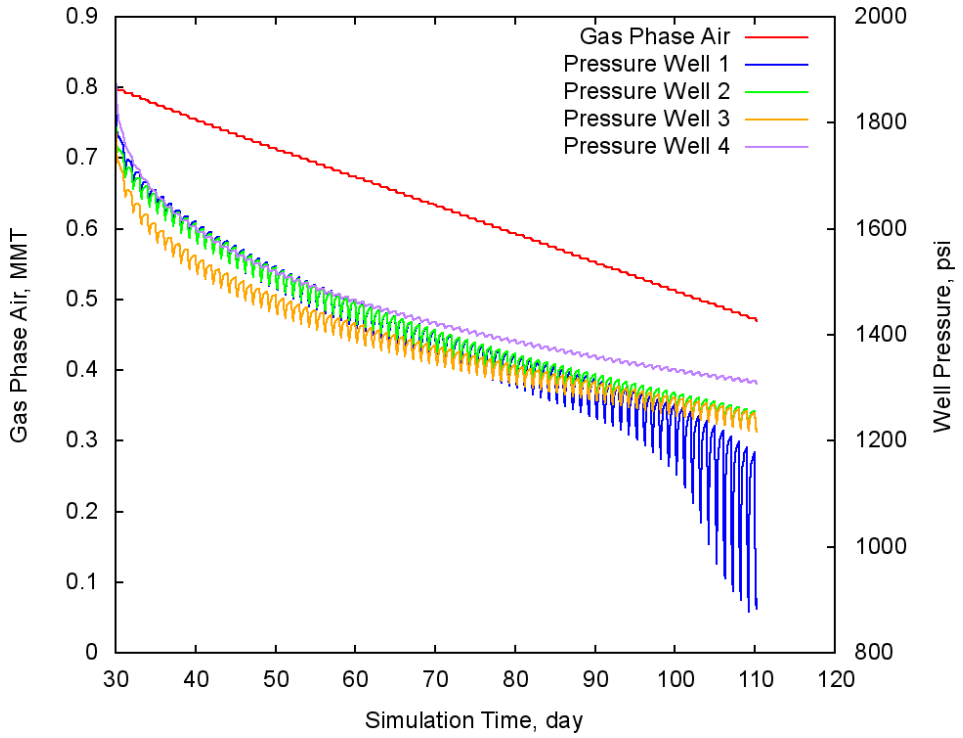

Figure 36. Total amount of remaining air at Columbia Hills site during extraction period

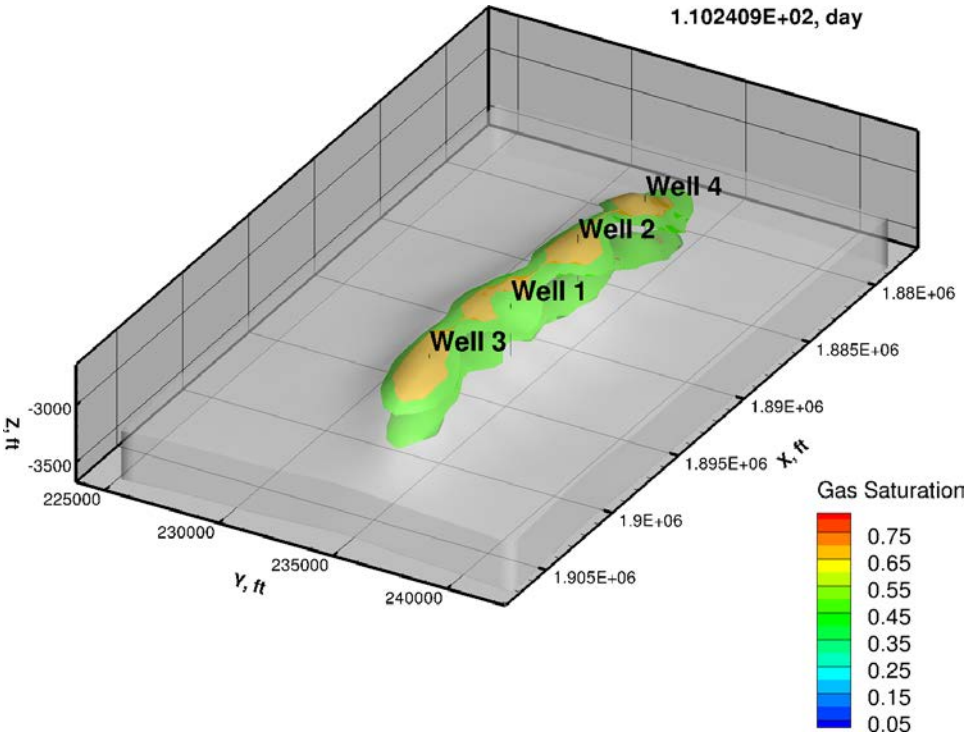

Figure 37. Air plume in Columbia Hills formation after 30 days of injection followed by 80 days of extraction

3.4.3 Diurnal Injection/Extraction

For this scenario, 30 days of continuous injection was followed by 30 days of cyclical injection and extraction. The injection rate is 353 kg/s, and the extraction rate is 189 kg/s divided between the four wells. The 24-hour cycle consists of a 3-hour injection period, 3-hour rest, 3-hour extraction, 6-hour rest, 3-hour extraction, and 6 hours of rest. Therefore, during the 3-hour injection period, 3,812 metric tons of air will be injected, whereas during the two 3-hour extraction periods, a total of 4,082 metric tons of air will be withdrawn. At 60 days, the total air mass has decreased from 0.8 to 0.784 MMT (Figure 38). About half of this decrease, 0.081 MMT tons, is due to the slight imbalance between injection and extraction rates, while the rest is due to increased dissolution of air due to the pumping cycles and buoyant redistribution. The diurnal injection/extraction simulation proceeded without breakthrough, with the injected air plume compacting slightly (Figure 39), indicating that this is a feasible long-term operation scenario.

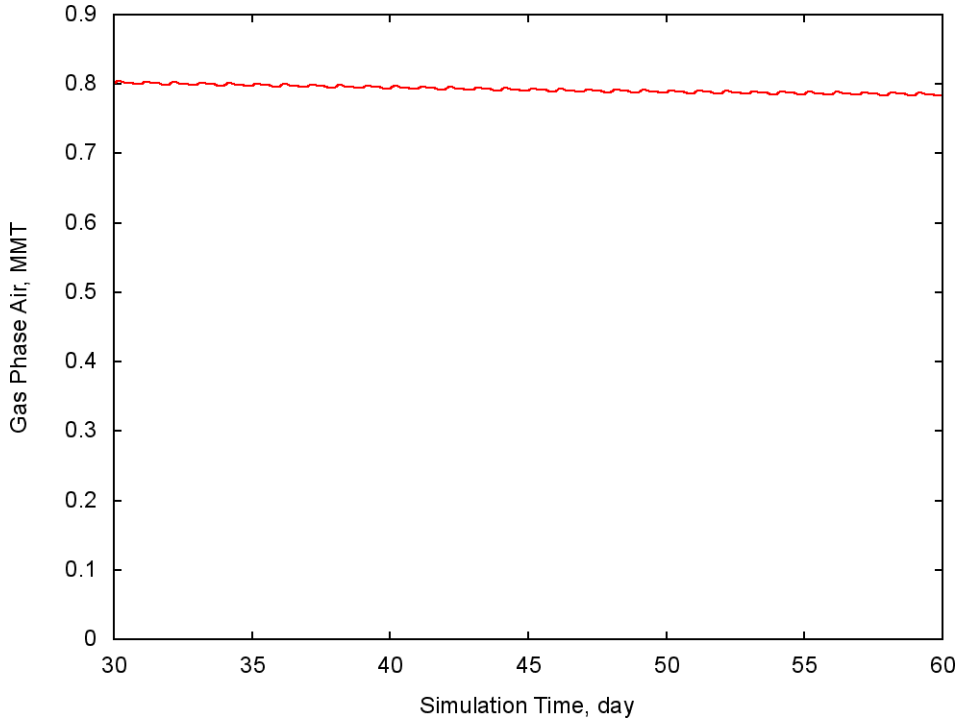

Figure 38. Total mass of compressed air at the Columbia Hills site during 30 days of diurnal injection/extraction cycles

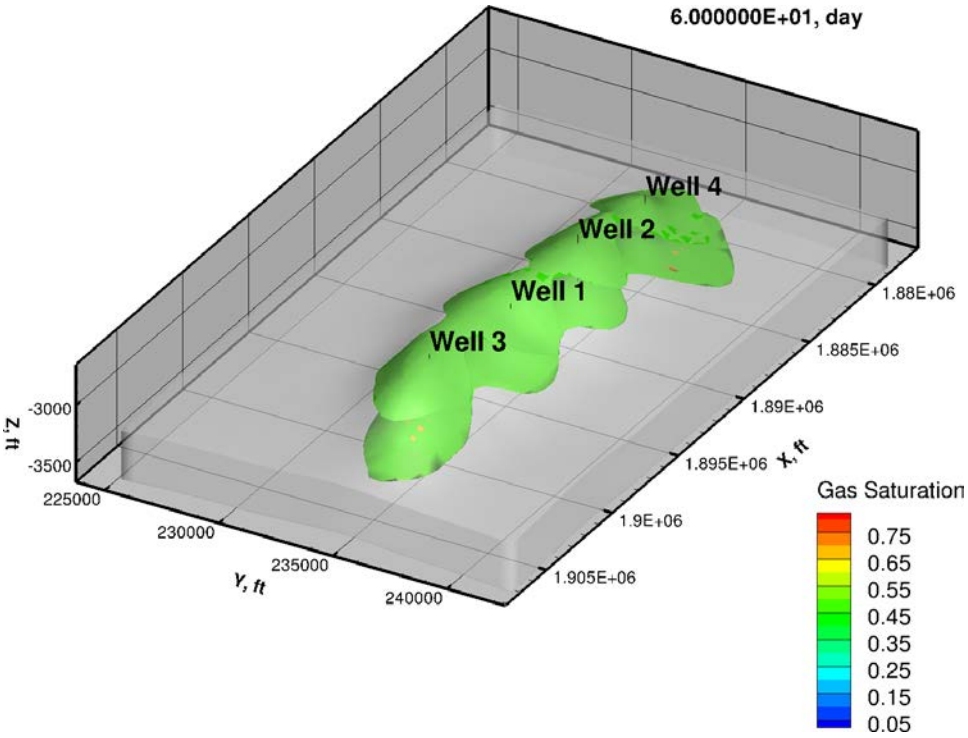

Figure 39. Extent of compressed air plume at the Columbia Hills site after 30 days of injection and an additional 30 days of diurnal injection/extraction cycles

3.5 CAES Simulation: Yakima Minerals Site

Simulations of compressed air storage in a sub-basalt sandstone layer at the Yakima Minerals site were performed using STOMP (WHITE and OOSTROM, 2006). In the horizontal direction, the grid contains 66 x 23 cells with dimensions of 250 x 250 m. In the vertical direction, the model contains two layers: the lower reservoir with a porosity of 0.1 and hydraulic conductivity of 0.48 ft per day, and the overlying caprock with a porosity of 0.05 and hydraulic conductivity of 2.7×10^{-4} ft per day. The ratio of horizontal to vertical hydraulic conductivity was assumed to be 10:1. The grid is shown in Figure 40.

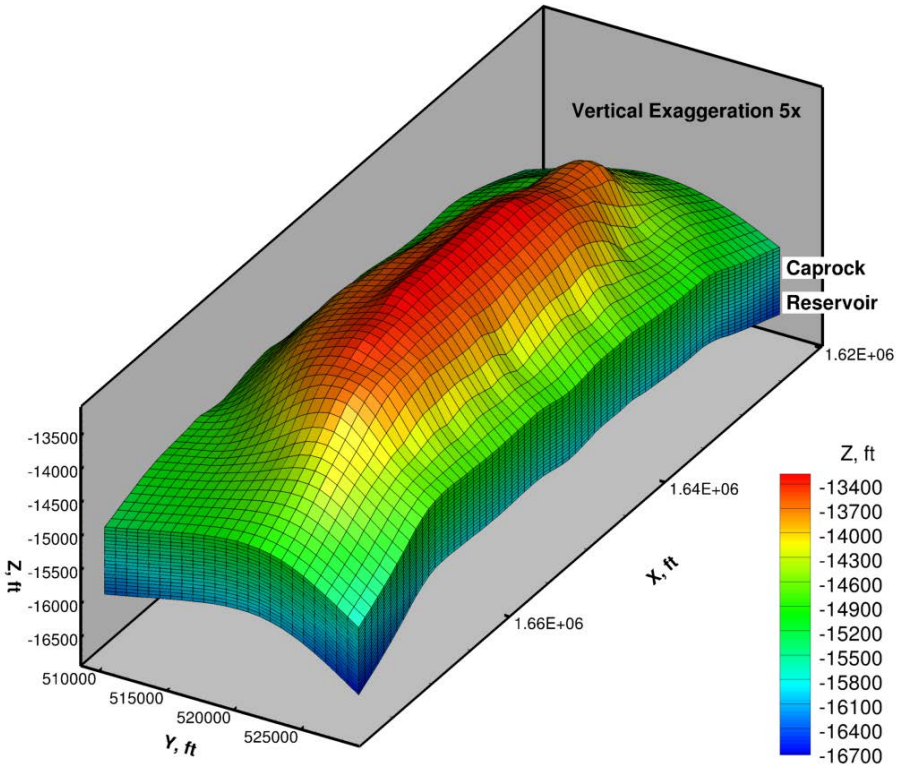

Figure 40. Grid and layering in the sub-basalt region at the Yakima Minerals site. Depths are below the mean surface elevation of 2,085 ft.

For the base case simulation, a hydrostatic gradient of 0.433 psi/ft, a fracture pressure gradient of 0.7 psi/ft, and a geothermal gradient of 0.02°F/ft was assumed. The injection well was located near the horizontal center of the grid, at X = 502,770 m, Y = 157,972 m and was screened throughout the entire depth of the sub-basalt reservoir, with a well diameter of 6.125 inches. At this location, the depth from the average ground surface elevation of 2,085 ft to the top of the reservoir is 13,843 ft. Under the assumed vertical gradients, the formation pressure at this depth would be 5,994 psi, the fracture pressure 9,690 psi, and the initial temperature 352°F.

Air was injected for a period of 30 days at 126 kg/s, with the pressure in the injection well held at 530 psi above the formation pressure. The total mass of air injected was 0.324 MMT (Figure 41). The injected mass of air is contained within a very small area, relative to the projected size of the anticline (Figure 42).

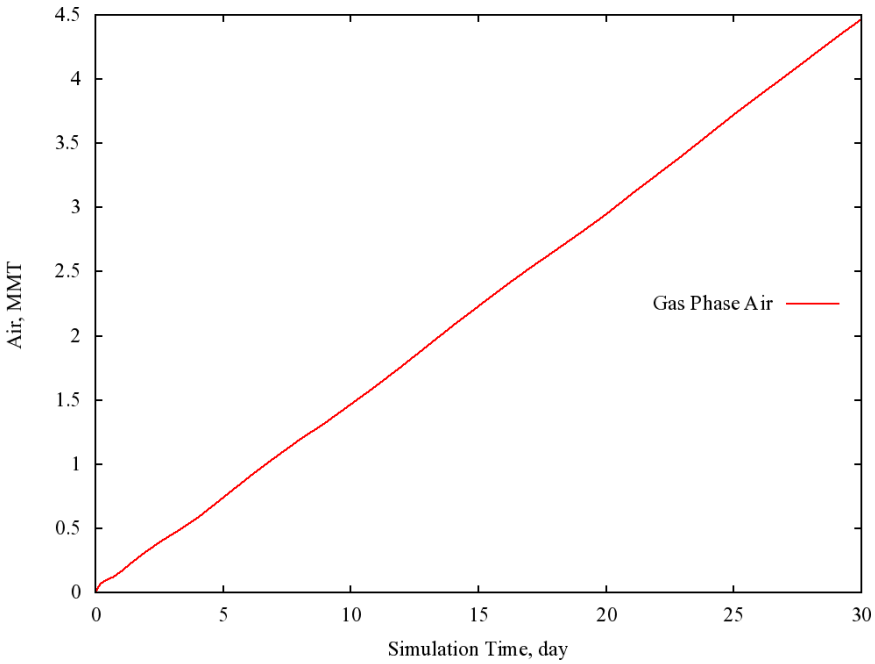

Figure 41. Cumulative mass of air injected over 30 days at the Yakima Minerals site

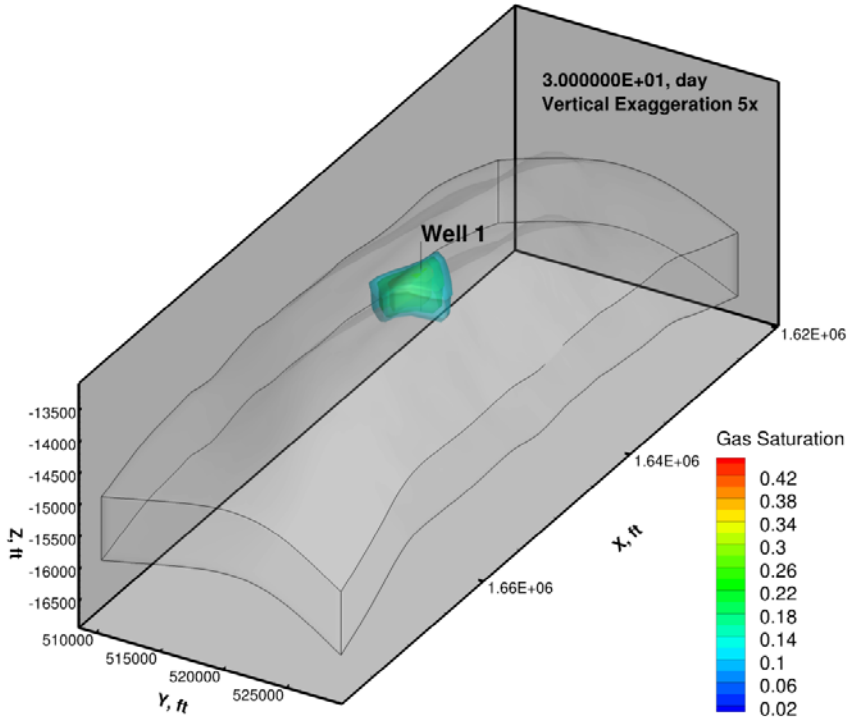

Figure 42. Gas saturation after 30 days of injection at the Yakima Minerals site

Several extended simulations were run beyond the initial 30-day compressed air injection. First, an extended injection simulation was run to determine how long it would take to reach the spill point of the anticline. Second, an extended extraction simulation was run to determine how long it would take until

the well began to draw water. Finally, a 30-day simulation was run with diurnally alternating injection and extraction periods.

3.5.1 Spill Point

Starting with the initial 30-day injection period, compressed air was injected assuming the same 126 kg/s injection rate used for the initial 30-day simulation. The injection continued until 1 year of total injection time. The portion of the pore space occupied by air is variable throughout the plume, with higher air saturations nearer the well and lower air saturations further away. For this analysis, the edge of the plume is conservatively taken to be the 0.1 (10%) saturation contour. There is no discernible spill point in the Yakima Minerals anticlinal structure, so the spill point is taken to be the edge of the model grid. After 1 year of injection totaling approximately 4 MMT, the injected air plume has not reached the model boundary. Consequently, capacity expansion at the Yakima Minerals site appears to be nearly unlimited relative to realistic sizes of CAES power plants.

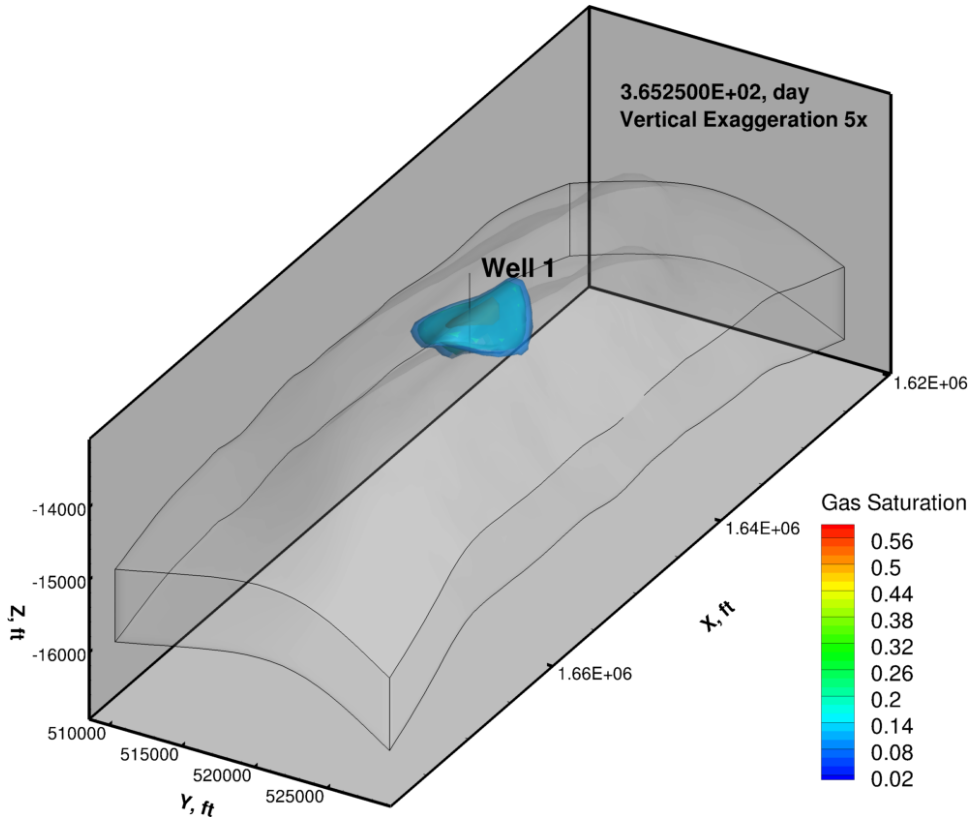

Figure 43. Injected air plume at the Yakima Minerals site after 1 year of continuous injection

3.5.2 Water Breakthrough

For this scenario, 30 days of injection is followed by air extraction for 6 hours a day at a rate of 126 kg/s into one well. Breakthrough occurs at 86 days, which is 56 days after the start of extraction (Figure 44). Well pressures decrease steadily with time before slowly leveling off, although pressure variations increase with time. The total mass of air decreases from 0.324 to 0.170 MMT. Fifty-three percent of the injected air mass remains in the formation (Figure 45).

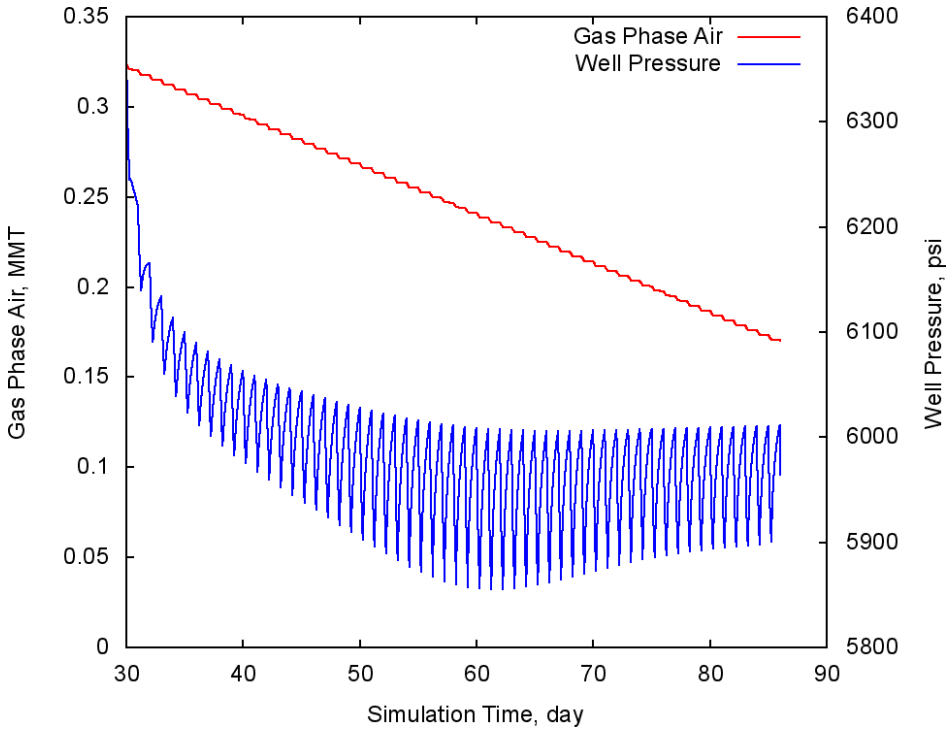

Figure 44. Total amount of remaining air at Yakima Minerals site during extraction period

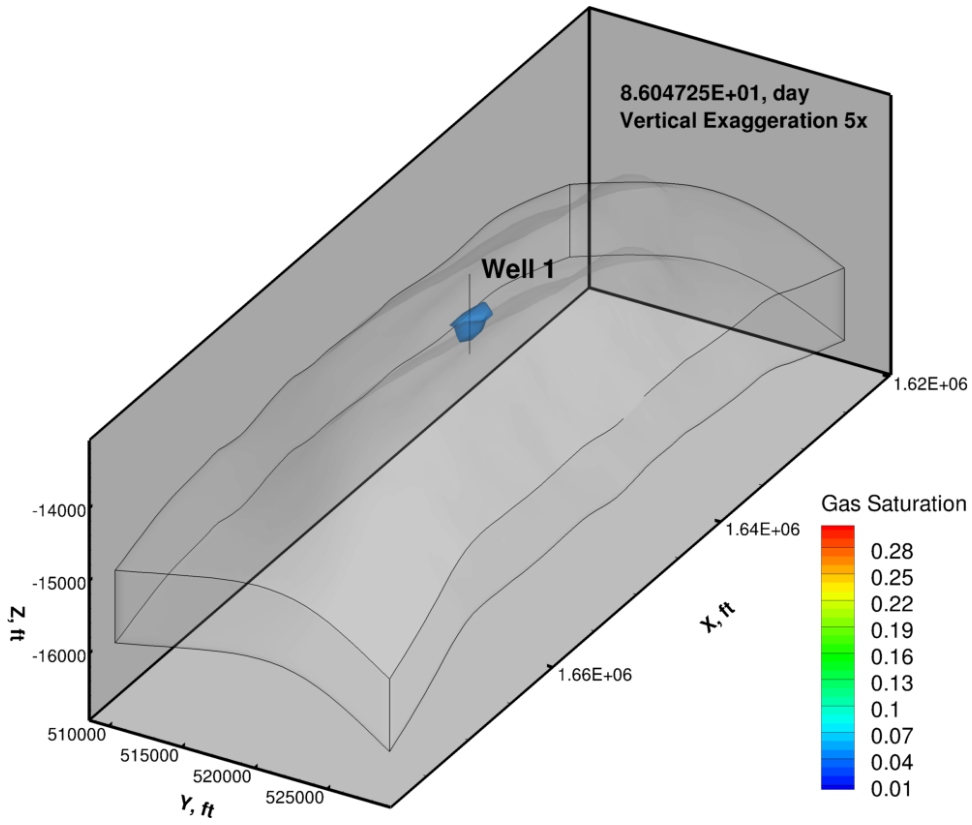

Figure 45. Air plume at the Yakima Minerals site after 30 days of injection followed by 56 days of extraction

3.5.3 Diurnal Injection/Extraction

For this scenario, 30 days of injection is followed by 30 days of cyclical injection and extraction. The injection and extraction rates are equal, 126 kg/s from one well. The 24-hour cycle consists of a 6-hour injection period, 3-hour rest, 3-hour extraction, 3-hour rest, 3-hour extraction, and 6 hours of rest.

The diurnal injection/extraction simulation proceeded without incident, indicating that this is a feasible long-term operation scenario. At 60 days, the change in total air mass is very slight, decreasing from 0.324 to 0.321 MMT (Figure 46). This decrease in air mass is due to dissolution of air in the formation water near the edges of the plume as the plume rises buoyantly with time (Figure 47).

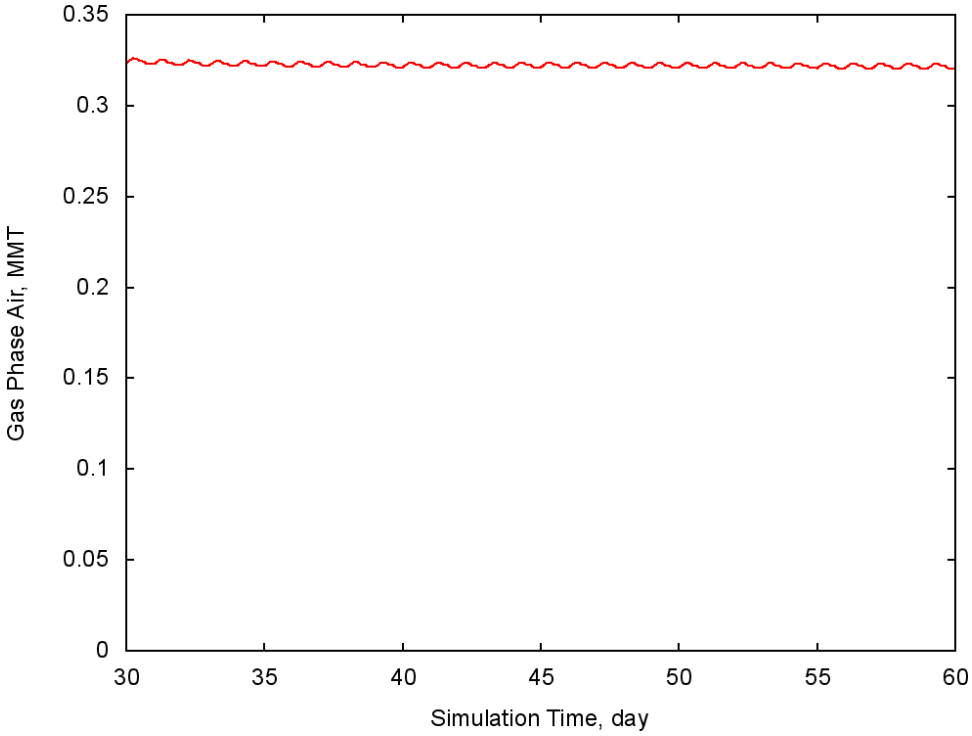

Figure 46. Total mass of compressed air at the Yakima Minerals site during 30 days of diurnal injection/extraction cycles

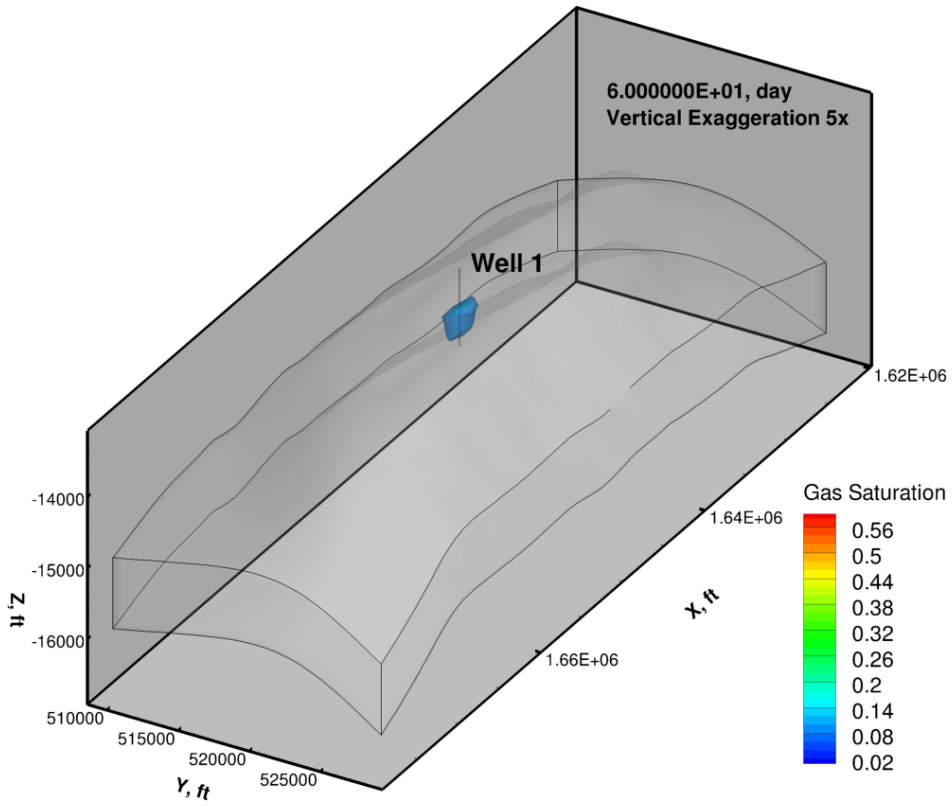

Figure 47. Extent of compressed air plume at the Yakima Minerals site after 30 days of injection and an additional 30 days of diurnal injection/extraction cycles

3.6 Yakima Minerals Site Geothermal Heat Recovery

As is discussed in more detail in Section 7.0, a new kind of hybrid CAES/geothermal power plant configuration was developed for the Yakima Minerals site due to lack of a natural gas source to provide heat. Hot water extracted from the sub-basalt sandstone is used for both reheating compressed air as it expands in the turbines and for a thermally driven chiller to provide cooling water for the compressors. A simulation with a pair of wells for water extraction and reinjection was conducted using STOMP. The two wells were separated by a distance of 500 feet. For initial modeling purposes, geothermal water at a temperature of 185°C was extracted at a rate of 2,500 gpm, 6 hours daily for 14 days. Water cooled to a temperature of 100°C was reinjected into another well during the same period each day.[1]

Because the model domain was on a smaller scale than that required for CAES, a flat, three-dimensional, three-layer model was constructed with a minimum 50-ft grid spacing, compared to the 250-ft horizontal grid spacing used for the CAES simulations (Figure 48). The model domain is 3,000 ft wide in the horizontal X-direction and 2,000 ft wide in the horizontal Y-direction. In the vertical Z-direction, the domain is 1,500 ft thick. The middle layer represents the high-permeability sandstone layer, sandwiched between two low-permeability layers. The sandstone layer was assumed to have a relative porosity of 0.1 (10%) and the confining layers a porosity of 0.05 (5%). The sandstone layer was given an intrinsic permeability of 178 mD, while the confining layers were assumed to have an intrinsic permeability of 0.1 mD. The ratio of horizontal to vertical permeability was assumed to be 10:1. The rock layers were assumed to have a rock thermal conductivity of 0.582 watt per meter kelvin (W/m-K) and a water-saturated thermal conductivity of 1.13 W/m-K. The specific heat of the rock layers was assumed to be 700 joules per kilogram kelvin (J/kg-K).

The sandstone layer was assumed to be 500 ft thick at a depth between 14,450 and 14,950 ft. The initial temperature in the sandstone was 185°C and the pressure 6,267 psi based on thermal and hydraulic gradients described previously for CAES modeling. Pressures and temperatures at all model boundaries were held constant at their initial values.

Injection/extraction of 2,500 gpm, distributed over the 500-ft thickness of the aquifer, has a minimal impact on formation pressures (Figure 49). After 14 days, cooler water is confined to the region around the injection well due to mixing with warmer formation water (Figure 50). During the 14-day period, water from the extraction well remains at the initial temperature (Figure 51).

[1] Flow rates and temperatures of geothermal resources were refined for the surface power plant model, and are slightly different than the ones initially modeled.

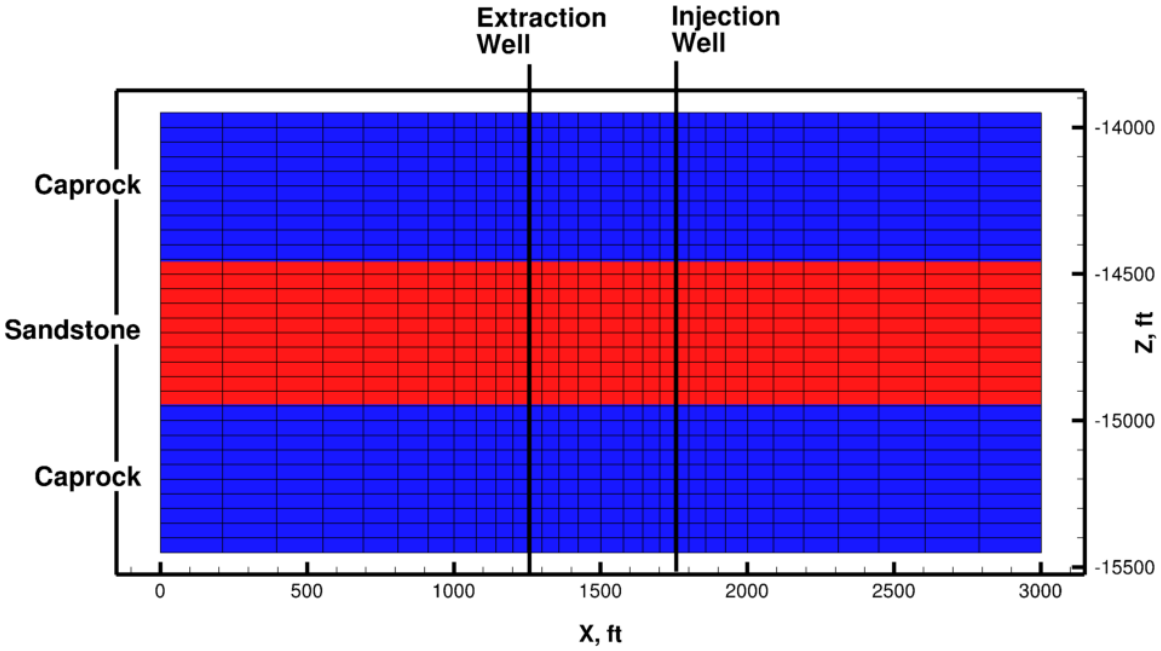

Figure 48. Cross-section of model grid and layering for Yakima Minerals deep geothermal wells simulation

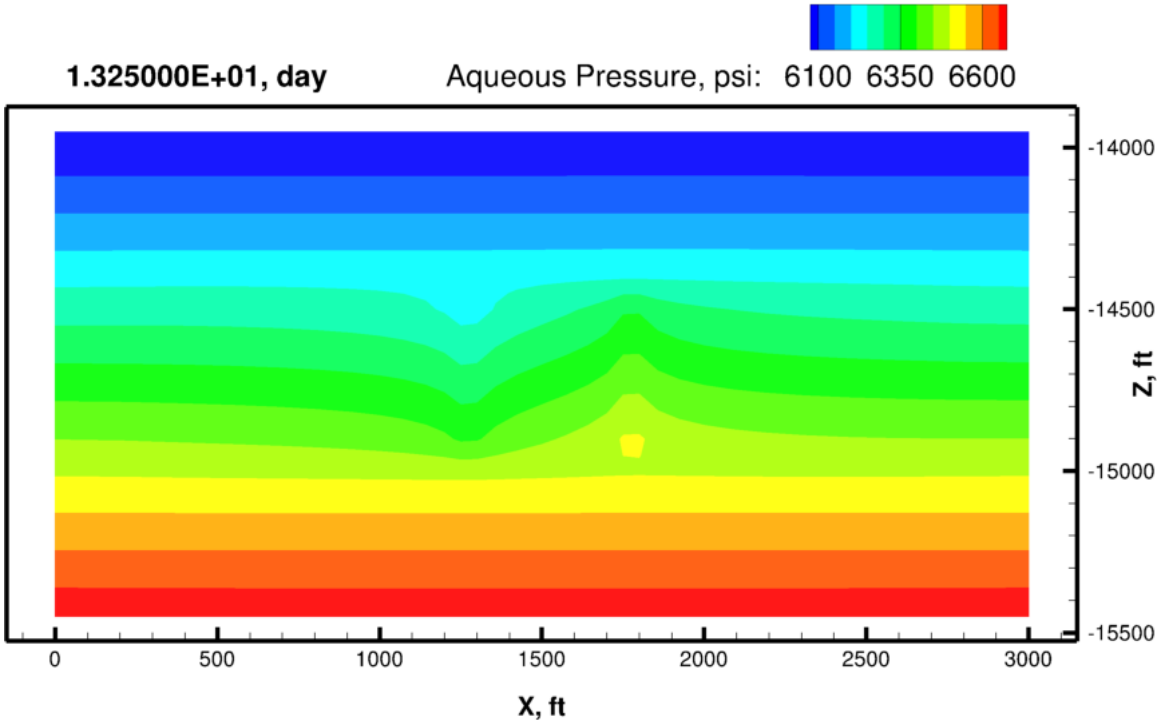

Figure 49. Pressure distribution in formation at the end of a 6-hr injection period

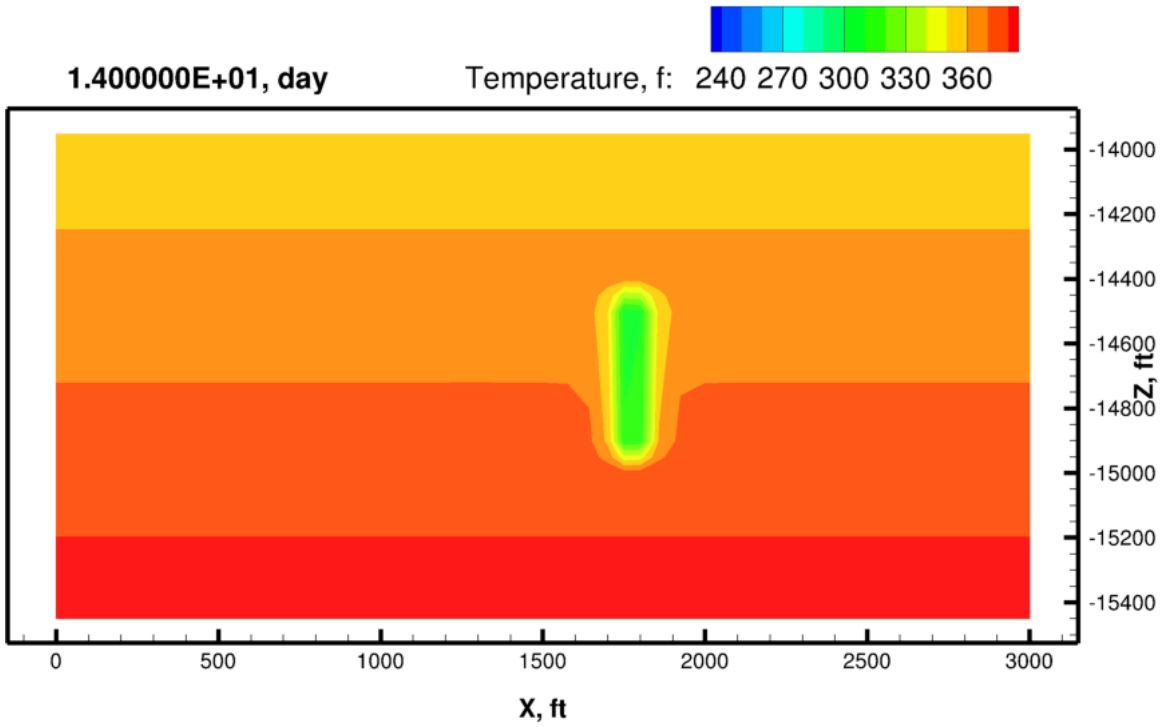

Figure 50. Formation temperature after 14 days of water injection at 220°F

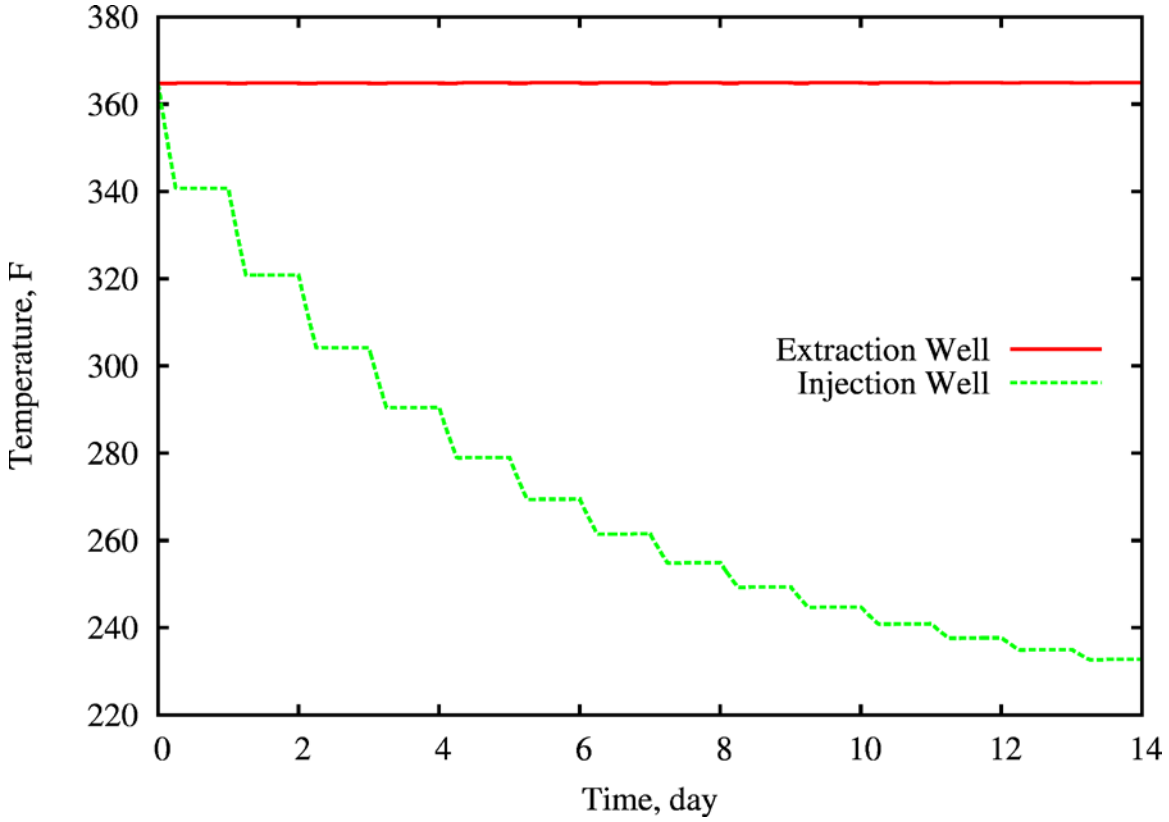

Figure 51. Water temperature at geothermal extraction and injection wells

3.7 Summary of Simulation Results

Compressed air injected into a tilted basalt flow top could migrate a significant distance in a few months, depending on the degree of tilt. Doubly plunging anticlinal structures like the Columbia Hills and Yakima Minerals sites appear capable of containing the injected air, though additional site characterization is needed.

At the Columbia Hills site, up to four wells can be used in tandem without interference between the wells. The amount of time air can be injected into four wells before the injected air reaches the spill point of the anticline is limited, between 60 and 90 days. After injecting for 30 days, extraction may proceed for 6 hours a day at 189 kg/s from four wells for 50 to 80 days before water breakthrough limits the performance of Well 1, which is slightly off the peak of the anticline. A nearly balanced diurnal injection/extraction scenario is feasible for virtually unlimited duration operations after a 30-day air cushion bubble is established.

At the Yakima Minerals site, an appreciable amount of air can be injected using only one well. In comparison to the Columbia Hills site, more air can be injected in the sub-basalt reservoir of the Yakima Minerals site because the density of compressed air is significantly higher at the greater depth of the Yakima Minerals site. Air injected at a rate of 126 kg/s does not reach the spill point of the anticline with even a full year of continuous injection. After injecting for 30 days, extraction may proceed for 6 hours a day at 126 kg/s from one well for 56 days before water breakthrough occurs. A balanced diurnal injection/extraction scenario is again feasible for virtually unlimited duration operations after a 30-day air cushion bubble is established.

4.0 Basalt-Air Reactivity Experimental Results

As is discussed in more detail in Section 6.0, the CAES plant design uses air extracted from the Columbia Hills basalt reservoir to directly feed a high-pressure turboexpander followed by a combustion turbine stage. Because of tight O_2 partial pressure constraints in the air feed to a natural gas turbine, a set of experiments was performed to check for oxygen consumption from reaction with ferrous silicate minerals in Columbia River basalts. A series of static high-pressure batch experiments were initiated March, 28, 2012 to examine rock-air-water interactions of basalts exposed to air at 50°C and 138 bar (2,000 psi). Basalt chips collected from the Wallula Test well at a depth of 1,460 ft and representing the Columbia River (Wanapum formation) were used for this study. Approximately 15 g of basalt was placed into four different stainless steel 25-ml Parr reactors with 7 ml of deionized water; water covered the basalt chips. After heating to 50°C, each reactor was pressurized with compressed air to ~138 bar. Pressure and temperature of each reactor was monitored weekly. A blank reactor containing water and compressed air was also included in the testing matrix. One of the four tests and the blank were terminated on January 18, 2013 following nearly 10 months of testing.

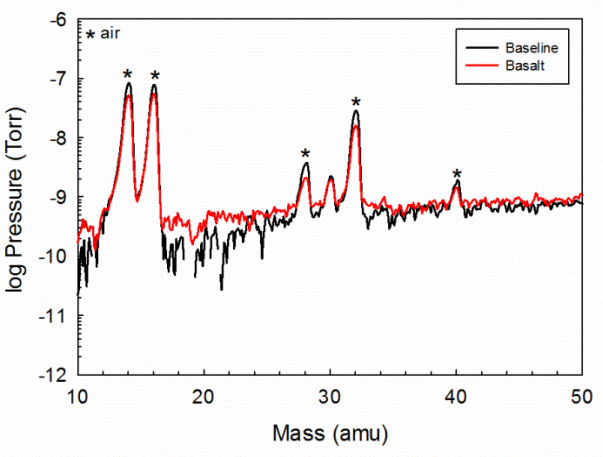

Figure 52. Residual gas analyses of gases obtained from the reactor containing basalt, water, and air (red) and the reactor with only water and air (black)

Prior to depressurization, gas samples were collected from these reactors and analyzed with a residual gas analyzer. These results, shown in Figure 52, illustrate the similarities observed between the two reactors. Identical components observed in both reactors include masses representing nitrogen (14, 28 atomic mass units (amu)), oxygen (16, 32 amu), and nitric oxide (40 amu). The reactor with the basalt had slightly lower concentrations of all the gas components but no significant oxygen depletion was detected.

Immediately following depressurization, the reactor was opened to reveal wet basalt grains; nearly 5 ml of the original 7 ml of solution were extracted from the vessel. Grains were allowed to dry on a clean piece of filter paper at room temperature for several hours. Visual observations detected a subtle amount of iron staining occurring on a portion of the grains. The inside of the reactor also contained a small amount of iron staining coinciding with the water level. Generally, grains obtained their original unreacted grayish color, remaining as individual particles with no evidence of cementation. More detailed characterization of the both the reacted and unreacted grains was obtained with scanning electron microscopy (SEM).

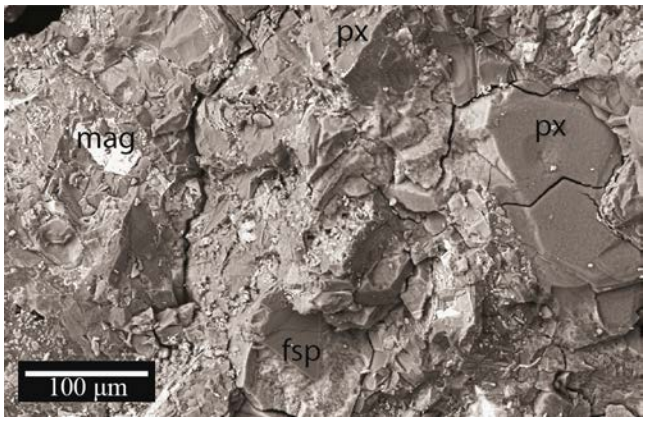

Figure 53. Microphotograph of an unreacted basalt chip (Wanapum formation) with distinguishable grains of titanium rich magnetite (mag), feldspar (fsp), and pyroxene (px) as observed by SEM

A representative example of surface features from an unreacted grain (Wanapum formation) is shown in Figure 53. Visible are individual components of the basalt including pyroxene (px), plagioclase feldspar (fsp), a bright grain of titan-magnesite (mag). Chemistries of these grains, obtained by SEM energy dispersive x-ray technique, were consistent with the individual mineral phases shown. Pyroxenes contained silica and iron with lesser amounts of aluminum and magnesium. Plagioclase feldspars generally contained twice the amount of calcium compared to sodium, with the balance consisting of aluminum and silica. The bright, dense magnetite grains were iron dominant mixtures with lesser concentrations of titanium. Also observed as surface features on the unreacted samples were zeolites and clays (secondary minerals) commonly identified within the vugs of this basalt.

In comparison, SEM characterization of the reacted basalt grains revealed unaltered plagioclase and magnetite particles along with direct evidence of minimal fluid interaction with the pyroxene minerals. Plagioclase feldspar grains, such as shown in Figure 54 (fsp), appeared smooth and intact. Additionally, tiny grains of titano-magnetite (mag), visible as bright spots on the SEM microphotographs, continued to maintain their Fe-Ti chemical ratio as compared to the unreacted grains.

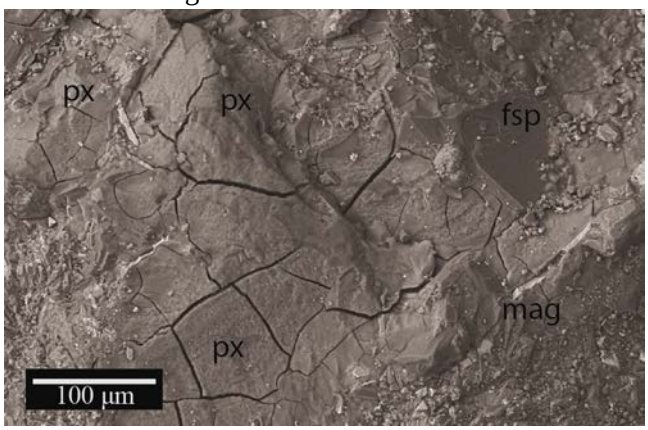

Figure 54. Microphotograph of an reacted basalt chip (Wanapum formation) with distinguishable grains of titanium rich magnetite (mag), feldspar (fsp), and pyroxene (px) as observed by SEM

In contrast, pyroxene grains (px), shown in Figure 54, were cracked and contained rougher surfaces in comparison to the unreacted pyroxenes. These features were more extensive and concentrated within the pyroxene phase contrasted to the feldspar plagioclase grains. Notable changes to chemistry were confined to the iron content of pyroxenes; iron-depleted regions were observed occurring within individual grains. It is plausible that variations of iron content resulted from isolated and discontinuous coatings of iron precipitates, which were visible on the reacted grains. Moreover, iron-enriched coatings appeared as larger precipitates and were distinguishable from titano-magnetite particles due to the lack of titanium. Overall, the reacted basalts maintained discrete grain boundaries and displayed no evidence of mineral carbonation. Given the minimal extent of alteration observed from the extended duration tests, chemical reactivity effects – including oxygen depletion and formation of alteration products that could reduce formation permeability near the wellbore – do not appear to be of concern for CAES operations in the Columbia River Basalt.

5.0 Energy Storage and Demand Analysis

The Pacific Northwest is blessed with large sources of renewable energy in the form of hydro and wind generating capacity, as well as other conventional non-renewable sources. Among the challenges of utilizing these resources are inherent fluctuations in demand, generation, and balancing, particularly during peak generation events, and the utility level need to provide reliable power in the most cost-effective manner. While traditionally BPA has used the Federal Columbia River Power System to balance load and generation, with the rapid expansion of regional wind capacity (Figure 55), BPA faces a rapidly expanding need for balancing capacity and operational flexibility from generators.

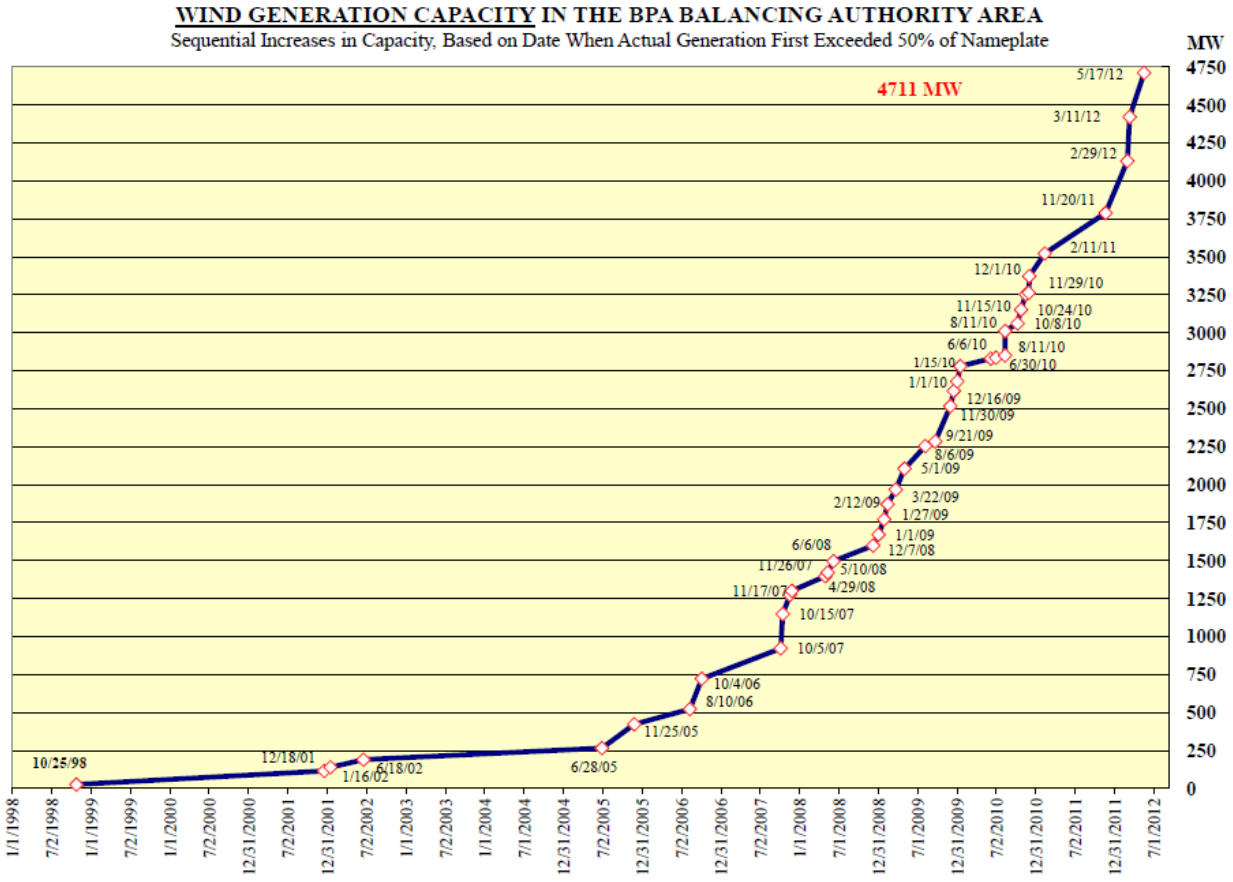

Figure 55. Wind installed capacity in BPA balancing authority area[1]

At times, wind energy generated in the BPA system can amount to nearly 70% of the total electricity demand in the BPA system (BPA, 2012b). Large amounts of wind generation combined with large amounts of hydropower produced by springtime high river conditions can generate electricity in excess of total demand, including export power. Though additional water can be spilled without generating electricity, excess spill can increase the total dissolved gas in the water, threatening the health of the ecosystem and fish.

[1] Wind Installed Capacity Plot. Accessed at: http://transmission.bpa.gov/business/operations/Wind/WIND_InstalledCapacity_Plot.pdf.

Regionally, large-scale energy storage could potentially offer a solution for two distinct types of events. The first scenario addresses significant springtime runoff events, where a large compressor would be consuming grid-supplied load and injecting air into a subsurface reservoir as much as 24 hours per day continuously over a 30-day period, thereby reducing forced spill at the dams. Once the subsurface compressed air reservoir is established, generation (air extraction) could be dispatched for on-peak use until the reservoir had been drawn down to the point where either the air flow or the pressure limits power production. The second scenario assumes diurnal operation, whereby the facility would be compressing during off-peak hours and generating during on-peak hours. Collectively, the two scenarios frame the cost evaluation of the CAES plant by providing operational constraints and influence on likely capacity factors.

On the broadest scale, over-generation events as occurred in spring 2010 are not rare, with a one-in-three probability that flows similar to those could happen in any year, lasting for 30 days or more (BPA, 2011c). To that regard, the minimum compression (energy storage) capacity of the proposed system was bound to 30 days of continuous injection, or approximately 150,000 to 165,000 MWh based on the facility configured for the simulation. This isn't to suggest that the CAES systems modeled in this analysis represent an "optimal" design or storage capacity for a regional CAES facility. The 2010 event estimated an excess of 745,000 MWh (~1,000 MW continuous for a month) was spilled over the dams due to the lack of load, and that was after all other remedies had been exercised. The energy storage systems evaluated do however represent viable alternatives to storing at least a portion of the total demand for storage and balancing. Having established both subsurface characteristics and scalable plant designs, it is conceivable that multiple systems could be deployed contingent upon the need.

From a more condensed timeline perspective, Figure 56 provides a snapshot of the system imbalance, and the level of reserves required to address the imbalance: on June 5, 2012, over approximately 12 hours, BPA had to supply almost 400 MW of supply as well as almost 800 MW of decreasing reserve.

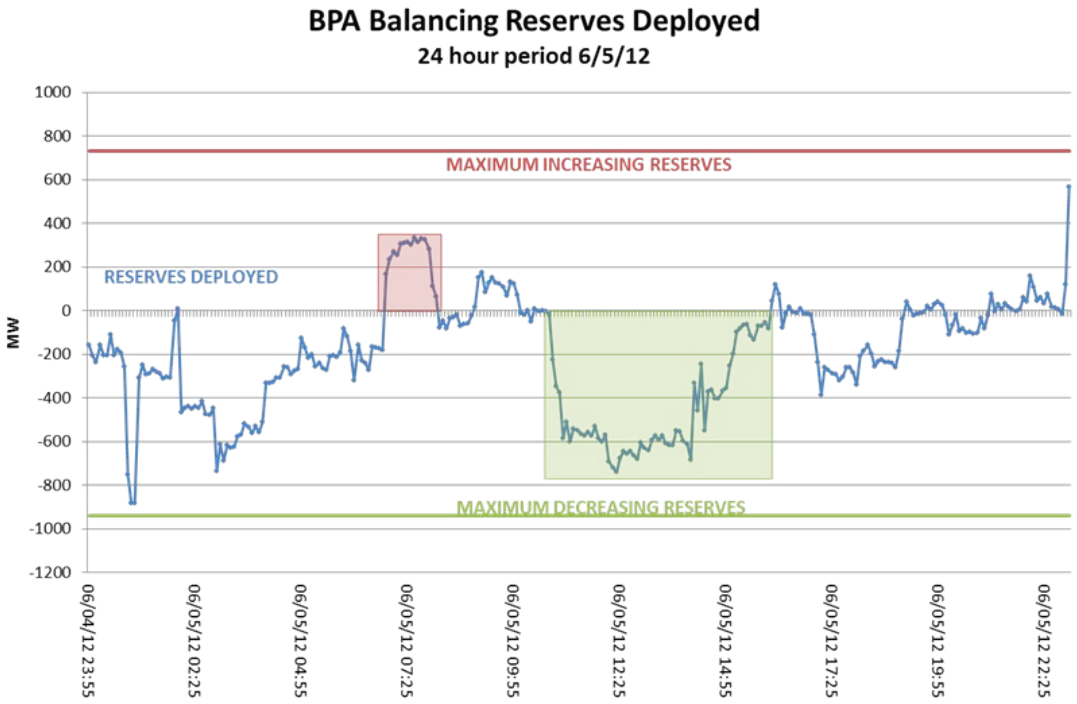

Figure 56. BPA Balancing and Reserves Deployed

Though in this case wind generation was forecast with enough certainty to avoid oversupply mitigation measures (such as curtailment), it clearly indicates the unique aspects of the system as a whole, and the relevance of evaluating mechanisms to shift surplus or off-peak generated power to use during on-peak times.

It is important to note that the single largest contingency in any site location for CAES is the reliance on geologic structures to accept, store, and deliver high-pressure air to the power train. Therefore, the primary objective of the analysis is to demonstrate that compressed air storage is viable in hard rock reservoirs by conceptually modeling commercially available technologies, working in conjunction with reservoir characteristics that ultimately govern the rate of injection and extraction air, and therefore the nameplate capacities that could be utilized. A secondary objective is to quantify the storage capacity in terms of energy consumed and energy produced through simulated injection (air compression) and extraction (generation) scenarios.

Numerous configurations can be deployed in a CAES facility, depending on location, storage reservoir size and characteristics, and capacity and energy requirements. Two distinct configurations of stored energy plants were evaluated for power production. The first was a CAES facility proposed for the Columbia Hills site that is based on conventional natural gas generation coupled with an economized turbo-expander and is included in the Figure 57.

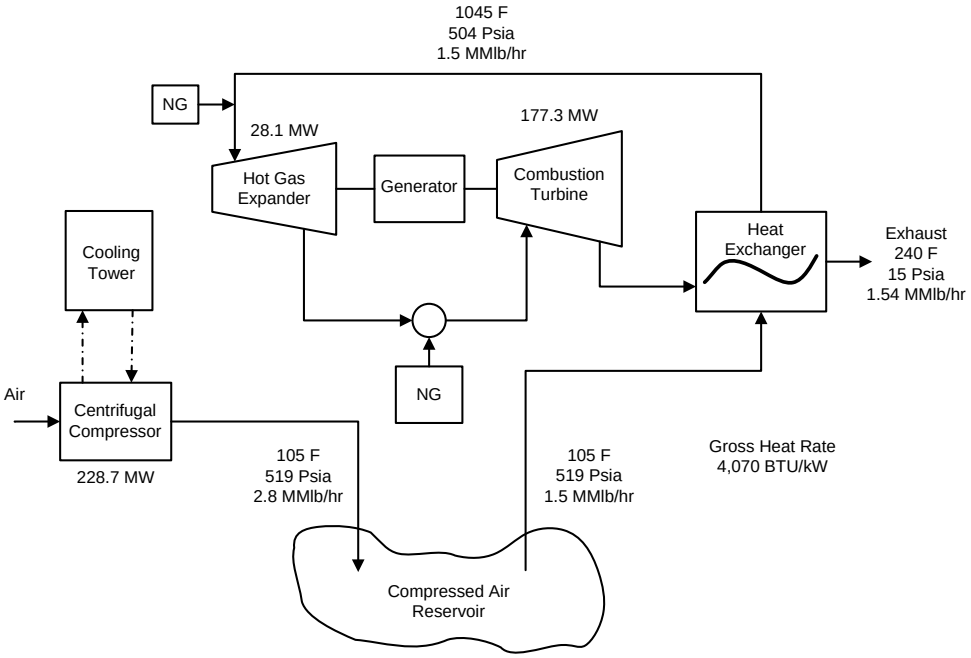

Figure 57. Columbia Hills CAES plant block flow diagram

Chosen primarily due to the subsurface reservoir characteristics, as well as ready access to natural gas and cooling water, the fossil fired CAES plant is the only approach that has been successfully built and operated at commercial scale to date. Equipment sizing was determined iteratively based on theoretical injection and extraction air flows offered by the subsurface model. The CAES plant simulated included the following:

- 228 MW intercooled, multistage centrifugal air compressor
- Distribution piping, four injection wells, casing, and underground compressed air storage reservoir
- Recuperative heat exchanger and 28 MW turboexpander
- 177 MW power turbine
- High voltage (230 kV) transformer and transmission
- Balance of plant including cooling towers, piping, instrumentation

The second compressed energy plant evaluated for the Yakima Minerals location is a new concept for a hybrid adiabatic CAES plant combined with geothermal heat recovery. The facility would utilize geothermal resources in addition to recovered heat of compression for use in expansion turbines for power generation. In an effort to capitalize on both above ground and below ground heat sources, two configurations were simulated: one that utilizes geothermal resources only and one that utilizes geothermal resources in conjunction with stored heat of compression in molten salt. Both configurations assume a single subsurface compressed air storage reservoir at ~14,000 ft and assume recovery of 175°C water from a subsurface geothermal source that will be used to preheat and/or reheat the compressed air supplying a power train. Conceptually, the geothermal water supply is a closed loop: the hot water is extracted and heat-exchanged with the compressed air, which cools the water. The water is then re-injected into the same formation at an appropriate distance away to avoid thermal contamination at the

extraction location, in this case representative of a loss of water temperature. Because the generation of power would typically coincide with 5 to 6 hours of operation per day, the distance between the geothermal water extraction and injection wells can be held to a minimum as indicated in Section 3.6.

There are advantages and disadvantages to each configuration, including impacts to the generation of power, compressor efficiency, modes and duration of operations, and capital costs. Table 4 provides cursory explanation of several of those aspects.

Table 4. Relative advantages and disadvantages to hybrid configurations

Configuration	Advantages	Disadvantages
Geothermal	• May use water cooling or air cooling for compressor duty • No surface storage required for thermal storage fluid • Can compress for 30 day over-generation event • Potentially lower total plant capital required for fewer heat exchangers	• Limit on total power output due to low energy heat recovery • Water cooled compressor would require two additional wells and a significant burden on cooling water supply • Air cooled compressor will experience loss in efficiency if required to operate at elevated dry-bulb temperatures
Geothermal + Molten Salt	• Molten salt captures heat of compression in aftercooler and utilizes it in generation cycle • Potentially lower capital with conventional axial flow compressor • Power generation would be greater • No additional wells required for groundwater sourced cooling: compression cooling provided by geothermal driven ammonia absorption refrigeration	• Above ground storage and supplemental heat required for molten salt • Potentially higher capital for more plant equipment such as molten salt and ammonia refrigeration

Given the qualitative distinctions, there is no apparent ranking of one configuration over another. One generates less power, but could potentially be more useful if needed for long, continuous periods of compression. The other configuration generates more power utilizing captured heat of compression, but may do so at a penalty to continuous compression requirements due to the finite heat capacity of the salt. A baseline configuration was simulated using geothermal resources only for power production. To quantify as many distinctions as possible, a second configuration and simulation was completed which included power production utilizing both geothermal resources and captured heat of compression; this configuration is included in the following Figure 58.

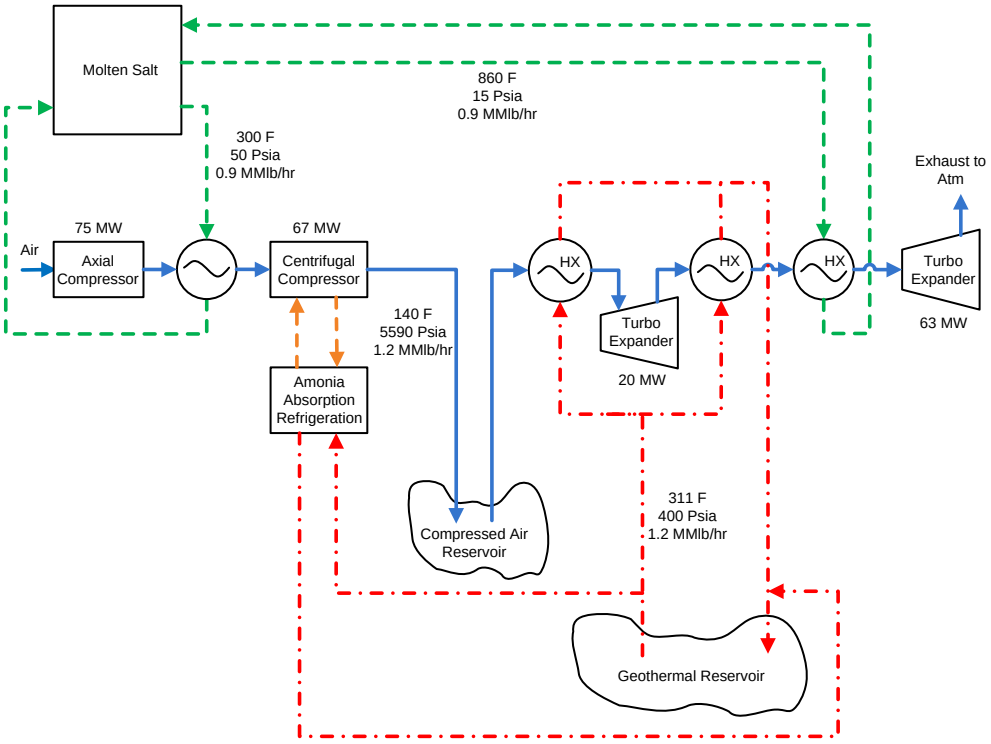

Figure 58. Yakima Minerals hybrid CAES plant block flow diagram

The baseline configuration of the hybrid CAES facility that was simulated for the Yakima Minerals includes the following:

- 75 MW after-cooled axial flow air compressor; 67 MW multistage intercooled centrifugal air compressor
- One compressed air injection-extraction well at approximately 14,000 ft below surface finished depth, and surface distribution piping of two miles
- Two geothermal wells (one for extraction and one for injection) located at the plant site
- 83 MW (3-stage) turboexpander exhausting to atmosphere
- High voltage (230 kV) transformer and transmission
- Balance of plant including ammonia absorption chiller for alternative cooling, molten salt storage and heat exchange, piping, instrumentation

6.0 Columbia Hills Site Design and Analysis

Globally, only two operating CAES facilities exist: the 290-MW Huntorf, Germany plant, which began operations in 1978, and the 110-MW McIntosh, Alabama plant, which began operations in 1991. Both facilities store air in solution-mined salt caverns that were constructed specifically for compressed air storage. Both CAES facilities are single-shaft plants that employ multi-stage compressors for air injection and use reheat cycle combustion turbines for power production from the extracted air. The McIntosh plant also contains a recuperative heat exchanger on the low-pressure turbine exhaust, which improves the plant's overall heat rate. Generic examples of the two reference plants are included in Figure 59 and Figure 60. These plant designs were used as reference points for the design of the CAES plant at the Columbia Hills site.

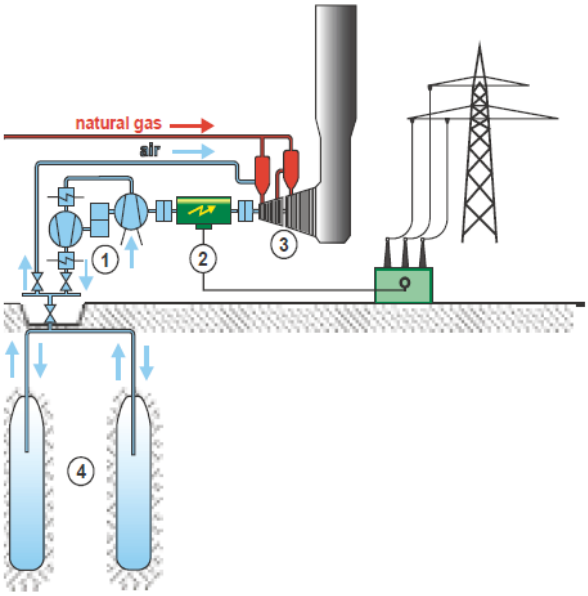

Figure 59. Schematic of the Huntorf CAES facility

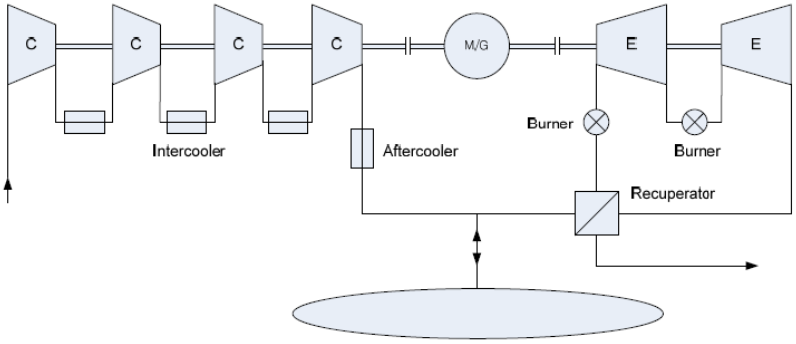

Figure 60. Schematic of the McIntosh CAES facility

6.1 Plant Design Assumptions

The concept of generating power from stored compressed air is predicated on the subsurface evaluations described previously. The feasibility of compressed air storage is contingent on an appropriately characterized reservoir that enables short-term storage (days and weeks vs. months) of the compressed air, and routine cycling between injection and extraction. Based on subsurface characterization models, it is appropriate and therefore assumed that the subsurface reservoir is capable of this type of cyclic operation once the initial subsurface air bubble is established during the continuous injection only cycle, which would occur in springtime.

6.1.1 Injection

As previously discussed (Section 3.4), subsurface modeling quantified the maximum amount of air that could be injected continuously over a 30-day period without fracturing the reservoir. Four wells could be used at the Columbia Hills site while maintaining a linear increase in the amount of air that could be injected. With Wells 5 through 7 indicating diminishing storage capacities, plant simulations assumed injection and extraction from four wells and the corresponding maximum air mass.

In addition to determining the total mass of air and number of wells, the hydrogeologic model and subsurface reservoir characteristics also helped to frame the CAES facility by quantifying well depth and spacing, the maximum injection and formation pressures, and necessary attributes of the compressed air recovery cycle such as well bottom pressure. From a physical layout perspective, the four wells were located linearly on 2,000-m centers, and the CAES facility was centrally located between Wells 2 and 3 to minimize piping runs and capital cost as seen in Figure 61.

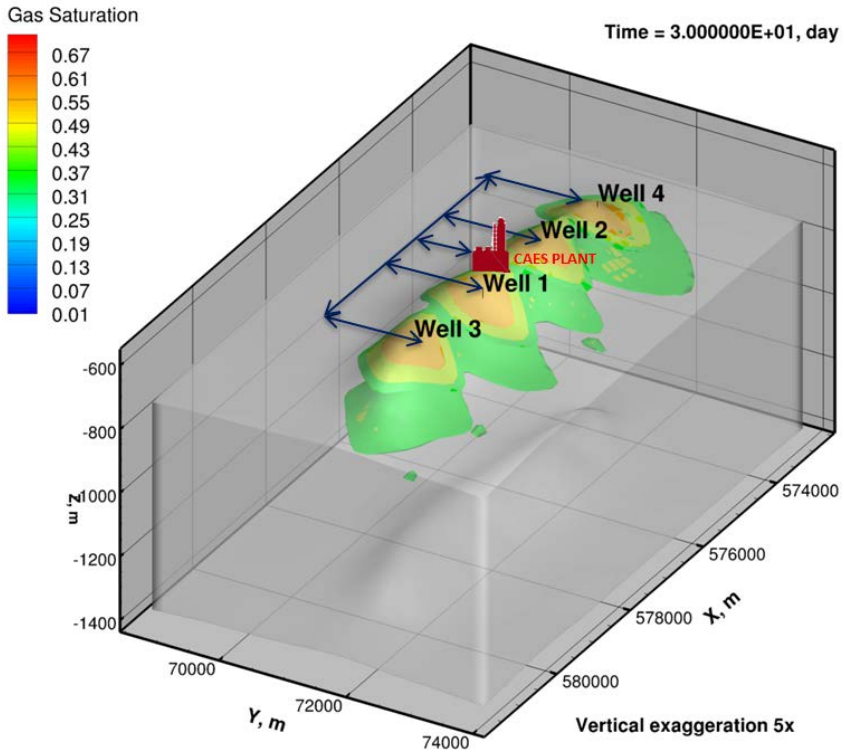

Figure 61. Well field conceptual layout

The subsurface model provided several governing attributes that informed the CAES facility simulation, such as initial formation pressure (1,200 psia), injection pressure at the bottom of the well (1,800 psia), and extraction pressure at the bottom of the well (600 psia). For continuity, all four wells were considered to have a drilled depth of 2,800 ft.[1] Collectively, the values served to help quantify the required compressor discharge pressure (adjusted to obtain bottom of well pressure), as well as the simulated mass flow rate and pressure of the compressed air during the extraction cycle.

For both the subsurface model and CAES facility simulation, injection rates were held at 2.8 million pounds (Mlb) per hour (353 kg/s), though subsurface modeling did indicate some variability over the 30-day initial injection period (see Figure 31).

6.1.2 Extraction

For simulation purposes, determining the minimum acceptable extraction flow rate and duration required reconciling several variables. The first variable was the effect of flow rate on turbo-expander and power turbine output. As mass flow machines, a large decline in available air flow or pressure from the reservoir would cause the total power output to decrease significantly as well as affect the round trip heat rate and plant efficiency. Considering nearly all commercially available machines do have adequate turn-down capability, it was necessary to ensure that on-peak power generation needs could be met with adequate extraction air flow. As a single event, this represented a minimum of 4 hours continuous operation analogous with high-load hours experienced in the afternoon and evening. Analysis of the

[1] STOMP model maximum well depths: Well 1 (2,763 ft), Well 2 (2,719 ft), Well 3 (2,719 ft), Well 4 (2,863 ft)

extraction air flow rate over this period indicates that essentially 100% of the flow can be maintained for this period (a reduction of 1.2%) over any 4-hour period assuming no reinjection has taken place. Consideration was also afforded to potential dual peak days where capacity might be utilized for one peak in the morning and one peak in the evening for a total of 6 hours of operations.

As indicated in Figure 32, the extraction flow rate decreases steadily down to approximately 200 kg/s assuming the reservoir starts off "full" and at constant formation pressure and extraction is continuous without shut in periods. Additional simulations would be required to ascertain whether extraction rates recover after extended shut in periods. For the present analysis, it was assumed that the extraction rate would follow the same decline curve irrespective of shut-in periods that would occur in an actual operating scenario. Considering a maximum of 6 hours operation per day for a 30-day period (assuming no reinjection), the capacity of the turboexpander and power turbine was fixed (206 MW) based on the minimum acceptable flow rate of 1.5 Mlb/hr (189 kg/s), or 37,000 MWh. Hence, over this 30-day period, 23% of the original energy of compression is recovered. This air flow is comparable to a Frame 6 power turbine (ISO flow at 1.6 Mlb/hr is reasonably close to the 1.5 Mlb/hr at Columbia Hills site conditions) (BROOKS, 2000).

6.1.3 Well Bore Diameter

An analysis was performed to understand the effect of well bore diameter on compressed air recovery. The air injection model assumed a casing diameter of 6.125 inches. To initiate the extraction simulation, and in light of trying to utilize a single bore and casing string for injection and extraction, a 6.25-inch production string was simulated at the prescribed air flow of 375,000 lb/hr in each of the four wells with a well bottom pressure of 600 psia. The simulation failed due to a choking condition in the production string. To ensure adequate air flow could be maintained to the CAES plant, the sensitivity analysis compared air flow and power output to pipe diameter as seen in Figure 62.

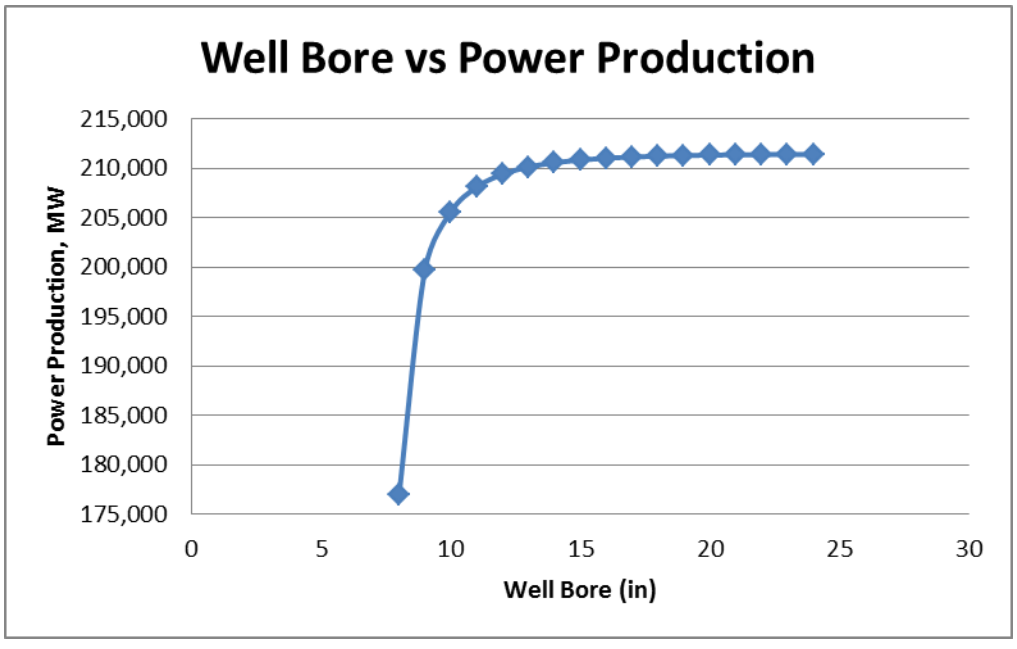

Figure 62. Gross power vs. well bore diameter

The results indicated that a 10- to 12-inch casing diameter would allow adequate air flow to the turbo-expander and power turbine to the point where larger diameter casings would not necessarily be advantageous relative to cost. Reservoir simulations showed that because the screened formation interval is relatively short at the Columbia Hills location, the impact of increasing the wellbore size from 6 inches to 12 inches had very little impact on the air injection/extraction rates.

6.2 CAES Plant Model and Aspen Plus Simulation

Discrete models were developed for the injection and extraction cycle, the CAES plant, and the water balance including cooling tower used for interstage cooling of the compressor. Aspen Plus was used to perform the simulations bound by the assumptions provided in Section 3.1. The goal of the simulation was to demonstrate behaviors of the entire system operating in steady-state condition at a specific site rather than to provide exact numeric and economic values over a wide range of potential operating scenarios. The results are valuable in that they address whether a CAES plant can be operated in a specific location with a specific subsurface geology, and the constraints therein.

6.2.1 Injection and Extraction Simulation

The accompanying material balance with relevant streams identified is provided in Table 5. For the injection cycle, the pipeline from the compressor (Stream 100) would supply a total of 2.8 Mlb/hr with a compressor discharge pressure of 1,677 psia corresponding to an injection pressure of 1,800 psia at the well bottom. The compressor air flow would be divided (Stream 120), distributed equally among the four wells (Stream 111), and injected into the formation (Stream 101). Pressure differentials were calculated based on proposed depth of wells, and piping distances between the injection locations.

The extraction cycle assumes a formation pressure of 1,200 psia, and a well bottom starting pressure of 600 psia. This provides a surface pressure of 519 psia (Stream 200), and a supply of 375,000 lb/hr from each well. At the surface (Stream 211), flow is combined from a pair of wells (Stream 240), and then combined with flow from the other pair of wells for a total flow to the recuperator of 1.5 Mlb/hr at 519 psia (Stream 200).

Table 5. Material balance for injection and extraction

Stream	100	101	111	120	200	201	211	240
Temperature (°F)	105	105	105	105	105	105	105	105
Pressure (psia)	1677	1799	1673	1677	519	600	522	519
Mass Flow (lb/hr)	2,799,997	699,999	699,999	1,399,998	1,500,000	375,000	375,000	750,000

The process flow diagram of the injection and extraction modeled in the Aspen Plus simulation is provided in Figure 63.

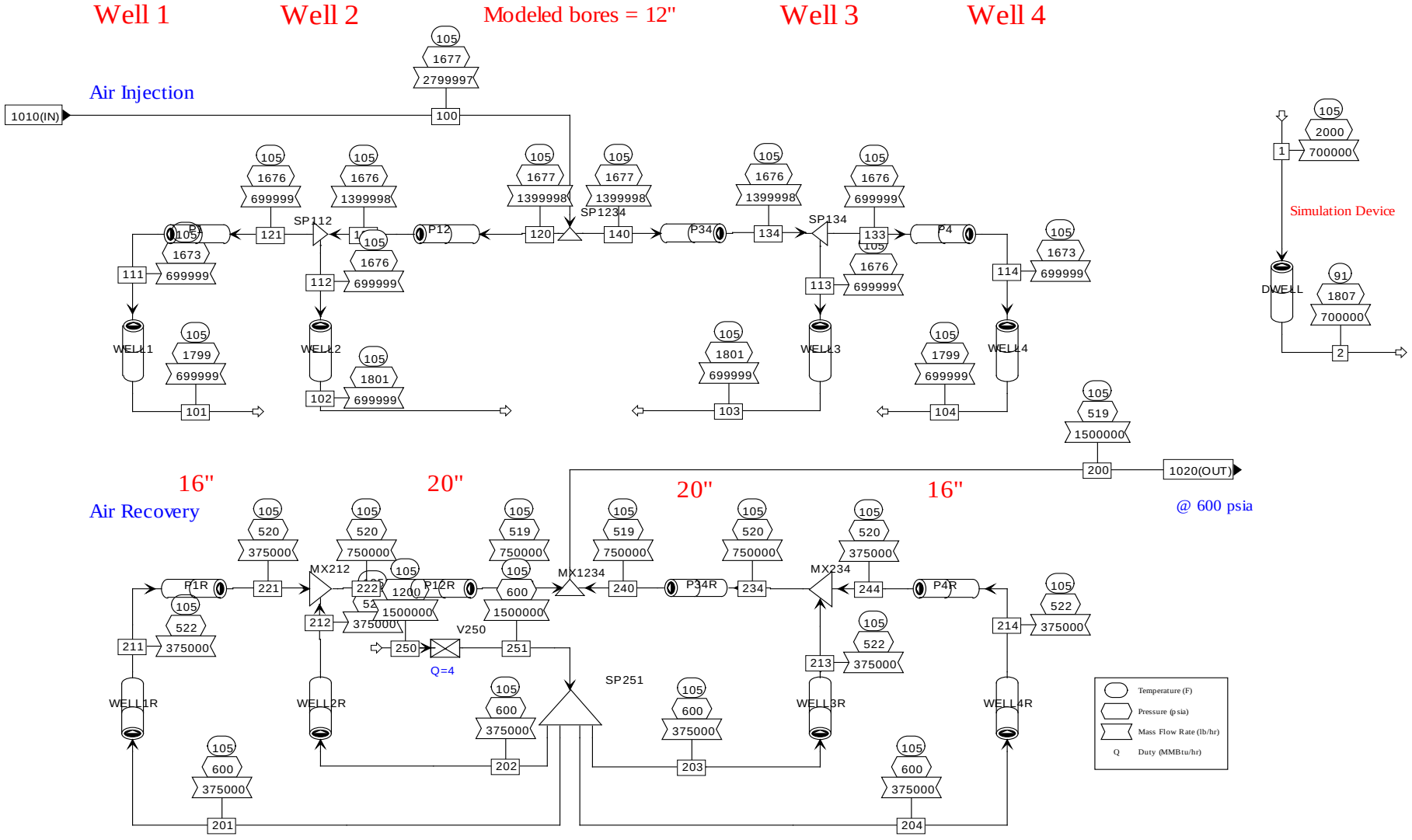

Figure 63. Injection and extraction process flow diagram

6.2.2 CAES Plant Simulation

The CAES plant model is configured similarly to the successfully operated McIntosh, Alabama plant, with the following notable exceptions. Air compression at the Columbia Hills location is performed with a multi-stage centrifugal compressor with more intercooled stages (6) than the McIntosh plant, which has a combination of a multi-stage axial flow compressor (analogous to a combustion turbine compressor) followed by two high-pressure centrifugal stages. Utilizing centrifugal compression with more intercooled stages reduces the gross energy demand of the machine and therefore improves operating efficiency. This, however, increases the capital cost and cooling water demand when compared to the McIntosh plant. Also, a higher turbine inlet temperature is assumed, which increases the gross power output of the power turbine. The power turbine capacity of the CAES plant was not prescriptively assigned; rather, it was sized to correspond to the extraction flow rate from the reservoir assuming a minimum well bottom pressure of 600 psia. In this configuration, the power turbine receives pressurized, heated air from the reservoir via the recuperator. The power turbine therefore does not require a compressor for the delivery of combustion air, nor is it subject to the energy penalty normally associated with operation of the compressor. The output of the power turbine is therefore significantly higher than a traditional compressor/power turbine layout, but is otherwise configured with supply and discharge conditions that are similar to conventional turbo-machinery. The CAES plant modeled has discrete operating units for compression and generation; the McIntosh plant is a single-shaft machine utilizing clutches to engage the motor/generator. For the plant capacity offered in this model, clutches of the appropriate size were considered prohibitively large, whereas the conventional machinery proposed is commercially available. The above exceptions were based on currently established equipment limitations; to verify the equipment choice and operating conditions, further consultation with original equipment manufacturers would be necessary.

The process flow diagram of the CAES plant modeled in the Aspen Plus simulation is provided in Figure 64. Starting with the supply of ambient air at ISO conditions, the air compressor (228,670 kW) receives filtered air and a small amount of fogging water (Stream 1008), compresses it, and supplies the well field (Stream 1010) with 2.8 Mlb/hr at 1,677 psia. Condensate collected during the compression cycle is provided to the cooling tower at approximately 33 gpm.

From the reservoir (Stream 1020), the compressed air is supplied to the recuperator (HRU1030); the flow (Stream 1030) is supplementally fired with a small amount of natural gas (Stream 1004) to meet appropriate inlet conditions (Stream 1035) of the 28,109 kW axial flow, hot gas turboexpander (CT-1040) (DRESSER-RAND, 2007). Turboexpander discharge at 1,015°F (Stream 1040) is refired with natural gas (Stream 1002) to supply the 177,283 kW power turbine (CT-1050) with 1.54 Mlb/hr of 2,429°F combustion gas (Stream 1045). Exhaust from the power turbine (Stream 1050) flows to the recuperator, which recovers 360 million British thermal units (MMBtu) per hour. Final stack conditions (Stream 25) are 1.54 Mlb/hr of exhaust flow at 240°F.

Minor auxiliary loads such as lube oil pumps and heat exchange equipment (pumps or fans) for generator cooling would be expected in a plant with this configuration. These systems would not be expected to contribute significantly to parasitic loads and are therefore not included in the simulation. The accompanying material balance with relevant streams identified is provided in Table 6.

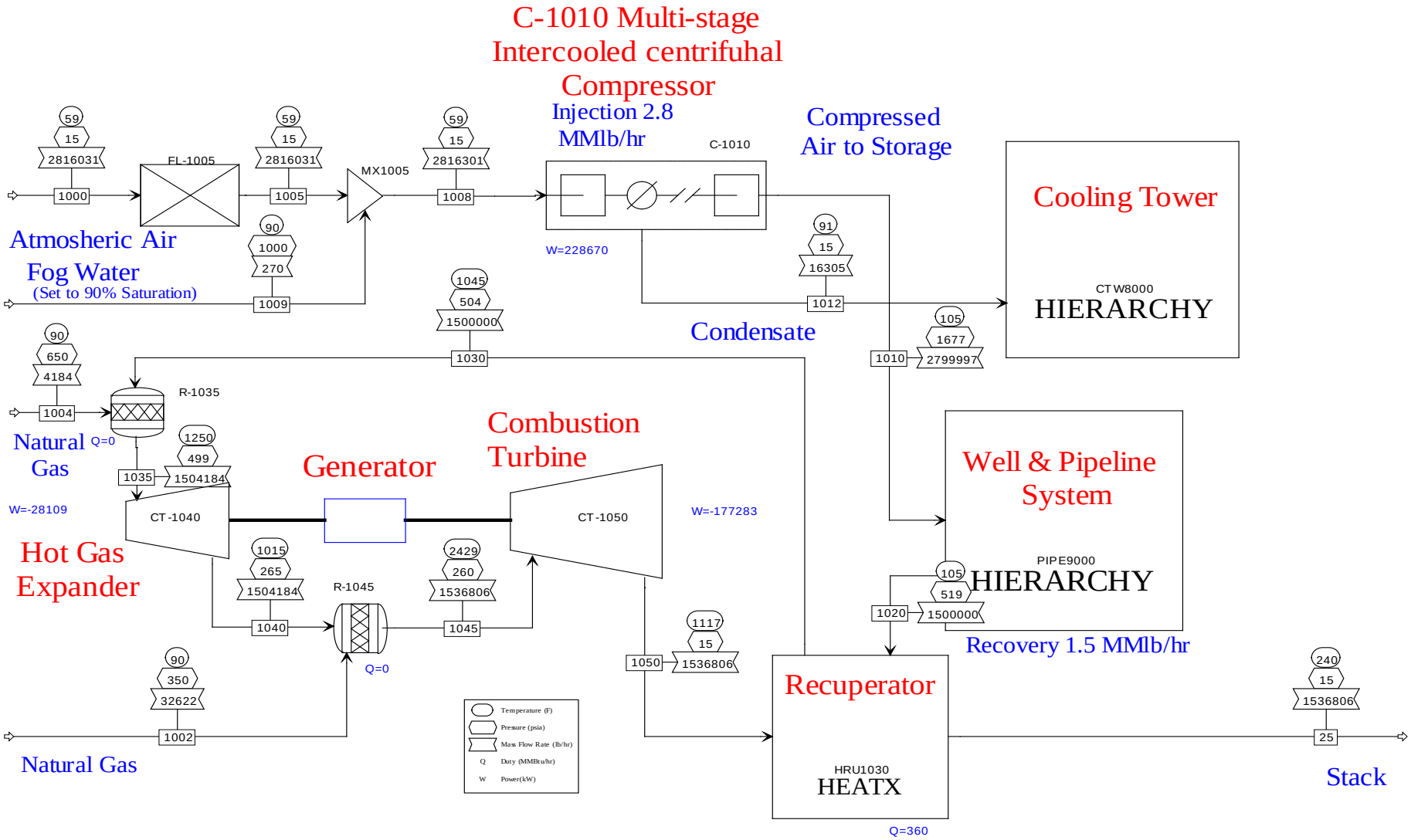

Figure 64. CAES plant process flow diagram

Table 6. Material balance for CAES plant

Stream	25	1002	1004	1008	1010	1020	1030	1035	1040	1045	1050
Temperature (°F)	240	90	90	58.6	105	105	1045	1250	1015	2429	1117
Pressure (psia)	14.8	350	650.0	14.6	1677	519	504	499	265	260.0	14.8
Mass Flow (lb/hr)	1,536,806	32,622	4184	2,816,301	2,799,997	1,500,000	1,500,000	1,504,184	1,504,184	1,536,806	1,536,806
Enthalpy (MMBtu/hr)	-772	-62	-8.0	-121.8	-18.4	-1.3	358	350.3	254	192	-413

6.2.3 CAES Plant Water Balance

Due to the large compressor load and intercooling requirements, a water balance was simulated to indicate potential water demands from the plant in addition to describing auxiliary motor loads such as recirculating water pumps and cooling tower fans. For a plant of this size, understanding the water balance was also a useful consideration in terms of siting and operations as the duty on the air compressor at almost 800 MMBtu/hr (ED 8080) would require a significant volume of water.

The water balance simulation was based on a 20°F cooling tower range (inlet – outlet), and a 20°F range on air compressor heat exchangers. Based on those assumptions, the cooling tower required 1,498 gpm of make-up water (Streams 8005 and 1012) to accommodate the compressor intercooling duty provided above. The recirculating water rate was 79,600 gpm (Stream 8023). For water discharge purposes (cooling tower blowdown), the simulation assumed 5 cycles of concentration in the cooling tower, which could be expected utilizing Columbia River water as the source. At 5 cycles of concentration, 300 gpm of cooling tower blowdown was produced (Stream 8063). Auxiliary loads include cooling tower fans at 1,243 kW, and recirculating cooling water pumps at 1,592 kW.

Given the proximity of the Columbia Hills locations to existing agricultural land, it would be reasonable to expect that during a significant portion of the year the cooling tower blowdown could be utilized for irrigation purposes, rather than discharged to a non-secondary use source. This activity is currently being done by two combined cycle power plants in the same geographic area as the proposed location, and would likely aid in the permitting process.

The material balance with relevant streams identified is provided in Table 7.

Table 7. Material balance for water and cooling system

Stream	8005	1012	8023	8063
Temperature (°F)	68	91	60.2	60.2
Pressure (psia)	30	15	14.31	44
Mass Flow (lb/hr)	748,751	16,305	39,784,017	149,750

The process flow diagram of the water balance and cooling system modeled in the Aspen Plus simulation is provided in Figure 65.

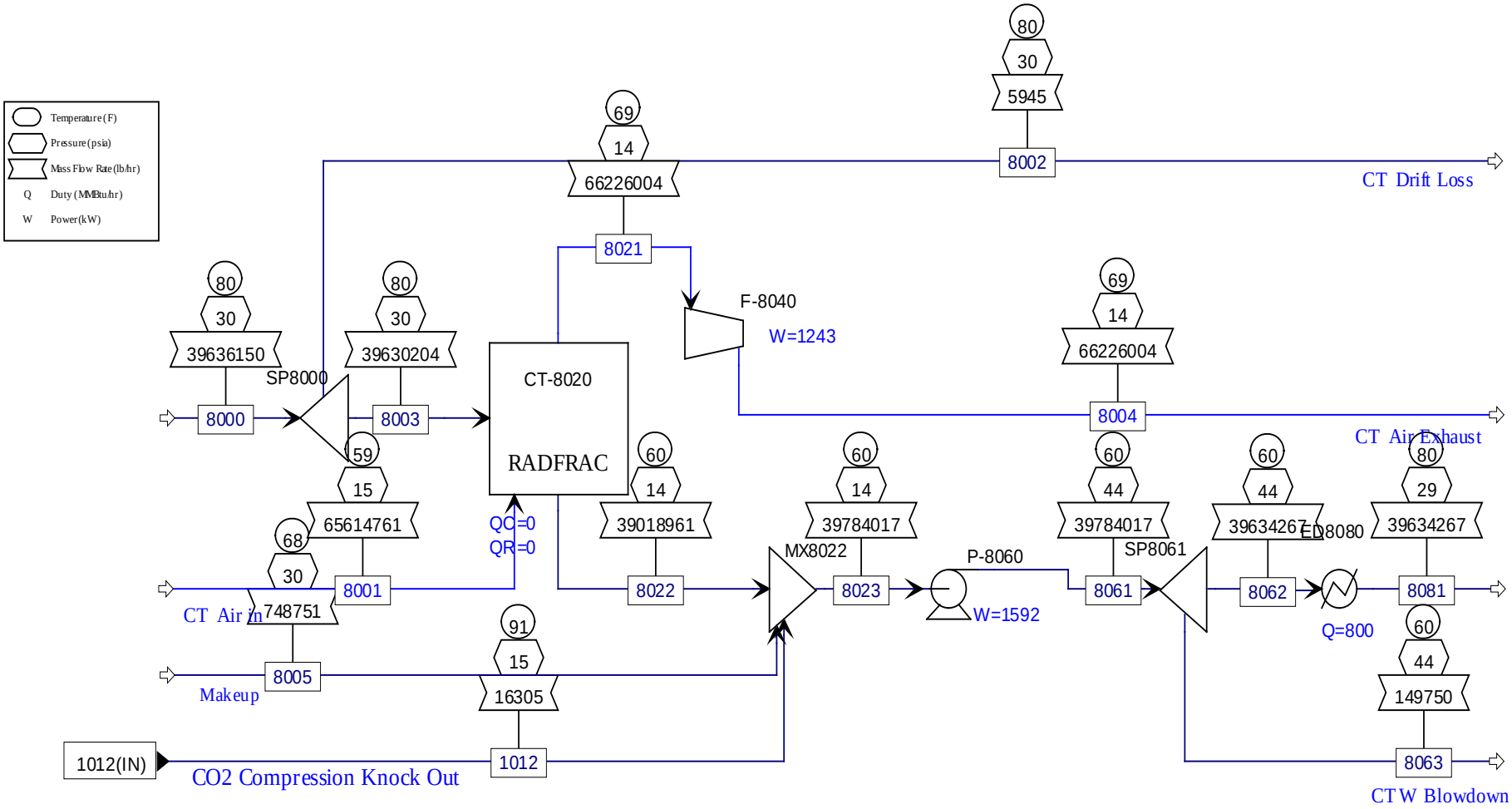

Figure 65. Compressor cooling water process flow diagram

6.3 Plant Operations

Operation of the energy storage facilities is predicated on being able to address two fundamental needs:

- Short-term storage and utilization of excess hydro (or wind) energy that would otherwise be lost to excess spill or environmental re-dispatch
- Capitalizing on daily pricing arbitrage between low-load and high-load hours, or use as a peak-shaving mechanism

Additional operating scenarios could be considered, such as balancing, spinning, and non-spinning reserves, as well as capacity based payments. A review of publically available literature indicates that conventional CAES plants (natural gas fired) are being designed to meet full load production within 10-minute response time standards. The non-thermal unit (compressor) would be expected to be operating well within the response time required (DRESSER-RAND, 2010; GE-ENERGY, 2013). However, given the size of the power turbine (analogous to a Frame 6F unit), and the known impact of start equivalencies on service and maintenance intervals (as well as load and fired hours), it is recommended that determining best use of the capacity (energy production, spinning reserve, non-spinning reserve, etc.) should be done in conjunction with the original equipment manufacturer. Best-use and additional revenue sources are discussed qualitatively in Section 8.0.

6.3.1 Capacity and Heat Rate

For the purposes of this section, steady-state operations were considered reflective of the plant configuration evaluated in Section 6.2. Table 8 provides a list of inputs used to calculate gross output and energy production, calculated heat rate, and emissions.

Table 8. Flow sheet load and duty

Description	Duty (MMBtu/hr)	Usage (kW)
Power Consumption		
Air Compression	779	228,177
Cooling Tower Fan	4	1,240
Cooling Tower Pumps	5	1,588
TOTAL		231,005
Power Generation		
Turboexpander	100	29,251
Combustion Turbine	605	177,312
TOTAL		206,562

The calculated heat rate based on natural gas combustion (HHV basis) is provided in Table 9.

Table 9. Calculated CAES heat rate

Description	Flow Rate (lb/hr)	Output (kW)
Combustion Turbine	32,622	177,312
Turboexpander	4184	29,251
TOTAL	36,806	206,562
Natural Gas	22,841 Btu/lb	
Fuel Consumption	841 MMBtu/hr	
Gross Generation Heat Rate	4,070 Btu/kWh	

As calculated, the heat rate of 4,070 British thermal units per kilowatt-hour (Btu/kWh) very closely aligns with published information for expander-combustion turbine generator sets operating during the generating cycle (EPRI, 2002). In light of the non-thermal-based generating resources available in the BPA balancing authority area, the effect of the compressor load on the net round-trip heat rate is worth discussion as well. Review of 2011 and 2012 BPA total load and generating resource data indicates that of the average 14,000+ MW total (including Interchange), approximately 88% are derived from non-thermal resources (hydro and wind) (BPA, 2012a). While additional thermal resources are utilized in the area (fossil and nuclear) and contribute to the regional heat rate (such as those owned by investor owned utilizes and publically owned utilities), from a percentage standpoint, the compressor would likely be consuming power that was predominantly generated by hydro and wind capacity thereby maintaining an aggressive net heat rate.

6.3.2 Energy Production

Operationally, the CAES plant envisioned at Columbia Hills would have at least two distinct compression and extraction cycles. The first cycle addresses utilization of excess grid capacity during springtime runoff events, or periods of acute oversupply of power. This is currently framed as continuous compression for a 30-day period, followed by generation only for 50 days at 6 hours per day.[1] Based on the selected machine capacities, the compression only cycle would consume approximately 164,000 MWh of grid-supplied energy. The generation only cycle was based on the minimum stable extraction flow rate from the reservoir, over a period of 50 days post-injection, and would recover approximately 62,000 MWh by operating 6 hours per day aligned with high-load hours, or 38% of the original energy investment. For an additional data point, breakthrough as reviewed in Section 3.4.2 indicated the potential to run for up to 80 days without reinjection; this is equivalent recovery of 99,150 MWh or 60% of the original energy investment. From a reservoir management standpoint, it would certainly be advantageous to extend the generation-only timeframe as long as feasible to recover the highest percentage of megawatt-hours prior to transitioning to diurnal operations. This would also be required prior to continuous compression, which would occur in the spring.

To maintain stable reservoir capacity over time, diurnal operation of the plant is based on the flow rates modeled for injection and extraction cycles, and adjusted for duration. Steady-state operation of the plant assumes 3 hours of compression (693 MWh), and approximately 5 1/2 hours of generation (1136 MWh) per cycle for a net generation of 443 MWh, or a net energy ratio of 1.67:1 (kWh produced/kWh consumed).

[1] Framed in Section 3.4.2; representing conservative duration with limited impact to well bottom pressure, although 80 days extraction was observed until complete breakthrough.

Based on this operations model, about 55% of the original working volume would be unrecoverable. The stored energy could theoretically be reduced by extracting air and generating power without reinjection, which would need to be done to the greatest extent possible prior to spring to accommodate runoff or excess capacity issues. It is also proposed that a minimum working supply of compressed air would need to be maintained in the reservoir at all times to maintain the reservoir conditions (formation and well bottom pressures), as well as meet minimum flow requirements for the power train if being used for balancing or peak shaving. These conditions are addressed in Section 3.4.2.

An additional distinction is that the operational scenario is only reflective of Year 1. Qualitatively, once the initial working and cushion volume is established in the reservoir, ensuing compression activities (in Year 2 through Year *n*) would be expected to enable a longer drawdown of the compressed air reservoir prior to reinjection. Though this scenario was not modeled, this could potentially enable a higher recovery of stored MWh's during the first post-injection duration.

6.4 CAES Capital and Levelized Costs

The cost estimate used a variety of resources reflective of the level of definition afforded to each project area. Where process units were defined and simulated, the Aspen Process Economic Analyzer (Aspen IPE) V7.3 was utilized. This included the CAES plant, cooling water system, and well field compressed gas supply and distribution piping. Site civil, mechanical, and electrical requirements were determined using factored estimates from Aspen IPE templates assuming an undeveloped greenfield site. Where Aspen templates did not have costs for individual equipment pieces such as axial compressors, turbo-expanders, and generator step-up transformer, the template was augmented with factored estimates from publicly available literature or similar plant. Costs for the injection and extraction wells were provided by a drilling contractor based on a 12-inch production string. Transmission and interconnection costs were provided by BPA. All capital costs are in overnight 2012 dollars (2012$). Gas and water connections were not determined or provided for the estimate.

The estimate is framed against the Association for the Advancement of Cost Engineering (AACE, 2005) requirement for a Class 4 estimate, which can have a range of estimate accuracies. The level of estimate chosen for this activity was -20% to +40% representative of a conceptual study characterized by vendor supplied information and process flow diagrams for the main CAES facility. The overall estimate is broken into three elements consistent with the segregated portions of project, including well field drilling and development, compression and generation (CAES plant), and transmission and interconnection. Table 10 provides a summary of estimated capital costs and cost per kilowatt.

Table 10. Estimated capital costs for CAES plant at Columbia Hills

Description	Total ($ million)
Well Drilling and Development	11.2
CAES Plant	207.5
Transmission and Interconnection	10.9
TOTAL CAPITAL COST	229.6
TOTAL GENERATION (kW)	206,500
TOTAL CAPITAL COST/kW	$1,112

Additional costs such as environmental surveying and permitting if environmentally or culturally sensitive areas are identified, well drilling and well injection permitting relative to the final location and well classification, and interconnection studies should be expected as well. Based on similar development activities, these costs are considered to be minor contributors to owner cost requirements for the development of the project at any location and are expected to be less than 1% of the total capital required (NETL, 2012).

6.4.1 Well Field Drilling and Development

Drilling and well development cost information was completed by PNNL in conjunction with a drilling contractor. The primary impacts to total cost are depth of drilling required, pipe diameter size, and length of pipe. Costs for the 4-well field were based on a 13-3/8-inch casing string for each well, and included budgetary line items for mobilization, drilling, well build out, and additional job cost categories such as drilling water and fluid containment. Additional costs would be expected to be incurred such as permitting and formal well completion, as well as costs associated with drilling such as wireline logging, mud logging, and formation testing. These additional costs are not provided at this time. The itemized estimate is provided in Table 11.

Table 11. Well drilling estimate for Columbia Hills locations[1]

Description	Cost per Well ($ thousands)	Total ($ thousands)
Mobilization	100	400
Drilling		
36” Hole and Cement to Surface	50	200
28” Drill to 1000’	658	2632
19” Drill to 3000’	950	3800
Well Build		
Furnish/Install 20” Casing	155	620
Furnish/Install 12” Casing	300	1,200
Cement Each Casing to Surface	248	992
Additional Job Costs	57	228
Subtotal Direct Costs	2,518	10,072
Engineering and Design		1,100
Total		11,170

The preceding compares favorably to an EPRI estimate for naturally occurring porous rock/aquifer reservoirs at $0.10/kWh of stored energy (EPRI, 2002). With the initial storage estimate of approximately 160,000 MWh, the Columbia Hills location would be approximately $16 million.

6.4.2 CAES Plant

The cost estimate contained herein was based on the configurations provided in Section 6.2.2 and includes the well field, compression and generation cycle, and balance of plant items such as buildings, fencing, and roads. Where necessary, specific pieces of equipment such as generator step-up transformer were determined using a factored estimate from a similarly sized transformer (13.8/230 kV), and escalated to 2012$. Table 12 includes costs for the CAES facility as calculated.

[1] Boart Longyear Drilling Services cost estimate. November 2012.

Table 12. Overnight capital cost of CAES facility

Project Title:	PROJECT:			***Scenario Name:***	Low Flow	
Project Name:	CAES System Columbia Hills					
Proj. Location:	North America	***Job No:***	--	***Prep. By:***	--	
	25NOV12				DOLLARS	
Estimate Date:	18:35:30	***Est. Class:***		***Currency:***	USD	
Account	MH	Labor Cost	Matl Cost	Total Cost	Percentages	
(2) Equipment	13,529	676,467	102,675,848	103,352,315	70.7%	of TDC
(3) Piping	100,057	5,002,842	11,951,615	16,954,457	11.6%	of TDC
(4) Civil	104,051	5,202,527	6,111,861	11,314,388	7.7%	of TDC
(6) Instruments	5,080	253,981	813,430	1,067,411	0.7%	of TDC
(7) Electrical	42,698	2,134,915	10,498,286	12,633,201	8.6%	of TDC
(8) Insulation	2,093	104,671	80,188	184,858	0.1%	of TDC
(9) Paint	9,583	479,172	180,953	660,125	0.5%	of TDC
						of TDC
Total Direct Field Costs	**277,092**	**13,854,575**	**132,312,179**	**146,166,754**	100.0%	of TDC
	(TDMH)	(TDL)	(TDM)	(TDC)		
Indirect Field Costs	**36,869**			**2,974,900**	21.5%	of TDL
	(IFMH)			(IFC)		
Total Field Costs	**313,961**			**149,141,654**	71.9%	of TIC
	(TFMH)			(TFC)		
Freight				5,292,500	4.0%	of TDM
Taxes and Permits				8,269,500	5.7%	of TDC
Engineering and HO	38,881			4,038,900	1.9%	of TIC
Other Project Costs				9,143,506	4.4%	of TIC
Contingency				31,659,490	15.3%	of TIC
Total Non-Field Costs	**38,881**			**58,403,896**	28.1%	of TIC
	(HOMH)					
Project Total Costs				**207,545,550**	142.0%	of TDC

The breakdown of significant cost contributors is heavily weighted to the equipment area where the combustion turbine, expansion turbine, generator, and compressor costs combined make up the highest percentage of the total. Additional costs for cooling towers, recuperative heat exchanger, and rotating equipment spare parts rounds out the cost area. The bulk of the piping costs are for the straight runs of 16- and 20-inch Sch. 100 pipe lengths between the CAES plant and the well field, and associated field erection activities. Electrical costs are predominantly weighted towards transformer and breaker requirements, as well as high voltage distribution wire.

Considered in isolation (without additional transmission and well field costs), the capital costs for the proposed CAES facility compare favorably to analogous generation resources such as natural gas combustion turbines, and natural gas combined cycle which range from $750/kW to more than $1,000/kW. Though there is no definitive like-for-like comparison available for CAES plants, given the high percentage of conventional machinery in the design, the capital cost of $1,005/kW is well within the margin of error described for this analysis.

6.4.3 Transmission and Interconnection

Switching, transmission, and interconnection costs were provided by BPA.[1] The estimate included details regarding geographic location of the sites and required lengths of laterals; options for interconnection voltages depending on the size of the generators (230 or 500 kV); and points of interconnection into existing substations or where necessary the cost of new substation. Annual operations and maintenance for each option was also included.

The gross capacity provided in the simulation aligned closely with the selection criteria that determined the step-up transformer output; therefore, the capital cost estimate considered the 230 kV option as the most representative of a likely configuration. For comparative purposes, both kilovolt ratings are provided. Table 13 provides summarized interconnection costs by geographic area including provisions for right-of-way, cost of substation or switching (where available), total length of laterals and transmission line cost, access roads, and overheads.

Table 13. Interconnection costs by kV rating

Location	230 kV ($ million)	500 kV ($ million)
Columbia Hills	10.9	54.1

The low voltage (230 kV) point of interconnection at the Columbia Hills location is assumed to be the existing Horse Heaven substation. As indicated in Table 13, the cost provided is an average of two potential configurations: one configuration assumes a new switching station and tapping into existing 230-kV lines and the other assumes construction of a new substation. Both Columbia Hills locations would require approximately 8 miles of new transmission line lateral for interconnection.

The high voltage (500 kV) point of interconnect at the Columbia Hills location is assumed to be a new switching station that would tap into the existing McNary-John Day 500-kV line. The high-voltage option includes the construction of a transmission line lateral of approximately 3 miles to the tie-in point on the existing line, and the new station.

6.4.4 Levelized Cost of Electricity

The CAES plant is the only technology that can provide significant energy storage (tens of thousands of megawatt-hours) at relatively low cost with practically unlimited flexibility for providing load management at the utility or regional levels. For the cost of electricity evaluation, the following parameters were used for the simplified LCOE (sLCOE) model and found in Table 14 (NREL, 2012).

[1] Electric Interconnection-4. BPA. October 2012 (proprietary).

Table 14. Simplified LCOE calculation for conventional CAES plant

Description	Value
CAES Project Capital Cost ($/ kW)	1,112
Project Lifetime (years)	20
Discount Rate (%)	4
Capital Recovery Factor	.074
Fixed O&M Cost ($/kW-year)	11.00
Variable O&M ($/kWh)	.003
Capacity Factor (%)	25
Heat Rate (Btu/kWh)	4070
Fuel Cost ($/MMBtu)	4.60
sLCOE (cents/kWh)	6.41

The following sLCOE model was used to calculate the price to produce electricity, which was adequate considering no project financial structures were known or proposed. The sLCOE was calculated as follows:

*sLCOE = {(overnight capital cost * capital recovery factor + fixed O&M cost)/(8760 * capacity factor)}+ (fuel cost * heat rate) + variable O&M cost*

Explanation of contributing data points is provided below:

- Overnight capital cost is the estimated total project cost measured in dollars per installed kilowatt ($/kW). This value was determined by Aspen IPE and supplementary cost information.
- A capital recovery factor CRF = {i(1 + i)^n} / {[(1 + i)^n]-1} is determined from specifying the project life and discount rate. This factor was calculated on a project life of 20 years and a discount rate of 4% commonly used for federal projects.
- Fixed O&M costs provided in dollars per kilowatt-year ($/kW-yr) and variable O&M costs in dollars per kilowatt-hour ($/kWh). These values were determined based on data obtained from the National Renewable Energy Laboratory (NREL) database for transparent costs (natural gas combustion turbines).[1]
- The capacity factor for the CAES plant was determined by estimating the total hours of generation expected over the course of a year.
- Fuel costs were determined from forward pricing curves from the U.S. Energy Information Administration's *Annual Energy Outlook* 2012 (delivered prices for electric power 2012).
- Heat rate was determined from the Aspen simulation; the calculated heat rates agree with estimations for conventional CAES plants available in public literature.

There are two significant impacts affecting the potential LCOE of the facility: the future price of natural gas, and the capacity factor. For comparative purposes, multiple curves are provided which demonstrate the impact of these conditions. Figure 66 demonstrates the impact of increased capacity factor (blue line) on the LCOE of the plant with two different compressor selections offered (red and green). The first Frame 6 type compressor option is representative of the compressor modeled in ASPEN. Based on utilization, a large aero-derivative compressor was also considered (capital impact only). At

[1] Open Energy Info Transparent Cost Database. Accessed at http://en.openei.org/apps/TCDB/.

approximately $20 million less than the Frame 6 compressor, the impact to LCOE was an improvement of 8% between the two options.

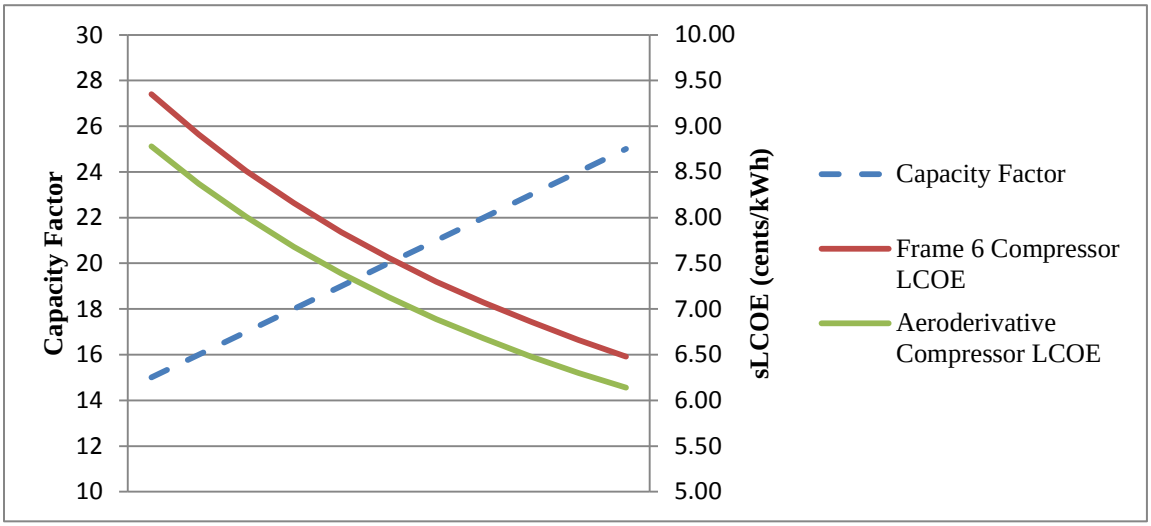

Figure 66. Impact of capacity factors on sLCOE for CAES plant

The second curve (Figure 67) considers the future price of natural gas obtained from EIA data (delivered cost/electric utility). The evaluation assumes the plant as modeled in ASPEN is the representative plant over the 20-year time frame.

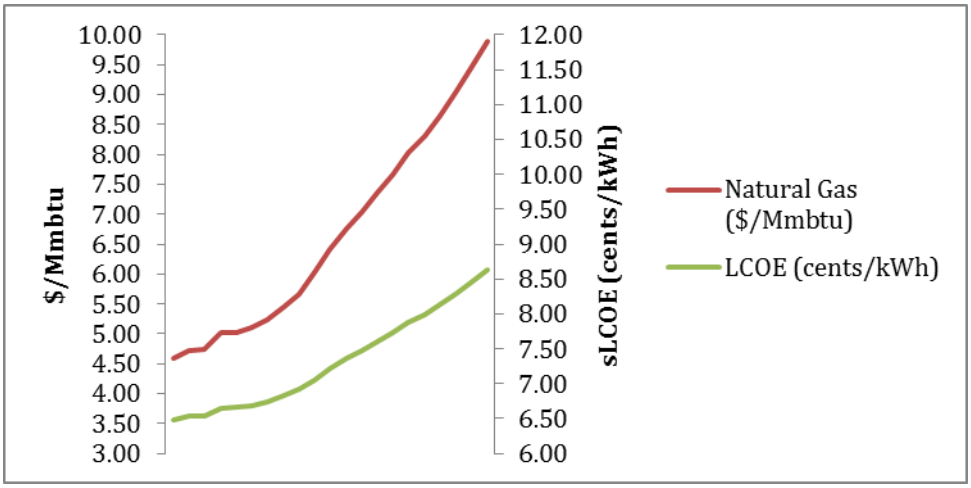

Figure 67. Impact of natural gas price on future sLCOE

Particularly relevant to the Northwest is a comparison of the CAES technology against other generating options in the region. For illustrative purposes, several options are provided as well as assumed capacity factors. Data used for the analysis included fuel pricing from EIA, and capital and operating data from the transparent database similar to the calculations provided for the CAES sLCOE evaluation.

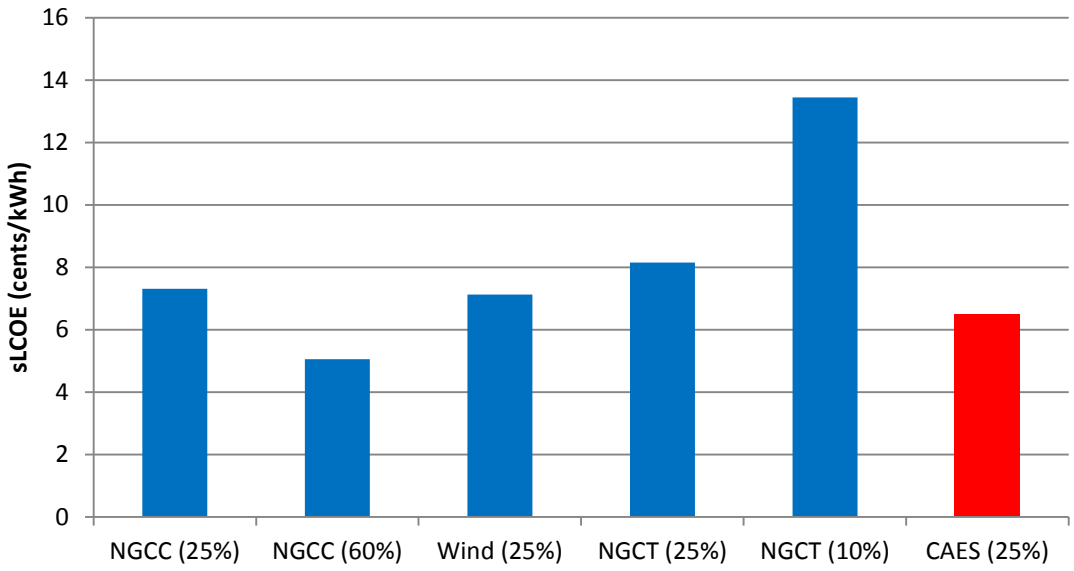

Figure 68. Comparative LCOE for new build generating options

The CAES plant designed for the Columbia Hills location is competitive against most *new-build* options available to the region, noting that the wind LCOE is "unsubsidized." The range of capacity factors offered for the natural gas fired facilities have both the baseline (25% capacity factor) for comparative purposes, and also what the capacity factors are more likely to be given the technology selection and typical dispatching scenarios (i.e., natural gas combustion turbines frequently have very low capacity factors as they are used for peaking duty). Perhaps the most useful observation is that the CAES plant, as designed, has a production cost that is competitive with all presented options, with exception to the higher capacity factor natural gas combined cycle. Considering the plant is capable of addressing multiple system level needs such as oversupply, on-peak power production, and balancing; the total value proposition would be even greater than the very reasonable cost of production.

7.0 Yakima Minerals Hybrid CAES Plant

The Yakima Minerals location was conceptually evaluated to determine if adequate thermal resources could be recovered and used to drive conventional turbo machinery. Here again, the subsurface conditions and parameters inform and control the surface facility design for aspects of flow, pressures, and temperature. Given the complexity of the collective design (surface and subsurface working together), the primary objective for the Yakima Minerals location was to evaluate potential configurations of a compressed energy plant utilizing geothermal heat recovery for power generation. Two plant designs were proposed for simulation: one that uses geothermal energy only for power generation and one that uses geothermal energy supplemented with recovered heat of compression. Given the unknown long-term impacts to the geothermal reservoir, neither configuration is necessarily optimized. However, the simulations do provide viable configurations of an adiabatic power plant utilizing geothermal resources, and where applicable, enable the identification and clarification of key mechanical and operational attributes.

7.1 Compression and Cooling Requirements

The hybrid CAES plant model began with a compressor configuration that was based on injection simulations and reservoir characteristics described in Section 3.0. The injection scenarios were conservatively bound by the formation fracture pressure. The initial injection scenario resulted in a calculated reservoir capacity of 2.4 MMT over 30 days of continuous injection, a corresponding compressor air flow of approximately 7.4 Mlb/hr, and well bottom injection pressure of 8,305 psia. Plant operations under these bounding conditions would have required an excessive amount of compression capacity (relative to generating capacity), a significant compressor cooling demand, and disproportionately large diameter piping to accommodate the compressor air flow both above and below ground. Accordingly, an iterative analysis was initiated to minimize compressor capacity, flow, and discharge pressure while still maintaining suitable subsurface reservoir conditions. The analysis also needed to demonstrate that the extraction and power generation cycle would not be materially impacted by the reduction in storage capacity. Based on the analysis, the final compressor configuration proposed includes a conventional 75-MW after-cooled axial flow compressor; followed by a 4-stage, 67-MW intercooled centrifugal compressor. Having determined the appropriate compressor configuration, multiple cooling options were considered including air-to-air, water-cooled, molten salt, and a geothermal driven ammonia absorption chiller.

Given the strict limits on cooling water expected at the Yakima Minerals location, two configurations of the hybrid CAES plant were developed. The first configuration uses a combination of air-cooling in conjunction with trim cooling provided by geothermal source driven ammonia absorption refrigeration during the compression (injection) cycle. For aftercooling the axial flow machine, air-to-air heat exchange is used to drop the compressor outlet temperature from 886°F down to approximately 140°F; the ammonia absorption chiller provides trim cooling to drop the compressed gas down to 105°F, which supplies ensuing compression stages. Likewise, at each stage on the centrifugal compressor, intercoolers utilize air-to-air heat exchange to reduce compressor outlet temperatures from approximately 300°F down to 140°F; and ammonia absorption heat exchange provides trim cooling to drop the compressed gas down to 105°F prior to supplying the next stage of compression.

Considering steady-state operations would most likely involve compression (and thereby cooling demand) during off-peak hours in the middle of the night, the air-cooled configuration could in theory capitalize on the lowest expected dry-bulb temperatures over the course of a day. An additional advantage to using dry-cooling is simply that it reduces the need for additional wells, pumps, piping, as well as reducing the thermal burden in the subsurface cooling reservoir. One disadvantage of using air-cooled heat exchange is the loss of compressor efficiency as the dry-bulb temperature increases, and increased parasitic load from cooling fin-fans. In the case of continuous compression over 30 days to store excess hydro capacity in the springtime, this could prove problematic if coinciding with unseasonably warm weather. Operationally, the impact could be moderated by lowering compressor output, or by operating only during times when the dry-bulb accommodated the load required. One additional consideration is that springtime dry-bulb temperatures are relatively mild (coinciding with the 30 days continuous compression); for conservative purposes, the simulations assumed a 90°F design dry bulb temperature, recognizing this value is conservatively higher than what would be expected.

The final cooling demand for ammonia absorption at steady state conditions is approximately 52 MMBtu/hr from the combined intercooler duty, and use of this configuration eliminates the need for compressor cooling water. Modeling further indicated that when balanced appropriately, the flow of geothermal water required for ammonia absorption refrigeration during the compression cycle is reasonably close to the flow required for the generation cycle. In this regard, only one set of geothermal wells (one extraction well and one injection well) would be constructed, and is expected to be utilized for both the compression and the extraction cycles. Additional details can be found in Section 7.3.

The second configuration proposed uses molten salt to capture and store the heat of compression produced by the axial flow compressor. This configuration is particularly valuable for diurnal type operations, where heat of compression can be captured and stored on the surface at temperature and used for reheat of compressed air during the power generation cycle. The use of molten salt can be considered as a “bolt on” type application; it capitalizes on the need to reduce compressor inlet air temperatures to the centrifugal machine, and is capable of capturing approximately 68% of the axial flow compressor duty before reaching material limitations (molten salt has a high freeze point).[1] Though air and ammonia absorption cooling is still required for the compressor train, the capture and use of heat of compression increases power output by 33% (from 62,447 to 83,138 kW). Additional details can be found in Section 0.

Respective of the location, an additional simulation addressed inherent advantages or disadvantages of siting with regards to elevation and impact to compression. Two plant site options were considered; one at 1,600 ft, which would require moving compressed air approximately two linear miles[2] to the injection/extraction wellhead at 3,100 ft; and one plant site on the top of the anticline at 3,100 ft, which would require no additional pumping of air. The simulation showed that there were slight advantages for the compressors (particularly the centrifugal) at the lower elevation and with larger distribution piping to the injection well (24 inches). The overall impact was negligible when simulated with the 20-inch diameter of pipe selected for the facility; the facility was modeled at the lower elevation (1,600 ft).

[1] HitecXL minimum operating temperature assumed to be 300°F.

[2] Two miles was considered the conservative distance required to locate the plant outside of any potential subsurface formation spill boundary and to limit formation interference between air and geothermal resources.

7.2 Injection and Extraction Simulation

With a common compressor train, both configurations of hybrid CAES plants were designed with similar injection and extraction parameters, and would utilize a single well bore for both cycles. There are distinctions, however, consistent with the alternate designs. The first configuration uses geothermal resources for power production in three low-temperature turbo-expanders; the flow rates therefore are maximized to provide usable heat in the power generation cycle. The second configuration has only one low-temperature turbo-expander utilizing geothermal resources, and one high temperature turbo-expander utilizing the molten salt; the geothermal flow rate in this case is about 20% less. Distinctions are provided in the following process flow descriptions.

Beginning with the injection cycle, the compressor would deliver approximately 1.2 Mlb/hr of 5,600 psia compressed air into the subsurface storage reservoir at a depth of 14,000 ft (Stream 200). This corresponds to a well bottom injection pressure of 7,200 psia (Stream 201), which is well above the formation pressure of 6,000 psia. The extraction cycle (power generation) assumes a flow rate of 1.2 Mlb/hr with a well bottom pressure of 4,800 psia and 350°F (Stream 250). Compressed air at the surface would be delivered to the first heat exchanger at slightly under 3,000 psia and 257°F (Stream 252).

Concurrent with the recovery of compressed air, the geothermal extraction cycle was simulated to provide 3,000 gpm (1.5 Mlb/hr) of 354°F water (Stream 260). At the surface, the geothermal water at 332°F and 400 psia (Stream 360) is fed to heat exchangers, and cross-exchanged with the compressed air. Once cooled, the water at 239°F (Stream 135) would be pumped back into the formation at a surface pressure of 2,000 psia, corresponding to a well bottom injection pressure of 8,000 psia (Stream 315). Figure 69 provides the conceptual process flow diagram of the compressed air and geothermal water injection and extraction cycles. As mentioned previously, the largest distinction of the molten salt supported adiabatic cycle is the lower demand for geothermal water indicated in Figure 70; the geothermal water supply drops to 2,400 gpm (Stream 260).

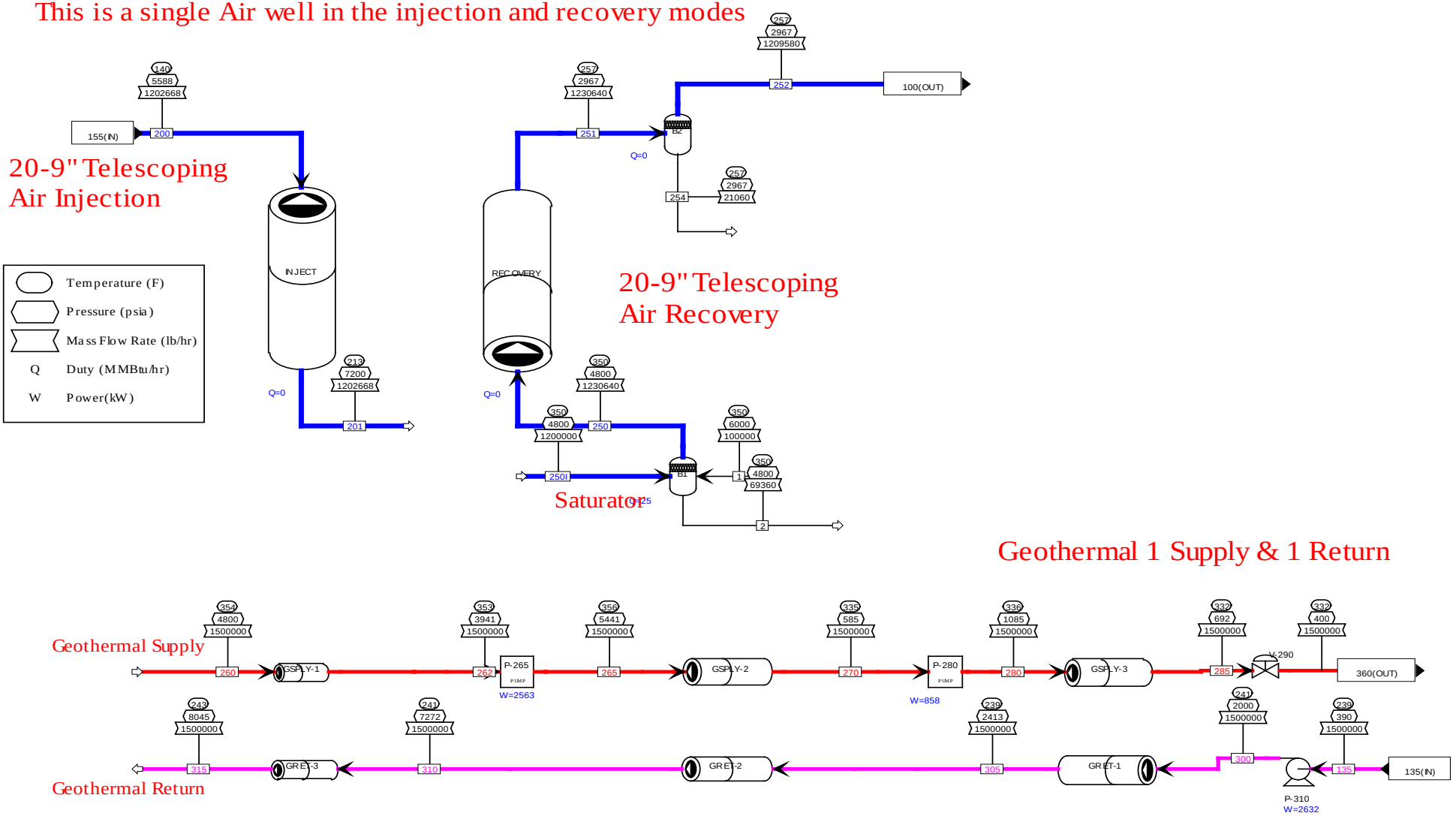

Figure 69. Injection and extraction for hybrid CAES plant

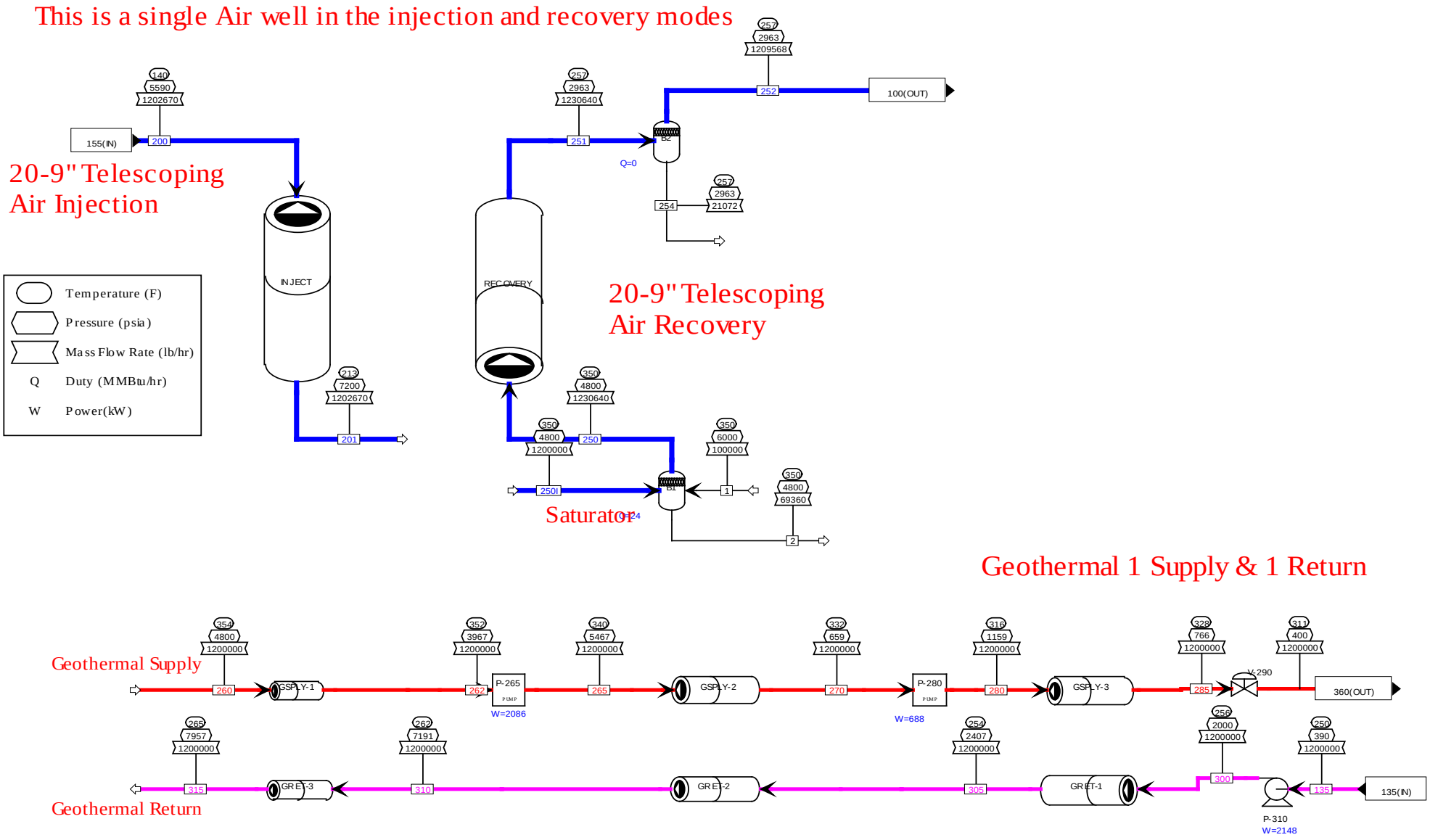

Figure 70. Injection and extraction for geothermal/molten salt hybrid CAES

7.3 Geothermal Cycle Hybrid CAES Plant Model and Simulation

The first configuration simulated recovers deep well geothermal energy only, and uses it in the power generation cycle using multiple reheat expansion turbines. Figure 71 shows the process flow diagram of the compression cycle of the proposed plant, and Figure 72 shows the process flow diagram of the extraction and power generation cycle. These are followed by the accompanying heat and material balances (Table 15 and Table 16), which provide the relevant flow streams.

The compression cycle starts with ambient air (Stream 145), and compresses 1.2 Mlb/hr in a 75-MW axial flow machine (C-150). Discharge from the compressor (Stream 150) supplies an air-cooled heat exchanger (ECA-155) where it is cooled to approximately 140°F; a trim cooler (ECW-156) using ammonia absorption drops the temperature to 105°F (Stream 157) and supplies the four-stage 67-MW centrifugal compressor (C-160). The duplicate flow stream (Stream 157B) was modeled to develop the heat and material balance required for each stage of four-stage centrifugal compressor, and to determine the operating characteristics of individual equipment pieces. In each successive stage of compression, intercoolers utilize both air and absorption heat exchange (ECA 160-E, F, G, and H and ECW 160-E, F, and G) producing a final compressed air flow of 1.2 Mlb/hr at 5,780 psia (Stream 160) supplying the compressed air injection well. The total cooling duty of the ECW heat exchangers (approximately 52 MMBtu/hr) could be removed either with cooling water or, in the configuration simulated, with ammonia absorption refrigeration depending on water source, permitting, and operability evaluations.

The extraction and generation cycle utilizes compressed air and geothermal heat for power production. For ease in following the process flow provided, all of the “cool” air is defined by the blue flow streams, all of the heated air is defined by the blue-green flow streams, all of the hot geothermal water is in red, and all of the cool geothermal water is magenta. From the compressed air reservoir, 1.2 Mlb/hr is recovered at 2,967 psia and 257°F (Stream 100), which supplies the first stage heat exchanger (EH-105). Concurrently, 332°F geothermal water at 1.5 Mlb/hr (Stream 360) is recovered and fed in parallel to each of the three primary heat exchangers (Streams 104, 114, and 124). After heat exchange, the heated compressed air is supplied to the first turboexpander at 2,957 psia and 290°F (Stream 105). Compressed air discharged from the turboexpander is re-heated in secondary heat exchangers, and supplied to the next primary heat exchanger and turboexpander (Streams 112, 115, 122, and 125) until completely depressurized (Stream 130). Once cross-exchanged with the compressed air, the geothermal water streams (Streams 111, 121, and 127) are combined, and supply the reservoir injection pump at 390 psia and 239°F (Stream 135). Total power production is estimated be 62 MW under conditions simulated in the model.

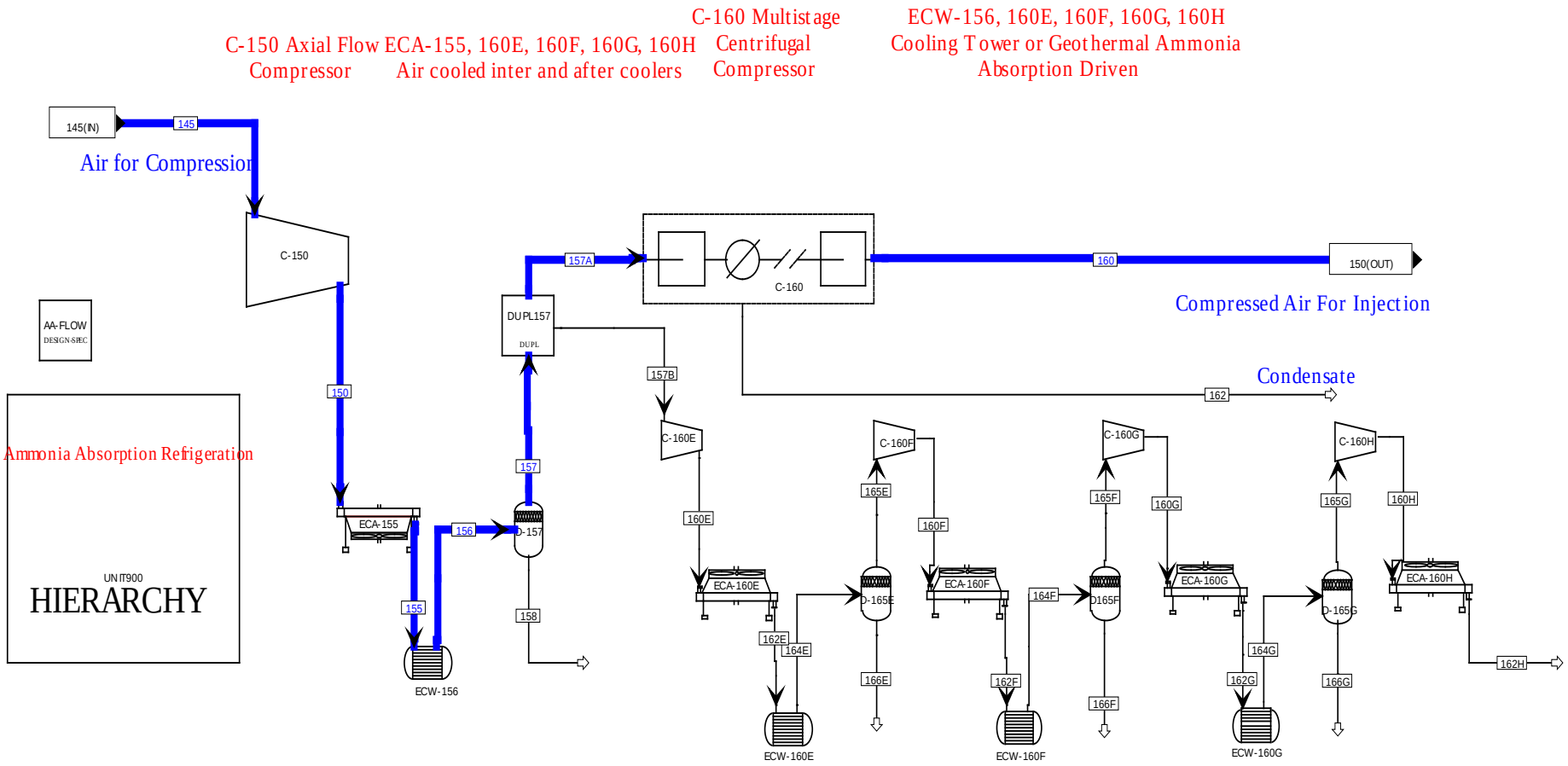

Figure 71. Adiabatic geothermal hybrid CAES plant (compression)

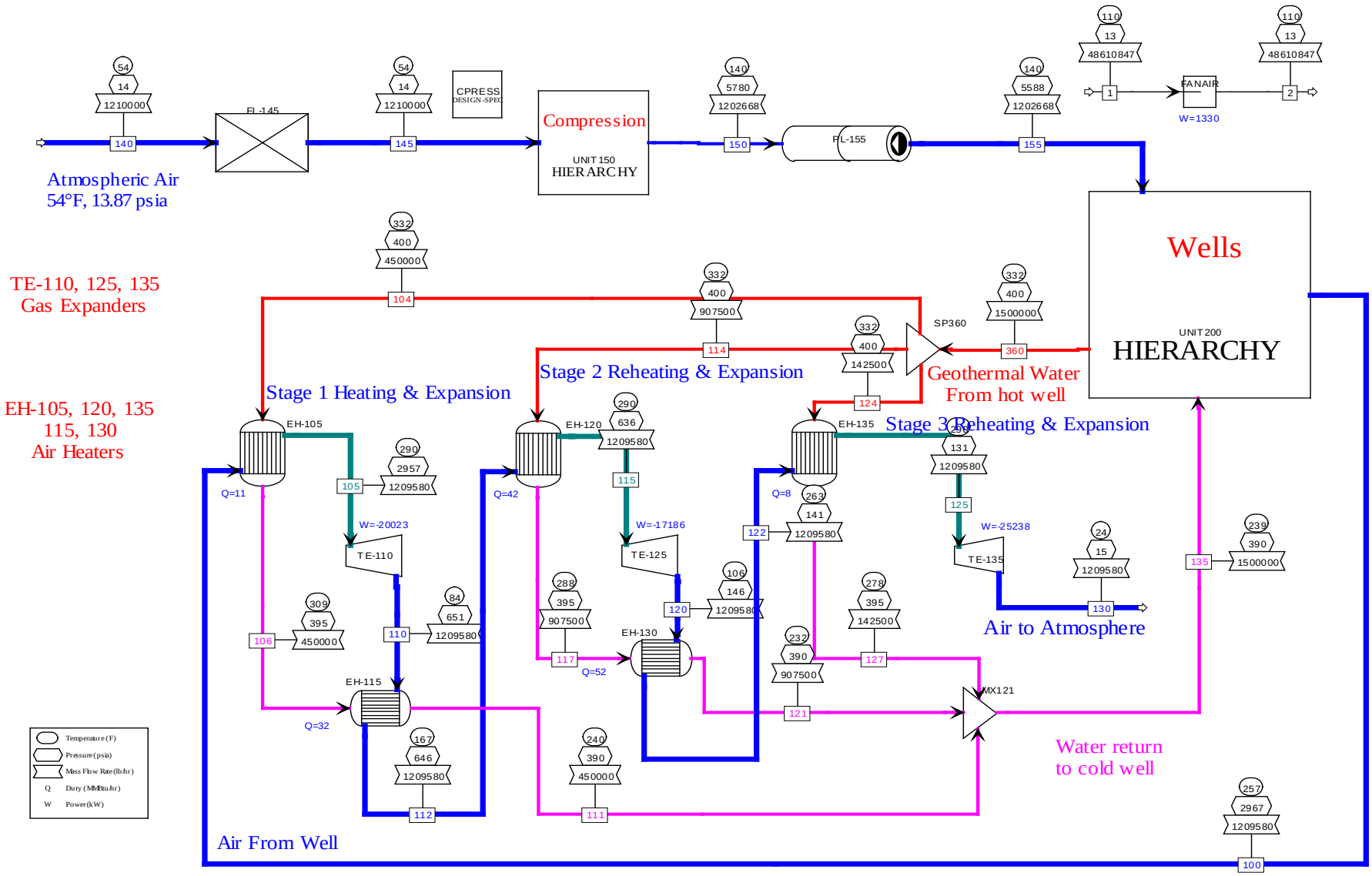

Figure 72. Adiabatic geothermal hybrid CAES plant (power generation)

Table 15. Heat and material balance for geothermal hybrid plant (compression)

Stream	145	150	157	160
Temperature (°F)	54	886	105	140
Pressure (psia)	14	247	232	5,780
Mass Flow (Mlb/hr)	1.2	1.2	1.2	1.2

Table 16. Heat and material balance for geothermal hybrid CAES plant (power generation)

Stream	100	104	105	114	115	124	125	130	135	360
Temperature (°F)	257	332	290	332	290	332	290	24	239	332
Pressure (psia)	2,967	400	2,957	400	636	400	131	15	390	400
Mass Flow (Mlb/hr)	1.2	.45	1.2	.9	1.2	.14	1.2	1.2	1.5	1.5

Table 17. Utility and consumption for geothermal hybrid CAES plant

Event	Block ID	Duty (MMBtu/hr)	Usage (kW)
Compression	Pump P-965	0.85	249
	Axial C-150	256.34	75,125
	Centr C-160	229.37	67,220
	Pump P-265	8.74	2,563
	Pump P-280	2.93	858
	Pump P-310	8.98	2,632
	Fan Cooling	4.54	1,330
		TOTAL	**149,978**
Generation	TurboExp	68.32	20,023
	TurboExp	58.64	17,186
	Turbo Exp	86.12	25,238
		TOTAL	**62,447**

The estimated round trip efficiency of the geothermal cycle hybrid CAES plant is 0.42; equivalent to 62,447 kW/149,978 kW.

7.4 Geothermal/Molten Salt Hybrid CAES Plant Model and Simulation

The second configuration proposed is an alternative to the adiabatic compressed air energy storage design developed by M. Nakhamkin (2012), with the distinction that the facility modeled would utilize two heat sources for power production: geothermal heat and a high heat capacity working fluid. During the compression cycle, an axial flow compressor would compress air to 250 psia and 885°F, which supplies an aftercooler. The heat of compression generated would be recovered and stored in molten salt (Hitec XL™) at atmospheric conditions. Compressed air is then supplied to an intercooled, four-stage centrifugal compressor that supplies compressed air for subsurface injection at 5,800 psia and 140°F.

Thermal storage at the surface is not without its difficulties though. Due to material restrictions (vapor pressure), the use of high-temperature thermal storage fluids such as Dowtherm A or Syltherm 800 would require pressurized storage to capture and retain the heat of compression. For the heat duties

modeled, calculations indicate that a pressure vessel of approximately 43 ft diameter would be required, which is prohibitive. Alternately, the molten salts such as HitecXL can be stored at 750°F at atmospheric conditions. They do, however, have a high freezing point (250°F to 280°F), and must be stored in a well-insulated vessel that includes a substantial amount of heat tracing or other supplemental supply of heat (such as geothermal) to avoid compromising the material. One additional advantage to using molten salt is that at the temperatures utilized for the model, the salt is much less likely to degrade over time (vs. thermal fluids), limiting material attrition and replacement costs.

The compression cycle for the molten salt configuration is characteristically similar to the compression model offered previously in Section 7.3 (see Figure 59). However, rather than rely on a very large air-cooled aftercooler duty, a molten salt heat exchanger captures approximately 75% of the available enthalpy. As indicated previously, molten salt material limitations enable cooling Stream 150 down to approximately 320°F prior to air cooling (duty of 174 MMBtu/hr), effectively reducing the air cooling requirement to 53 MMBtu/hr. As described in Section 7.1, aftercooler and intercooler duty (ECW-156 and ECW 160E, F, and G) is addressed with geothermal supported ammonia absorption refrigeration eliminating the need for cooling water. The design as simulated is provided in Figure 73, Figure 74, and Figure 75.

During the power generation cycle, 1.2 Mlb/hr compressed air is recovered, preheated with 350°F water from the geothermal resource, and expanded in a high-pressure (HP) expansion turbine. Discharge from the HP turbine is reheated with geothermal water up to 290°F, and then with the molten salt (750°F). The airflow is expanded again in a high-temperature/low-pressure (LP) four-stage power turbine. Given that the salt has a maximum heat absorption capacity relative to the fixed volume, the configuration would be optimal under the diurnal use scenario represented by steady state operations further clarified in Section 0. The power generation cycle as simulated is provided in Figure 76.

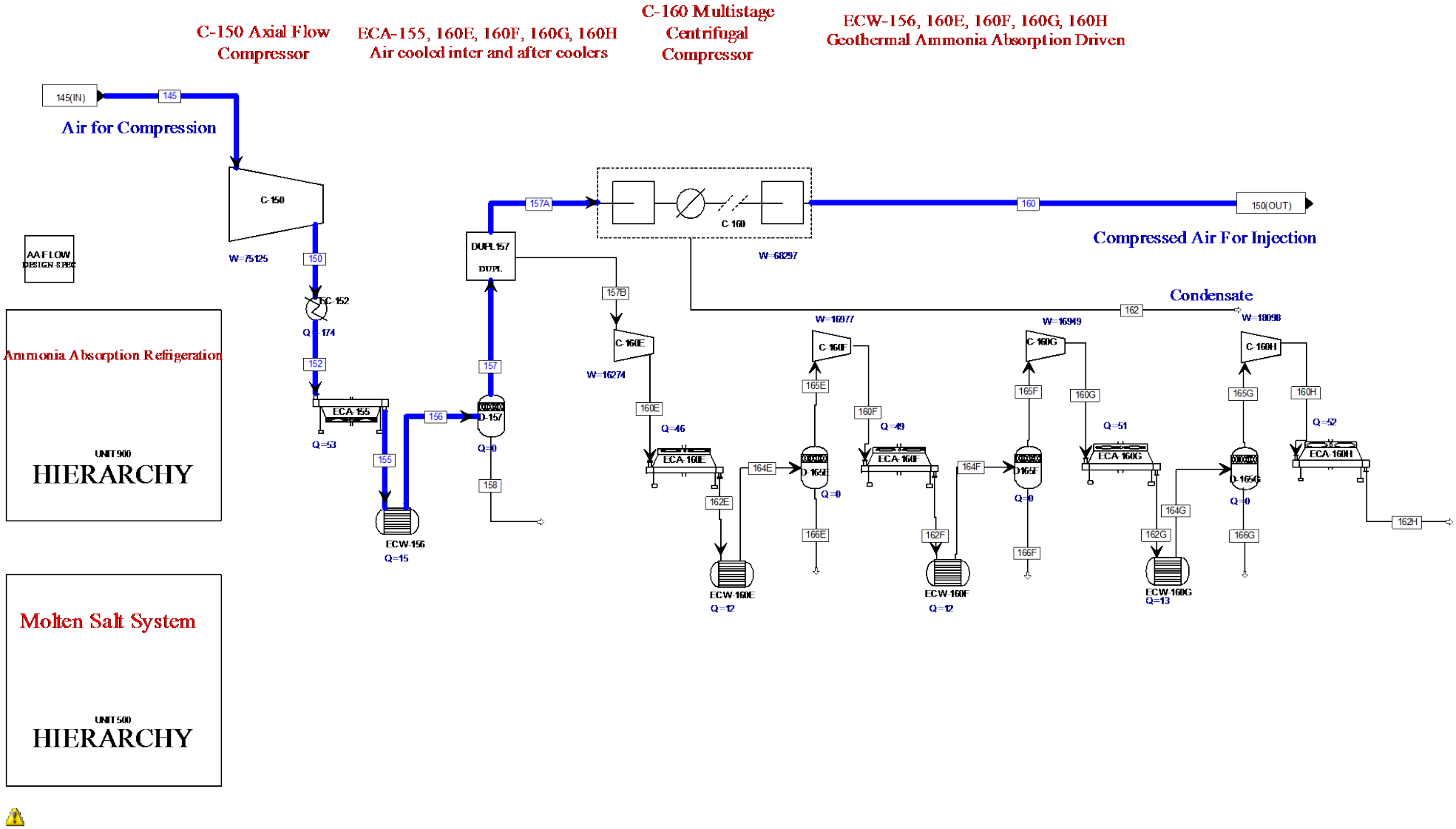

Figure 73. Geothermal/molten salt compression cycle

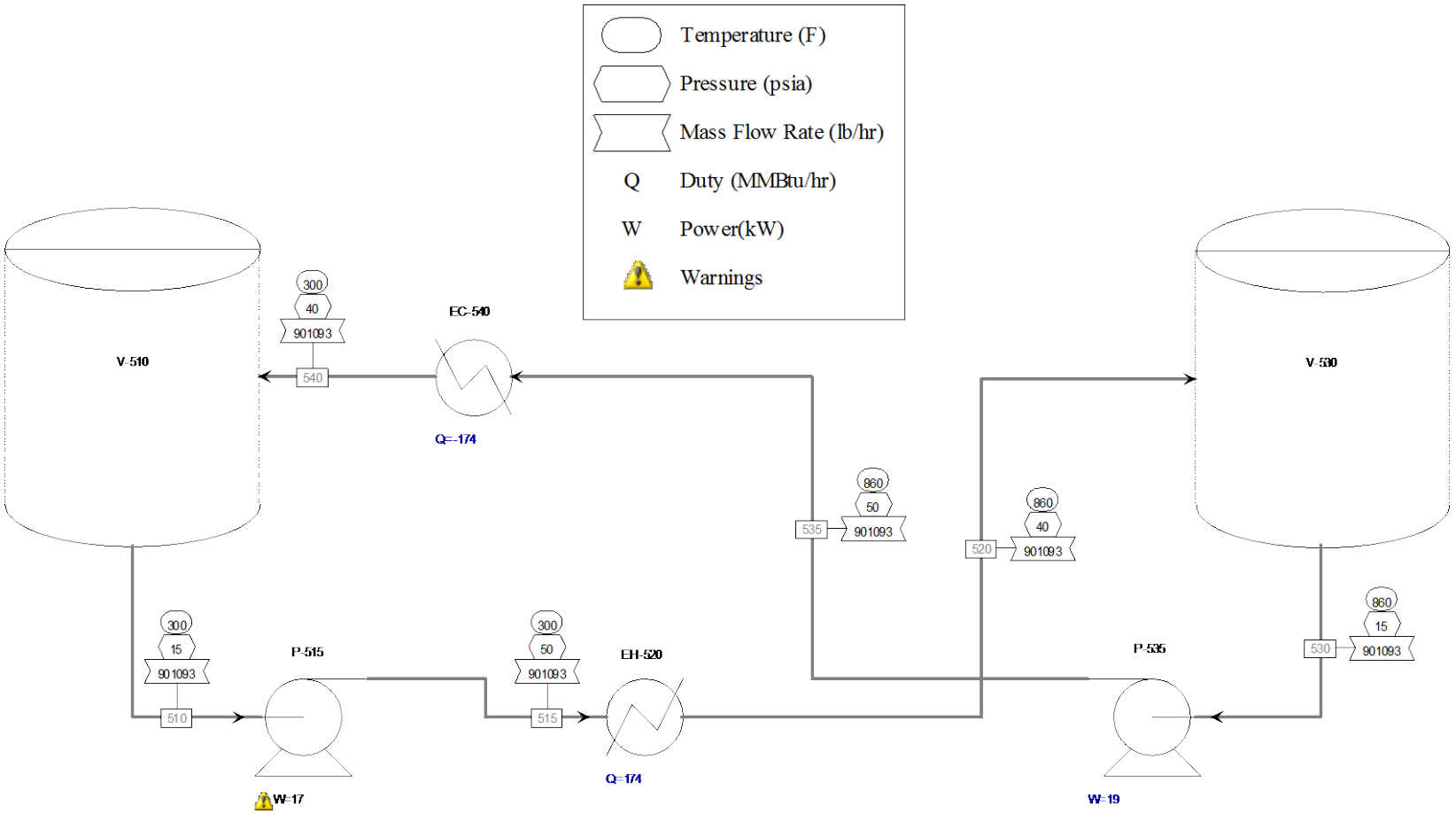

Figure 74. Molten salt process flow

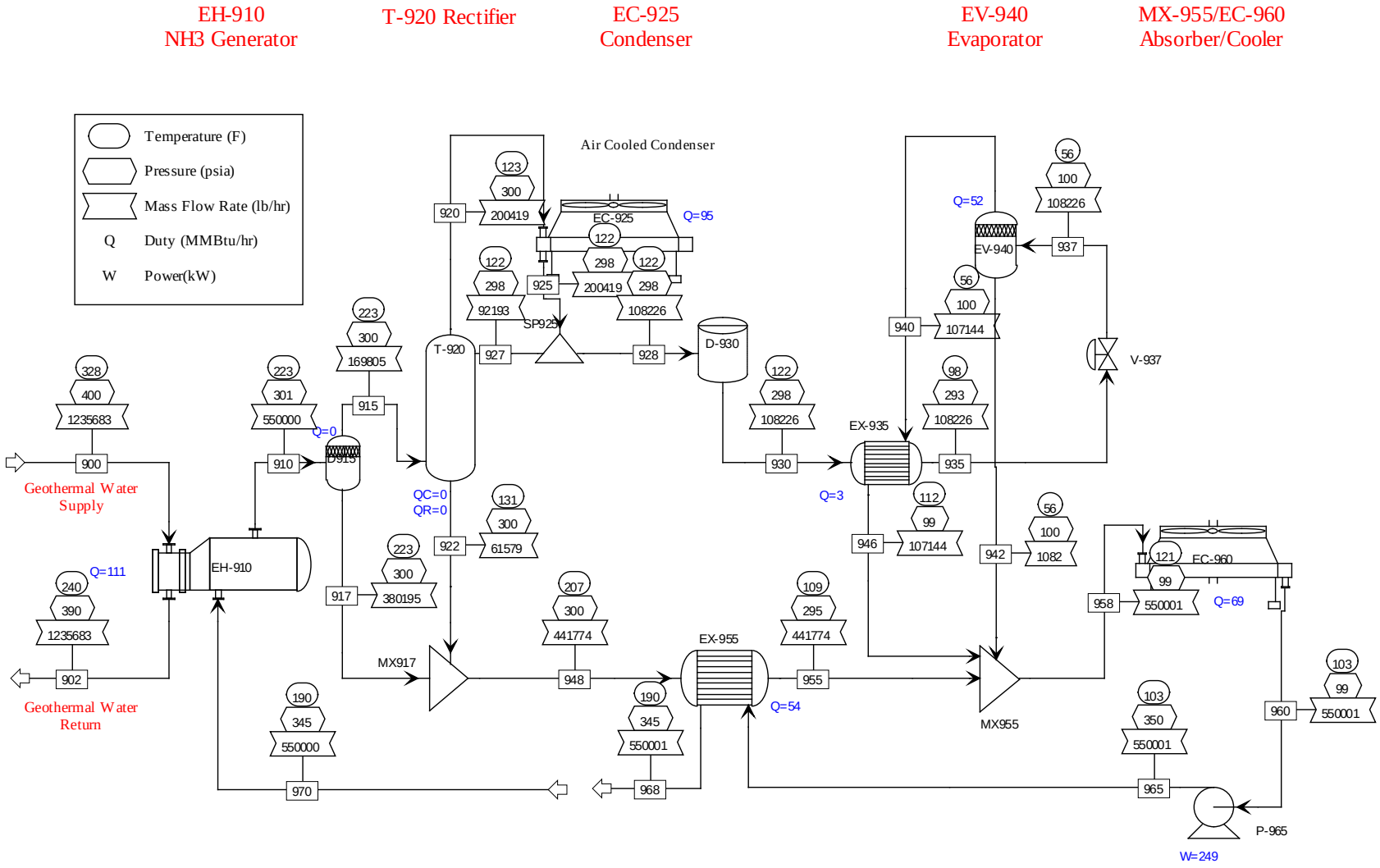

Figure 75. Geothermal driven ammonia absorption cooling for hybrid CAES plant

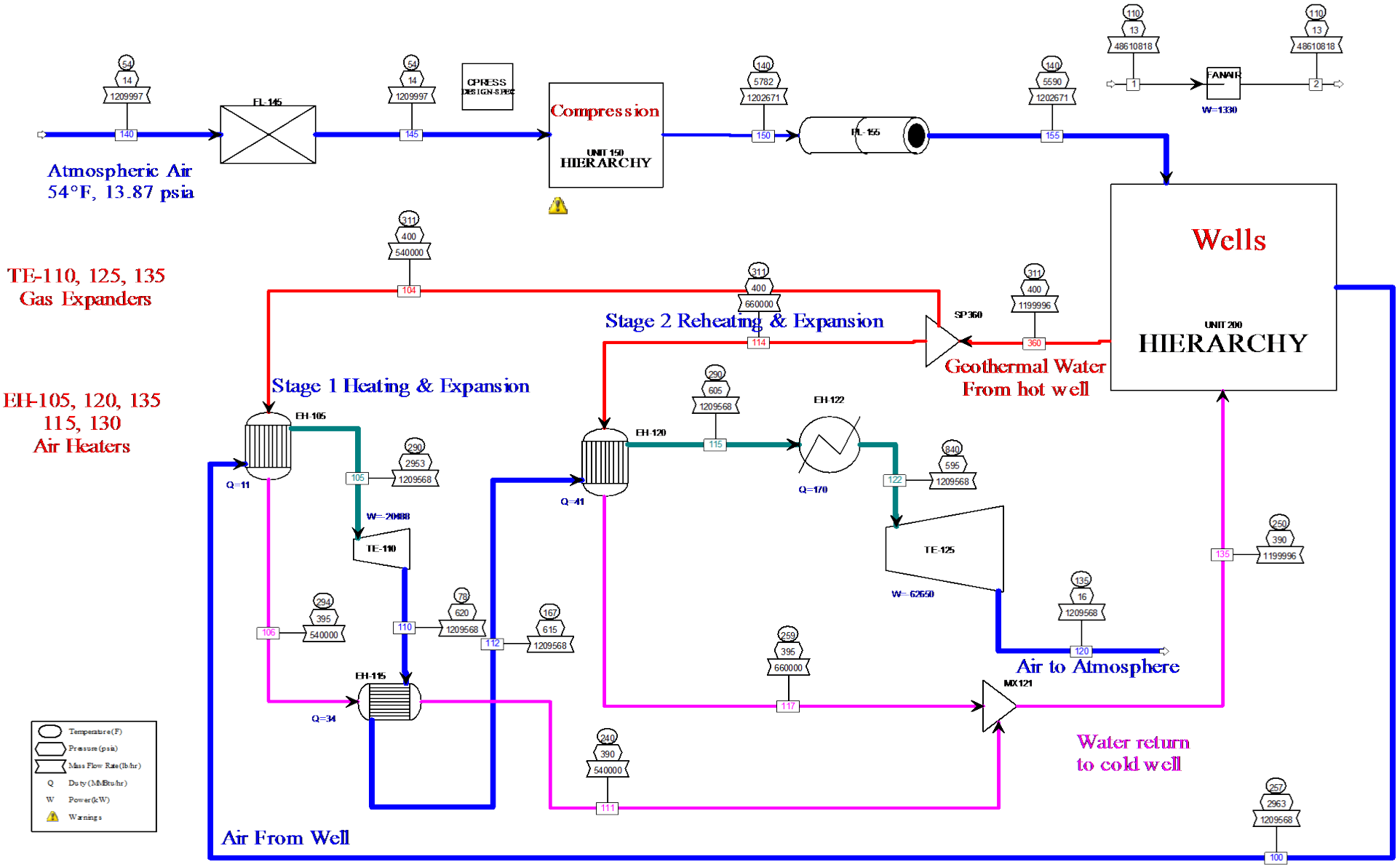

Figure 76. Adiabatic geothermal/molten salt hybrid CAES plant (generation)

The accompanying heat and material balance for the molten salt hybrid cycle plant is quite similar to the non-salt cycle from a flow rate standpoint. Relevant differences are identified by the process flow diagram for the molten salt cycle, and the overall impact to gross power production, which is included in Table 18 and Table 19.

Table 18. Heat and material balance for geothermal/molten salt hybrid CAES plant

Stream	Compressed Air		Geothermal (power)		Ammonia Absorption		Molten Salt	
	150	100	360	135	900	902	510	520
Temperature (°F)	140	257	311	250	328	240	300	860
Pressure (psia)	5,782	2,963	400	390	400	390	15	15
Mass Flow (Mlb/hr)	1.2	1.2	1.2	1.2	1.2	1.2	.9	.9

Table 19. Utility and consumption for geothermal/molten salt hybrid CAES plant

Event	Block ID	Duty (MMBtu/hr)	Usage (kW)
Compression	Pump P-515	0.06	19
	Pump P-535	0.07	21
	Pump P-965	0.85	249
	Axial C-150	256.34	75,125
	Centr C-160	233.04	68,297
	Pump P-265	7.12	2,086
	Pump P-280	2.35	688
	Pump P-310	7.330171	2,148
	Fan Cooling	3.21739	943
		TOTAL	**149,576**
Generation	TurboExp	70	20,488
	TurboExp	213.77	62,650
		TOTAL	**83,138**

The estimated round trip electrical efficiency of the molten salt supported hybrid CAES plant is 0.56; equivalent to 83,138 kW/149,576 kW.

7.5 Plant Operations

A hybrid CAES plant at Yakima Minerals would also be capable of two distinct compression and extraction cycles. One cycle would function to capture and store excess grid supplied energy during spring, and use the compressed air for power production once the over-generation event was complete. A second operational cycle is envisioned as routine daily operation including compression off-peak, and generation on-peak. Based on the configurations proposed, the plant would use geothermal resources for both compression and generation. The geothermal fluid source flows have been balanced to the extent that only a single extraction and single injection well would be required.

Based on gross machine capacity, the compression only cycle of 30 days would consume approximately 108,000 MWh of grid-supplied energy, storing approximately 0.4 MMT of compressed air. The generation only cycle was based on the minimum stable extraction flow rate from the reservoir

of 1.2 Mlb/hr, and was allowed to "produce" compressed air until well breakthrough was identified (see Section 3.5). Based on the findings, a hybrid CAES facility would be capable of generating power for 6 hours per day (coinciding with a single 6-hr peak, or two daily 3-hr peaks) for 86 days post-injection, allowing the recovery of 43,000 MWh without reinjection, or approximately 40% of the original consumed megawatt-hours. This is fairly consistent with the anticipated volume and characteristics of the cushion gas required also addressed in Section 3.5. From an operability standpoint, it is also useful to point out that during the initial generation only phase of up to 86 days, though the reservoir air volume is decreasing, well bottom pressures are stable and do not drop below approximately 5,850 psia as simulated. This is particularly important considering power generation models are predicated on minimum well bottom pressures of 4,800 psia, further indicating that the hybrid CAES plant is feasible, and is likely conservative in the estimation of power and energy production.

To maintain stable reservoir air volume over time, diurnal operation of the plant is based on the flow rates modeled for injection and extraction cycles, and adjusted for duration. Steady-state operation of the plant assumes maintaining consistent reservoir volume through matched injection and extraction rates characterized by 6 hours of compression (900 MWh), and approximately 6 hours of generation (498 MWh) per daily cycle. Adjusted annually to include the initial 30 days of compression and 86 days of post-injection generation, the plant would consume 324,000 MWh, and generate 163,000 MWh in Year 1. Again, respective of the minimum cushion gas requirement, Year 2 through Year *n* operations would be expected to increase the initial generation period recovering an additional 11,000 MWh assuming the same injection and extraction parameters were followed.

Though obviously mismatched (power consumption > power generation), the value of the hybrid CAES plant configuration lies in the basic notion that it is a dispatchable, non-fuel-based power source. The cost of electricity is therefore limited to meeting requirements for capitalization and non-fuel O&M (fixed and variable). In addition to energy production, the hybrid CAES plant is capable of providing multiple ancillary services via automatic generation control, and based on the configuration proposed, should readily be capable of meeting 10-minute standards for response time and possibly less.

Other uncertainties remain at the site predominantly based on the interactions between the plant and subsurface reservoir. For example, while phase-change geothermal plants (flash or binary cycle) commonly have issues with heat exchanger and turbine cleanliness, the geothermal resource at Yakima Minerals was intentionally maintained at adequate pressure and temperature to avoid phase change solubility concerns. This doesn't eliminate heat exchanger cleanliness and brine solubility issues, but it is a potential concern that isn't explored in this analysis.

7.6 Hybrid CAES Plant Capital and Levelized Cost

The cost estimate for the hybrid CAES facility used a variety of resources reflective of the level of definition afforded to each project area. Where process units were defined and simulated, Aspen IPE was utilized. Area costs for the hybrid plant, compressor cooling (air and water), and well field compressed gas supply and distribution piping were all completed using this methodology. Site civil, mechanical, and electrical requirements were determined using factored estimates from Aspen IPE templates assuming an undeveloped greenfield site and a well field layout described in Section 7.1. Unidentified costs within the areas such as the molten salt and high-temperature heat exchanger were obtained through publicly available literature. Additional costs were augmented from similar plant designs such as costs for the

compressor, turbo-expanders, and generator step-up transformer. Area costs for the injection and extraction wells were estimated by a drilling contractor based on production string sizing, and depth to well bottom. Transmission and interconnection costs were provided by BPA. All capital costs are in overnight 2012$.

Table 20. Estimated capital costs for hybrid CAES plant at Yakima Minerals

Description	Total ($ million)
Well Drilling and Development	38.6
CAES Plant	176
Transmission and Interconnection	13
TOTAL CAPITAL COST	227.6
TOTAL GENERATION (kW)	83,138
TOTAL CAPITAL COST/kW	$2,738

The plant's cost of capital at $2,738/kW is more than twice the cost of the conventional CAES facility on a per kilowatt basis. However, the cost does compare quite competitive with capital costs offered by the Geothermal Energy Association, which range from $1,891 to $2,767/kW (inflation adjusted) for non-specified geothermal power technologies (HANCE, 2005). Clear distinctions between the hybrid plant and the gas-fired CAES facility are discussed further in Section 7.6.4.

7.6.1 Well Field Drilling and Development

Due to the anticipated geologic similarities in drilling characteristics among sites (i.e., predominantly basalt layers), the well drilling and development cost information for the Yakima Minerals site was completed using similar inputs as the Columbia Hills site with modifications for casing diameters, depth, and well build-out. The Yakima Minerals location as proposed would have three deep wells: one well for injection and extraction of compressed air with a well bottom depth of ~14,000 ft; and two wells for geothermal water use (one for extraction and one for injection) with a well bottom depth of ~15,000 ft. Due to the overall depth of the wells (and inherent cost per well), costs for the 3-well field were developed based on casing sizes that could maximize air flow and surface pressure for the facility out of a single well starting with a known bottom-of-well casing diameter of 9-5/8 inches. Based on industry standards and data received from a drilling contractor,[1] this was the largest diameter of casing identified as being feasible for use at the depths considered for Yakima Minerals. As applicable, budgetary line items for ancillary cost categories are included, but the estimate does not include additional costs such as well permitting, testing, or standby rates if/as requested.

[1] Boart Longyear Drilling Services cost estimate. January 2013.

Table 21. Well drilling estimate for Yakima Minerals location

Description	Cost per Well ($ thousands)	Total ($ thousands)
Mobilization	795	2,385
Drilling		
38” Hole and Cement to Surface	70	210
28” Drill to 2,500’	1,823	5,469
19” Drill to 12,000’	5,035	15,105
12-1/4” Drill to 14,000’	794	2,382
Well Build		
Furnish/Install 22” Casing	313	939
Furnish/Install 13-3/8” Casing	996	2,988
Furnish/Install 9-5/8” Casing	202	606
Cut/Cement Each Casing to Surface	1,033	3,099
Additional Job Costs	524	1,572
Subtotal Direct Costs	11,585	34,755
Engineering and Design		3,823
Total		38,578

7.6.2 Hybrid CAES Plant Capital Equipment

The cost estimate contained herein was based on the configurations provided in Section 0, and includes the well field, compression and generation cycles, and balance of plant items such as ammonia absorption cooling; storage and use of molten salt; and balance of plant items such as buildings, fencing, and roads. Where necessary, specific pieces of equipment such as generator step-up transformer and deep well geothermal pump were determined using a factored estimate and escalated to 2012$.

Table 22. Overnight capital costs of hybrid CAES facility

Project Title:	PROJECT:			***Scenario Name:***	Low Flow	
Project Name:	Hybrid CAES Yakima Min.					
Proj. Location:	North America	***Job No:***	--	***Prep. By:***	--	
	08JAN13				DOLLARS	
Estimate Date:	18:35:30	***Est. Class:***		***Currency:***	USD	
Account	MH	Labor Cost	Matl Cost	Total Cost	Percentages	
(2) Equipment	31,040	1,552,000	77,141,100	78,693,100	70%	of TDC
(3) Piping	74,451	3,722,550	14,477,200	18,199,750	16%	of TDC
(4) Civil	70,889	3,544,450	3,163,500	6,707,950	6.0%	of TDC
(6) Instruments	7,085	354,250	1,151,400	1,505,650	1.0%	of TDC
(7) Electrical	14,270	713,500	4,380,400	5,093,900	5.0%	of TDC
(8) Insulation	21,762	1,088,100	796,100	1,884,200	2.0%	of TDC
(9) Paint	8,158	407,900	89,700	497,600	<1.0%	of TDC
						of TDC
Total Direct Field Costs	227,655	11,382,750	101,199,400	112,809,805	100.0%	of TDC
	(TDMH)	(TDL)	(TDM)	(TDC)		
Indirect Field Costs				9,154,156		
				(IFC)		
Total Field Costs	227,655			121,963,961	69%	of TIC
	(TFMH)			(TFC)		
Freight				4,047,976	4.0%	of TDM
Taxes and Permits				6,324,963	5.6%	of TDC
Engineering and HO	38,881			6,590,300	3.7%	of TIC
Other Project Costs				10,373,000	5.8%	of TIC
Contingency				26,874,100	15.3%	of TIC
Total Non-Field Costs	38,881			54,210,339	30.7%	of TIC
Project Total Costs				**176,174,300**	156.0%	of TDC

While there are no comparable plant configurations that can be used to frame the capital cost analysis, several components of the hybrid facility do compare reasonably well to other estimates. In assigning comparable values however, it's important to recognize that as a hybrid CAES facility it much more closely aligned with a geothermal plant, than a conventional turbo-machinery power plant.

For example, DOE proposed rules of thumb for a 20-MW geothermal power production plant with a total development cost of $4,000/kW, with $2,000/kW committed to power plant and surface facilities including transmission (in 2008$)(DOE, 2008). On comparable terms, the hybrid CAES plant comes in at $2,121/kW ($2,274 including transmission) in 2012$.

7.6.3 Transmission and Interconnection

Switching, transmission, and interconnection costs were provided by BPA.[1] The estimate included details regarding geographic location of the sites and required lengths of laterals; options for interconnection voltages depending on the size of the generators (230 or 500 kV); and points of interconnection into existing substations or where necessary the cost of new substation. Annual operations and maintenance for each option was also included.

[1] Electric Interconnection-4. BPA. October 2012 (proprietary).

The gross capacity provided in the simulation was well below the capacity criteria that determined the step-up transformer output; therefore, the capital cost estimate considered the 230 kV option as the most representative of a likely configuration. For comparative purposes, both kilovolt ratings are provided. Table 23 provides summarized interconnection costs for the Yakima Minerals location including provisions for right-of-way, cost of substation or switching (where available), total length of laterals and transmission line cost, access roads, and overheads.

Table 23. Interconnection costs by kV rating

Location	230 kV ($ million)	500 kV ($ million)
Yakima Minerals	13	66.2[a]

a. Average of the two Yakima locations

The low-voltage point of interconnection at the Yakima Minerals location is assumed to be a new switching station on the PacificCorp Vantage-Pomona Heights transmission line. Tying into the existing line would require the construction of a new substation, and transmission line laterals of approximately 4 miles.

The high-voltage point of interconnection at the Yakima Minerals location is assumed to be a new substation that would tap into the existing Schulz-Wautoma 500-kV line. The high-voltage option includes the construction of a transmission line lateral of approximately 4 miles to the tie-in point on the existing line, and the new substation.

7.6.4 Levelized Cost of Electricity

The experimental nature and lack of commercial scale deployments makes it difficult to provide a well-supported LCOE for the hybrid CAES plant simulated. Inherently, the plant has aspects of both conventional power production machinery (compressor, air coolers, turbo-expanders, etc.), but relies on a less well understood subsurface reservoirs (air and water), and recirculating brine for the continuous supply of both heat and pressure energy for stable power production. In any event, with no need for fuel, the LCOE will be dominated by capital repayment requirements, with the remainder to cover fixed and variable costs for plant maintenance and operations.

Due to a lack of referenced plant data, particularly for the hybrid CAES model offered, a modification to annual O&M costs is provided based on an average of O&M costs detailed by ERPI, DOE, and Sanyal (Hance, 2005) with the caveat that the costs are based on geothermal power production. Qualitatively, and in comparison to the conventional CAES facility or geothermal plant (binary or flash), fixed O&M costs should be lower due to a limited number of staff required to operate the unit, a lack of hot gas path repair and replacement costs, and a lack of phase change implications in the working fluids. However, a hybrid facility may also require additional costs committed for reservoir, well, and brine heat exchanger management activities in addition to annual well work-overs, packing inspection, and replacement. The non-fuel variable O&M should be modest as well for the hybrid CAES plant with limited requirements for consumables and a lack of pollution abatement needs (such as reagent for selective catalytic reduction), but could be heavily impacted by the number of run-time hours and starts on the compressor.

To that regard, a single inflation-adjusted O&M cost is offered reflective of the range of costs per annual megawatt-hours. For conservative purposes, a mid-point value of the ranges offered from a review of public literature was selected for the calculation (HANCE, 2005). For parity, the hybrid CAES plant was reviewed with a 25% capacity factor and similar line item values where appropriate. The following parameters were used for the simplified LCOE (sLCOE) model reported in Table 24.

Table 24. Simplified LCOE calculation for hybrid CAES plant

Description	Value
CAES Project Capital Cost ($/ kW)	2,738
Project Lifetime (years)	20
Discount Rate (%)	4
Capital Recovery Factor	.074
Annual O&M Cost ($/MWh-year)	26.44
Capacity Factor (%)	25
Heat Rate (Btu/kWh)	NA
Fuel Cost ($/MMBtu)	NA
sLCOE (cents/kWh)	11.84

There are widely varying comparative sources of public information regarding *geothermal* LCOEs, largely contingent on well depth, temperature of geothermal resources, and flow rates (inherently impacting power production ability) (INL, 2006). With a range of 4.1 to 104.9 cents per kilowatt-hour, it's not particularly valuable to put the LCOE of the hybrid CAES plant into context with other estimates other than to acknowledge it is representative of costs expected to be incurred based on the configuration, location, and operations proposed for the Yakima Minerals site. For comparative purposes, the hybrid CAES configuration proposed is provided in Figure 77 and compared against other new build options with the applicable capacity factors included in parenthesis.[1]

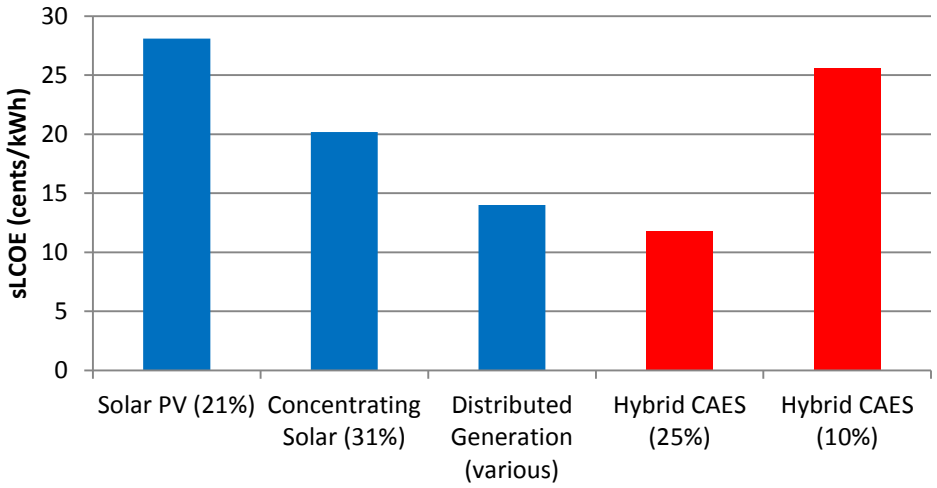

Figure 77. LCOE of hybrid CAES and additional generating resources

[1] Capacity factors and LCOE obtained from Transparent Cost Database. Accessed at http://en.openei.org/apps/TCDB/. January 15, 2013.

8.0 Ancillary Services and Revenue Sources

As energy generation from wind and other renewable sources have expanded to meet the renewable portfolio standards (RPS) targets imposed by 31 states and the District of Columbia, CAES and other energy storage options have received increasing attention as a means to provide balancing and other ancillary services. These grid services (e.g., energy arbitrage, spinning reserves, and capacity credits) have been the focus of several recent modeling exercises and published articles. Embedded in the value proposition assessments are a number of questions, including the following:

- Which grid services could CAES ultimately provide?
- What are the values of these grid services?
- How can these values vary based on the location of the CAES and other grid conditions?
- How can CAES be operated to maximize the total value generated through the provision of competing services?

This section attempts to answer the first two questions, as applied to the deployment of CAES in the Pacific Northwest, through an analysis of recent literature.

8.1 Balancing Services

PNNL recently completed a study focused on evaluating energy storage technologies as a means to resolving future grid reliability challenges caused by renewable energy penetration. In this study, PNNL estimated the market size for energy storage devices providing balancing and arbitrage services in the Western Electricity Coordinating Council (WECC) under a hypothetical 2020 grid scenario in which wind energy production comprises 20% of the region's generating capacity. The PNNL study evaluated nine competing technologies for meeting balancing requirements under the 2020 RPS case, and evaluated each based on their life-cycle cost, including all initial and recurrent costs, property and income taxes, depreciation, borrowing costs, and insurance premiums over a 50-year life cycle.

PNNL found that CAES was not cost competitive with the base-case technology, combustion turbines. However, this did not include an evaluation of the full range of services provided by each energy storage technology such as spinning reserve, non-spinning reserve, and reactive power supply. By isolating the cost of the base-case technology (i.e., combustion turbines), the value of balancing services can be derived. This value, which represents the cost to local electricity service providers of meeting 2020 RPS balancing requirements using existing technologies, was estimated at $72/kW-year (KINTNER-MEYER et al., 2012). At the capacities selected, this is approximately $30 million per year, recognizing that the plant can be utilized for both DEC and INC balancing, but only during times when the capacity is not being committed for other purposes.

8.2 Arbitrage

A number of studies have evaluated the feasibility of using standalone CAES or combined CAES-wind generation systems to balance wind output or provide reserve capacity, short-term energy arbitrage, or other capacity-based services. The findings of several recent studies are presented in Table 25. Each

study's findings are presented in terms of net revenue, which equates to gross revenue minus electricity purchases, natural gas costs, and O&M expenses. As shown, these values vary significantly based on the scope of the analysis, geographic region, grid conditions, and modeling procedures. It is important to note that these estimates do not include the value of seasonal arbitrage that would accrue to the ability to store low or zero priced energy during the PNW spring hydro runoff and deliver the stored energy back during summer and winter peak hours.

Table 25. Arbitrage values ($/kW-year) for CAES

Author	Region	Value of Arbitrage Services ($/kW-year)
DENHOLM and SIOSHANSI (2009)	Texas / ERCOT	$86
	Midwest / PJM	$49
	CAISO	$71
DRURY et al. (2011)	CAIS0	$30
	MISO	$21
	NYISO	$33
	PJM	$39
SIOSHANSI et al. (2009)	PJM	$60-$110
KINTNER-MEYER et al. (2012)	NWPP	$15
	CAMX	$18

DENHOLM and SIOSHANSI (2009) employed a model designed to optimally dispatch an energy storage device whether located near a load center or co-located with wind generation at three locations: the Midwestern U.S. (selling energy into the PJM market near Chicago), Texas, and the Western U.S. (selling energy into the California Independent System Operator [CAISO] market). The findings of this analysis suggest that arbitrage alone would be sufficient to meet annual capital requirements (10% to 12% of capital costs) in the ERCOT case ($86/kW-year) while the Midwest and CAISO cases ($49 and $71/kW-year, respectively) are limited somewhat by the relatively higher price of natural gas in those regions.

DRURY et al. (2011) also employs an optimized dispatch approach, modeling single and multiple applications based on historical market data. In addition to the results presented in Table 25, DRURY et al. (2011) also estimated gross arbitrage revenue ($121/kW-year for CAISO, $80/kW-year for MISO, $176/kW-year for NYISO, and $154/kW-year for PJM) and net revenue when arbitrage and capacity reserves are co-optimized.

SIOSHANSI et al. (2009) employed a dispatch model to estimate arbitrage values in the PJM at $60 to $110/kW-year. KINTNER-MEYER et al. (2012) examined the revenue potential of energy storage technologies in the WECC using PROMOD, which is a production cost model. A 2020 RPS grid scenario was built into PROMOD, congested paths were located, and energy storage systems were sited to maximize revenue potential. The findings of KINTNER-MEYER et al. (2012) which are in the $15 to $18/kW-year range, are lower than other referenced estimates in part because the study forecasts

production capacity forward and includes both planned capacity and that provided by the incremental investment in energy storage technologies. As the additional capacity is added to the model, the supply of energy expands and prices fall. This is consistent with current projections of WECC wholesale prices for on-peak and off-peak power (KNUDSEN, 2012).

8.3 Other Energy Services

In addition to balancing services and energy arbitrage, other benefits include spinning reserve and capacity values. The CAES system will be limited in terms of the services it ultimately provides; however, there are virtually no tradeoffs between energy and capacity in providing spinning reserve during charging periods. This service could increase annual revenue to the CAES device by 15% (DENHOLM and SIOSHANSI, 2009). Further, DRURY et al. (2011) estimated the value of spinning and non-spinning reserves at $23 to $29/kW-year. If the energy capacity is greater than 6 hours, the device could also contribute to the capacity requirements of a balancing authority. The values range from $100/kW-year to $200/kW-year in the New York Independent System Operator market (KINTNER-MEYER et al., 2012). A final benefit is the value associated with the deferral of capital for transmission and distribution upgrades or new builds. Though not quantified, given the ability of a single plant to provide multiple value streams (balancing, arbitrage, spinning reserve, etc.), the benefit of deferring capital could be quite significant.

When estimating the value of services provided by CAES, the analyst must consider local grid conditions, the charging and discharging capacity of the CAES system, the ability to vary the size of the storage cavern and components, operational characteristics, and local grid conditions. The evaluation of multiple value streams requires the optimization of the CAES device's operation in a manner that maximizes revenue while meeting operational constraints. Therefore, the revenue streams identified in this section cannot simply be summed to determine the value of a CAES system. A detailed valuation of CAES, which is beyond the scope of this analysis, is required to determine its total value.

9.0 Key Findings: Project Implementation

9.1 Core Considerations for CAES siting

This study began with a regional site suitability evaluation that identified five areas for deeper investigation. Of these, two were selected for core geologic simulation work used to inform modeling of preliminary plant configurations. The resulting implementations described here provide very different approaches, but in both cases a technologically viable configuration was devised to take the greatest advantage of local surface and subsurface conditions, and to best mitigate the challenges at each site. While the sites discussed below do reflect the most appealing locations based on the siting process described earlier, the flexibility of off-the-shelf component technologies to tailor a design to the specific strengths and challenges of a given site suggest an overall flexibility in CAES implementations. One primary finding of this study—that there are areas within the Columbia River Basalt where storage capacities, injectivities, and geometries comprise a suitable storage reservoir for compressed air—suggests that CAES projects may be viable at a number of sites beyond those examined here.

Regional identification of potentially suitable CAES sites began with the storage reservoir parameters required to implement a commercial scale storage project. Areas were evaluated for four key criteria:

- Reservoir thickness ($\geq$ 30 ft)
- Reservoir permeability ($k \geq 500$ mD
- Effective porosity ($\varepsilon \geq 0.1$), and
- Overlying low-permeability, caprock thickness ($\geq$ 100 ft; $\leq$ 10-1 μD)

Preliminary reservoir simulation work undertaken using the STOMP model showed that, while air injected into a dipping reservoir tends to migrate quite slowly, such a storage configuration does still pose a risk of loss of compressed air, and a corresponding decrease in overall system efficiency. For this reason, the above criteria were modified to include the presence of an anticlinal structure to contain injected air and prevent migration away from the storage project boundaries.

The requirements above imply a need for data upon which to base a quantitative evaluation. Because relatively few wells exist in this region at candidate storage depths, minimizing uncertainty in the site assessment process necessitated a focus in areas near the deep boreholes that exist into the CRBG. The limitations presented by this exclusive use of available data constrained the siting effort. However, because a high percentage of deep wells drilled outside the Hanford Site were sited based upon proprietary oil and gas exploration information, it is likely that these sites represent the most likely candidates for high injectivities, good capacities, and a strong likelihood for structural containment.

The following sections present additional considerations for siting a CAES facility at the Columbia Hills and Yakima Minerals sites. It is important to note that actual built plant configurations for these sites are heavily dependent upon geologic site characterization to quantitatively determine reservoir conditions, which will impact compression, injection, and production system design. The acquisition of additional geophysical and well data is essential to final facility design and management.

9.2 Columbia Hills CAES Plant

The Columbia Hills CAES plant design presented in this study represents a conventional system design that has achieved commercial success when paired with cavern-based air storage; the novel use of deep flood basalts as the air storage reservoir is the sole deviation from a "standard" CAES plant as deployed elsewhere. The net efficiency and heat rate of the gas fired CAES plant are very competitive. This qualitatively extends to the consumption of grid-supplied energy during the compression cycle, which is assumed to consist predominantly of wind and hydroelectric generation rather than thermally produced electricity. The total capital ($/kW) and levelized cost of electricity ($/kWh) are competitive with most regional utility based energy generating alternatives at the selected capacity factors, and are significantly better than a directly comparable simple-cycle combustion turbine. In addition to energy production, the plant as configured could be expected to capitalize on additional revenue streams, such as the provision of ancillary services.

The selected site offers numerous advantages in terms of land ownership, proximity to critical infrastructure (natural gas pipeline and transmission), and nearby exploration wells that reduce risk of encountering unexpected hydrogeologic conditions at the site. The geologic structure examined for storage in this case, while smaller relative to the storage capacity present at the Yakima Minerals site, is capable of meeting compression requirements for 40 days before injected air begins to transition beyond the boundaries of the storage area. Given simulation results suggesting that 59% of injected air remains in the formation at water breakthrough, this implies that approximately 40% of the stored air would be subject to injection and extraction. Flexibility of injection and extraction rates and timing would allow for the project to be designed and managed to most effectively utilize the storage reservoir.

Its relatively small storage capacity and the limited injectivity of the subsurface reservoir are the primary constraints at the Columbia Hills site. As shown in Figure 26, based on assumed reservoir properties, the four injection wells use up all available injection capacity at the site, which would effectively limit future expansion of the CAES facility beyond the 229-MW compression load under cases analyzed in this report. While the subsurface parameters are the limiting factor for maximum capacity of the surface facility, it's worth noting that the plant is both readily scalable (up or down) and capable of being sited anywhere the compressed air reservoir can be established and maintained.[1] If higher capacity or storage requirements are needed at the Columbia Hills site, fracture stimulation of the reservoir should be factored into any future analysis. Reservoir stimulation would offer two key benefits by: 1) significantly reducing uncertainty around encountering less favorable hydrologic properties than expected at the site, and 2) reducing the pressure required to achieve the targeted injection rate and increasing the air storage volume efficiency in the structure. Both factors will improve the plant operating efficiency and reduce financial risk associated with developing a project at this site.

As a consequence of the CO_2 sequestration pilot study underway near Wallula, Washington (MCGRAIL et al., 2011), the WADOE now has experience in permitting unique activities associated with large-scale injections of gases into the Columbia River Basalts. The injection wells envisioned for the Columbia Hills site would most likely be permitted as Class V wells under the state's Underground Injection Control Program. One aspect of the envisioned completions, however, will require concurrence from WADOE. Well completions that connect distinct aquifer units are prohibited in Washington State

[1] Subject to the availability of additional infrastructure required by the plant configuration (e.g., natural gas, cooling water, transmission).

under WAC 173-160-420. The well design for the Columbia Hills site envisions a completion across three members in the Grande Ronde Basalt. Compressed air storage results in a dewatered zone around an injection well. Hence, as long as the CAES plant was operational, water transfer between these interflow zones would not be possible and the injection wells would comply with the intent of the regulation in WAC 173-160-240. Nevertheless, WADOE would need to approve the well completion plan for a project utilizing a similar well design as outlined in this report.

9.3 Yakima Minerals Hybrid Plant

The Yakima Minerals plant necessitated an unconventional approach to the CAES plant design lacking readily available access to natural gas supplies and cooling water. First, the storage reservoir is far deeper (>10,000 ft) than any CAES plant that has been considered to date. The advantages of the deep storage reservoir include well completions in thick and permeable sands known to be present from exploratory drilling resulting in excellent injectivity and a very compact air bubble accumulation under the anticline. Based on subsurface modeling, the site would readily accommodate a large degree of capacity expansion should it be needed in the future.

A significant attribute of the hybrid plant is that the compressor and turbo-expander equipment will operate at substantially higher pressures than conventional CAES plants, enabling the hybrid plant to capitalize on both geopressure and geothermal characteristics. As designed and modeled, this results in maximum compression capacity relative to airflow directly addressing over-generation events as well as significant power output from a non-phase change geothermal plant. Other innovative concepts at this site include 1) short-term storage of the heat of compression in a molten salt reservoir, 2) an option for heat rejection using flow-balanced geothermal driven ammonia absorption or into shallow basalts via groundwater cooling water return, and 3) extraction of geothermal heat to supplement heat derived from the molten salt storage reservoir (and maintain its temperature above the melting point if needed) to drive the turbo-expander train. Perhaps the single most valuable aspect of the hybrid CAES plant based on the assumptions made is that it is a technically feasible, renewable energy source that can be dispatched to produce or consume energy with essentially no environmental releases.

Compressor cooling is a significant design issue at the Yakima Minerals site. Auxiliary cooling would be needed to allow for an operational period extending for the 30-day design basis applied for this study. For maximum compressor efficiency, implementation of a shallow groundwater source cooling water return system and/or cooling tower would be preferred over air-cooling if readily accessible. However, groundwater source cooling would require a substantial flow rate based on heat exchanger duty, access to shallow and very permeable sediment or basalts nearby the power plant site, and large diameter wellbore completions. Implementing a cooling tower option at this site drastically reduces the groundwater flow requirements, and would directly reduce capital and operating expenses from what is currently modeled.[1]

The nearest available surface water to implement this option would be the Yakima River. Due to excess demand on the Yakima River, obtaining a water right permit for out-of-stream use of Yakima River water may be difficult and would take an extended period. One mitigating factor is that the primary

[1] The air cooling (ECA heat exchangers) and Area 900 (ammonia absorption) equipment cost is $7.8M. Total cost would be higher including construction, instrumentation, piping, and ancillary line items such as insulation and paint.

withdrawals from the Yakima River would coincide with periods of excess spring runoff and the largest continuous compressor load; hence, a negligible impact on overall management of the resource would be possible. To address these concerns, staff incorporated the geothermal driven ammonia absorption cooling system into final process flow diagrams, and eliminated the need for cooling water. The geothermal flows required for the cooling process were balanced against the duty required for trim cooling, and are envisioned to be used for both compression and generation cycles. In Washington State, closed loop heating and cooling water return flow wells are rule authorized wells under WAC 173-218-100 provided no chemicals or other products are added to the water. Hence, both the geothermal heat extraction and injection wells would be rule authorized as envisioned for this plant. The air injection well(s) would be completed in a single defined sub-basalt sedimentary formation and hence should comply with all well construction requirements under WAC 173-160-420.

Other uncertainties remain at the site, predominantly based on the interactions between the plant and subsurface reservoir. For example, while phase-change geothermal plants (flash or binary cycle) commonly have issues with heat exchanger and turbine cleanliness, the geothermal resource at Yakima Minerals was intentionally maintained at adequate pressure and temperature to avoid phase change solubility concerns. This doesn't eliminate heat exchanger cleanliness and brine solubility issues, but it does reduce them. This is a potential concern that wasn't explored in this analysis.

Additionally, the modeled capacities of the plant were predicated on maximizing flow from the subsurface reservoirs at the imposed casing diameter restriction and limiting the design to a single well. With attributes of both CAES and geothermal plants, there is no comparable commercial equivalent to the design developed in this study. Appropriately, this simply acknowledges that the models (and therefore cost analyses) rely on technologies and assumptions that are in phases of development, but that currently require technical maturation. For example, as reported by DOE (2008), findings in an MIT study group evaluation of geothermal reservoir performance under production conditions indicated the following:

> The flow rate of circulating fluid in an enhanced geothermal system (EGS) reservoir and the thermal drawdown associated with this flow rate are major unknowns. The analysis assumed *a flow rate of 80 kg/sec at 200°C from each production well*, equivalent to a commercial hydrothermal reservoir. At present there is no experimental evidence to verify that this level of productivity can be achieved. As pointed out in the analysis, the EGS project at Soultz, which is the best-performing project to date, has had a maximum well productivity of about 25 kg/sec. Well productivity remains the greatest technological challenge for the commercialization of EGS.

The geothermal flow rate modeled for the Yakima Minerals plant is approximately two times the 80 kg/s flow rate discussed in the preceding, and six times the flow rate of the EGS project at Soultz, which successfully supplied 25 kg/s. That said, the Yakima Minerals plant is not an EGS plant and is not expected to rely on a fractured or enhanced subsurface reservoir. The caution is still relevant, but it is perhaps more reasonable to consider a facility that would utilize a lower flow rate to accommodate the current "state of the technology." The price per kilowatt would likely rise due to the fixed well depths (and cost to construct), but it is feasible knowing that the compression and generation machinery is readily scalable. This is also indirectly addressed by review of a current technology evaluation for deep well, high temperature, submersible production pumps (QI et al., 2012). Though the study was framed against DOE goals for efficient fluid lifting, the highest flow observed in the study was approximately 100 kg/s with the highest pump efficiencies (again, given design limitations) at 70 to 80 kg/s. Framed against the Yakima Minerals site, this commercially feasible option suggests that two well bores for

production would be necessary (rather than one), and could potentially add an additional $12 million to the capital of the plant.

9.4 Conclusions and Next Steps

The diversity of the plant designs and reservoir parameters for the two sites modeled here speaks to the breadth of settings across which CAES projects could potentially be developed in the Columbia Basin. This first-order effort to identify the best possible sites based on a number of surface and subsurface siting criteria, and to pair those sites with the suite of compression and generation technologies best suited to commercial-scale projects at each site, sheds light on the feasibility of CAES implementation in the Pacific Northwest. However, additional economic dispatch modeling—including baseload generation, balancing and power arbitrage, and ways to allow a portion of the rents associated with increased hydroelectric dispatch to accrue the CAES project operator—will enable more specific modeling of the revenue streams and allow greater iteration on plant design and storage reservoir management.

Design flexibility allows paired surface-subsurface systems to be tailored to the needs of the project, but the overall system would be designed to operate differently under an expectation to mitigate all wind oversupplies and maximize hydroelectric generation during off-peak hours than it would under an expectation of profit maximization via diurnal arbitrage. Their flexibility would allow either of the CAES configurations described in this report to serve a number of purposes, making it a unique resource within the BPA service territory, but economic optimization of the design and management of these systems requires information about expected power prices. In addition to providing a proof of concept that CAES is feasible in storage reservoirs within the CRBG, configurations and associated LCOEs presented here provide a starting point for discussing the value CAES may have in enabling the integration of intermittent renewables energy while maintaining stable, reliable availability of electricity in the BPA service area.

10.0 Literature Cited

AACE. 2005. *Aace International Recommended Practice No. 18r-97, Cost Estimate Classification System—as Applied in Engineering, Procurement, and Construction for the Process Industries.* AACE International, Morgantown, West Virginia.

Allen, R. D., T. J. Doherty, and L. D. Kannberg. 1985. *Summary of Selected Compressed Air Energy Storage Studies.* PNL-5091, Pacific Northwest Laboratory, Richland, Washington.

BPA. 2011a. *Transmission Technology Roadmap.* RM-06, Bonneville Power Administration, Technology Innovation Office, Portland, Oregon, URL= www.bpa.gov/corporate/business/innovation/.../2006/rm-06_transmission.pdf.

BPA. 2011b. *Northwest Overgeneration: An Assessment of Potential Magnitude and Cost.* http://www.bpa.gov/corporate/AgencyTopics/ColumbiaRiverHighWaterMgmnt/, Bonneville Power Administration.

BPA. 2011c. *Interim Environmental Redispatch and Negative Pricing Policies, Final Rod.* Bonneville Power Administration, Portland, Oregon.

BPA. 2012a. *2011 and 2012 Bpa Total Load and Wind Generation in the Bpa Control Area.* http://transmission.bpa.gov/business/operations/Wind/, Bonneville Power Administration, Portland, Oregon.

BPA. 2012b. *Oversupply*. http://www.bpa.gov/Projects/Initiatives/Oversupply/Pages/default.aspx, Bonneville Power Administration.

Brooks, F. J. 2000. *Ge Gas Turbine Performance Characteristics.* GER-3567H, GE Power Systems, Schenectady, New York.

Burns, E. R., D. S. Morgan, R. S. Peavler, and S. C. Kahle. 2011. *Three-Dimensional Model of the Geologic Framework for the Columbia Plateau Regional Aquifer System, Idaho, Oregon, and Washington.* Scientific Investigations Report 2010-5246, U.S. Geological Survey, Tacoma, Washington, URL= http://pubs.usgs.gov/sir/2010/5246/.

Denholm, P. and R. Sioshansi. 2009. "The Value of Compressed Air Energy Storage with Wind in Transmission-Constrained Electric Power Systems." *Energy Policy* **37**(8):3149-3158.

DOE. 2008. *Geothermal Tomorrow: 2008.* Geothermal Technologies Program, U.S. Department of Energy, Office of Energy Efficiency and Renewable Energy, Washington, DC.

DOGAMI. 2012. *Mineral Land Regulation and Reclamation Geothermal Well Logs.* http://www.oregongeology.org/mlrr/geothermal-logs.htm, Oregon Department of Geology and Mineral Industries.

Doty, G. N., D. L. McCree, and F. D. Doty. 2010. "Projections of Levelized Cost Benefit of Grid-Scale Energy Storage Options." In Proceedings of *ASME 4th International Conference on Energy Sustainability*, American Society of Mechanical Engineers, pp. 577-584.

Dresser-Rand. 2007. *Fcc Power Recovery Expanders.* Form 85211-09, Dresser-Rand, Houston, Texas, URL= http://www.dresser-rand.com/literature/turbo/85211_FCCExpanders.pdf.

Dresser-Rand. 2010. *Compressed Air Energy Storage (Caes).* Form 85230, Dresser-Rand, Houston, Texas, URL= http://www.dresser-rand.com/literature/general/85164-10-CAES.pdf.

Drury, E., P. Denholm, and R. Sioshansi. 2011. "The Value of Compressed Air Energy Storage in Energy and Reserve Markets." *Energy* **36**(8):4959-4973, 10.1016/j.energy.2011.05.041.

EPRI. 2002. *Handbook of Energy Storage for Transmission or Distribution Applications, Technical Update.* EPRI, Palo Alto, California.

GE-Energy. 2013. *7fa Heavy Duty Gas Turbine.* http://www.ge-energy.com/products_and_services/products/gas_turbines_heavy_duty/7fa_heavy_duty_gas_turbine.jsp, GE-Energy, Atlanta, Georgia.

Gephart, R. E., P. A. Eddy, and R. A. Deju. 1979. *Geophysical Logging and Hydrologic Testing of Deep Basalt Flow in the Rattlesnake Hills Well Number One.* RHO-BWI-ST-1, Rockwell Hanford Operations, Richland, Washington.

Hance, C. D. 2005. *Factors Affecting Costs of Geothermal Power Development.* Geothermal Energy Association, Washington, DC.

INL. 2006. *The Future of Geothermal Energy: Impact of Enhanced Geothermal Systems (Egs) on the United States in the 21st Century.* INL/EXT-06-11746, Idaho National Laboratory, Idaho Falls, Idaho.

Kintner-Meyer, M., P. Balducci, C. Jin, T. Nguyen, M. Elizondo, V. Viswanathan, X. Guo, and F. Tuffner. 2010. *Energy Storage for Power Systems Applications: A Regional Assessment for the Northwest Power Pool (Nwpp).* PNNL-19300, Pacific Northwest National Laboratory, Richland, Washington.

Kintner-Meyer, M., P. Balducci, W. Colella, M. Elizondo, C. Jin, T. Nguyen, V. Viswanathan, and Y. Zhang. 2012. *National Assessment of Energy Storage for Grid Balancing and Arbitrage: Phase 1, Wecc.* PNNL-21388, Pacific Northwest National Laboratory, Richland, Washington.

Knudsen, S. 2012. *Personal Communication: Bpa 2012 Forecast: On-Peak and Off-Peak Pricing (P50 Interval).* Email from Steve Knudsen, September 3, 2012.

McGrail, B. P., H. T. Schaef, A. M. Ho, Y. J. Chien, J. J. Dooley, and C. L. Davidson. 2006. "Potential for Carbon Dioxide Sequestration in Flood Basalts." *Journal of Geophysical Research-Solid Earth* **111**(B12), doi:10.1029/2005JB004169.

McGrail, B. P., E. C. Sullivan, F. A. Spane, D. H. Bacon, G. Hund, P. D. Thorne, C. J. Thompson, S. P. Reidel, and F. S. Colwell. 2009. *Preliminary Hydrogeologic Characterization Results from the Wallula Basalt Pilot Study.* PNWD-4129, Battelle Pacific Northwest Division, Richland, Washington.

McGrail, B. P., F. A. Spane, E. C. Sullivan, D. H. Bacon, and G. Hund. 2011. "The Wallula Basalt Sequestration Pilot Project." *Energy Procedia* **4**:5653-5660.

Nakhamkin, M. 2012. *Advanced Adiabatic Compressed Air Energy Storage System.* US Patent 8,261,552. September 11, 2012.

NETL. 2012. *Seneca Compressed Air Energy Storage (Caes) Project, Final Phase 1 Technical Report.* National Energy Technology Laboratory, Morgantown, West Virginia.

NREL. 2012. *Levelized Cost of Energy Calculator*. http://www.nrel.gov/analysis/tech_lcoe.html, National Renewable Energy Laboratory, Golden, Colorado.

Qi, X., N. Turnquist, and F. Gasripoor. 2012. "Advanced Electric Submersible Pump Design Tool for Geothermal Applications." Paper Submitted to: *Geothermal Resources Council's 36th Annual Meeting.* Reno, Nevada, USA. September 30 – October 3, 2012.

Reidel, S. P., K. R. Fecht, M. C. Hagood, and T. L. Tolan. 1989. The Grande Ronde Basalt, Columbia River Basalt Group; Stratigraphic Descriptions and Correlations in Washington, Oregon, and Idaho. In *Volcanism and Tectonism in the Columbia River Flood-Basalt Province*, Vol. Special Paper 239 (ed. S. P. Reidel and P. R. Hooper), pp. 21-54. Geologic Society of America.

Reidel, S. P., V. G. Johnson, and F. A. Spane. 2002. *Natural Gas Storage in Basalt Aquifers of the Columbia Basin, Pacific Northwest USA: A Guide to Site Characterization.* PNNL-13962, Pacific Northwest National Laboratory, Richland, Washington.

Reidel, S. P., F. A. Spane, and V. G. Johnson. 2005. *Potential for Natural Gas Storage in Deep Basalt Formations at Canoe Ridge, Washington State: A Hydrogeologic Assessment.* PNNL-15386, Pacific Northwest National Laboratory, Richland, Washington.

Schaef, H. T., B. P. McGrail, and A. T. Owen. 2010. "Carbonate Mineralization of Volcanic Province Basalts." *International Journal of Greenhouse Gas Control* **4**(2):249-261.

Schulte, R. H., N. Critelli, Jr., K. Holst, and G. Huff. 2012. *Lessons from Iowa: Development of a 270 Megawatt Compressed Air Energy Storage Project in Midwest Independent System Operator.* SAND2012-0388, Sandia National Laboratories, Albuquerque, New Mexico.

Sioshansi, R., P. Denholm, T. Jenkin, and J. Weiss. 2009. "Estimating the Value of Electricity Storage in Pjm: Arbitrage and Some Welfare Effects." *Energy Economics* **31**(2):269-277.

Tolan, T. L., S. P. Reidel, M. H. Beeson, J. L. Anderson, K. R. Fecht, and D. A. Swanson. 1989. Revisions to the Estimates of the Areal Extent and Volume of the Columbia River Basalt Group. In *Volcanism and Tectonism in the Columbia River Flood-Basalt Province*, Vol. Special Paper 239 (ed. S. P. Reidel and P. R. Hooper), pp. 1-20. Geological Society of America.

USGS. 2006. *National Elevation Dataset.* http://ned.usgs.gov/Ned/about.asp, U.S. Geological Survey, EROS Data Center, Sioux Falls, South Dakota.

WADOE. 2012. *Well Logs.* http://apps.ecy.wa.gov/welllog/, Washington State Department of Ecology.

WDNR. 2012a. *Earth Resource Permit Locations.* https://fortress.wa.gov/dnr/geology/?Site=erpl, Washington State Department of Natural Resources.

WDNR. 2012b. *Geothermal Resources of Washington.* https://fortress.wa.gov/dnr/geology/?Site=geothermal, Washington State Department of Natural Resources.

White, M. D. and M. Oostrom. 2006. *Stomp Subsurface Transport over Multiple Phases, Version 4.0, User's Guide.* PNNL-15782, Pacific Northwest National Laboratory, Richland, Washington.

Wilson, M. S., T. S. Dyman, and S. M. Condon. 2008. Evaluation of Well-Test Results and the Potential for Basin-Center Gas in the Columbia Basin, Central Washington. In *Geologic Assessment of Undiscovered Gas Resources of the Eastern Oregon and Washington Province*, pp. 12. U.S. Geological Survey Digital Data Series DDS-69-O.

Distribution

No. of Copies

11 Bonneville Power Administration
P.O. Box 3621
Portland, OR 97208-3621
Attn: Steve Knudsen (10)
Ryan Redmond

1 Dresser-Rand Company
500 Paul Clark Drive
Olean, NY 14760
Attn: Mark J. Kuzdzal

1 Dresser-Rand Company
9572 Whisper Ridge Trail
Weeki Wachee, FL 34613
Attn: James R. Heid

2 Greenfire Energy
5698 Park Place East
Salt Lake City, UT 84121
Attn: Mark Muir
Alan D. Eastman

1 Magnum
3165 East Millrock Drive
Suite 330
Holladay, UT 84121
Attn: Robert Webster

1 Northwest Natural Gas
220 NW Second Ave
Portland, OR 97209
Attn: Christopher F. Galati

1 Portland General Electric
121 SW Salmon St
3WTCBR03
Portland, OR 97204
Attn: Chris Dieterle

1 Puget Sound Energy
10885 NE 4th St
Bellevue, WA 98004-5579
Attn: Patrick Leslie

No. of Copies

1 Ramgen Power Systems
25 Mason Street
Winchester, MA 01890-3126
Attn: Peter Baldwin

1 Seattle City Light
Seattle City Light
700 5th Avenue, Suite 3200
P.O. Box 34023
Seattle, WA 98124-4023
Attn: Kimberly Pate

1 Snohomish PUD
2320 California Street
Everett, WA 98206
Attn: Craig W. Collar

1 Washington State University
2710 Crimson Way
Richland, WA 99354-1671
Attn: Steve Reidel

4 U.S. Department of Energy
Office of Energy Efficiency & Renewable Energy
1000 Independence Ave., S.W.
Washington, DC 20585
Attn: Jay Nathwani, EE-2C
Benjamin R. Phillips, EE-2C
Greg Stillman, EE-2C
Tim Reinhardt, EE-2C

1 Robert D. Kahn & Company
1117 Minor Avenue, Suite 200
Seattle, WA 98101
Attn: Robert Kahn

ONSITE

39 Pacific Northwest National Laboratory

D. H. Bacon, K9-33
S. Baskaran, K9-01
M. D. Bearden, K2-20
C. F. Brown, K6-81

No. of
Copies

T. M. Brouns, K9-69
J. E. Cabe, K6-05 (5)
M. A. Chamness, K6-85
C. L. Davidson, K6-10 (5)
M. J. Fayer, K9-33
C. J. Freeman, K2-20
J. D. Holladay, K2-12
J. A. Horner, K6-96
G. Hund, BSRC
E. O. Jones, K2-20
L. D. Kannberg, K1-85

No. of
Copies

D. A. King, K2-12
M. Kintner-Meyer, K1-85
J. Liu, K2-20
B. P. McGrail, K6-90 (5)
H. T. Schaef, K6-81
E. C. Sullivan, K6-81
P. D. Thorne, K6-96
F. A. Spane, K6-96
M. D. White, K9-33
Information Release, K1-06 (2)

Pacific Northwest
NATIONAL LABORATORY

Proudly Operated by **Battelle** *Since 1965*

U.S. DEPARTMENT OF
ENERGY

902 Battelle Boulevard
P.O. Box 999
Richland, WA 99352
1-888-375-PNNL (7665)
www.pnnl.gov